THE CHARACTERIZATION OF ATMOSPHERIC PRESSURE IONIZATION/TANDEM MASS SPECTROMETRY FOR DIRECT ATMOSPHERIC ANALYSIS

by

KENNETH PAUL MATUSZAK

A DISSERTATION PRESENTED TO THE GRADUATE SCHOOL
OF THE UNIVERSITY OF FLORIDA
IN PARTIAL FULFILLMENT OF THE REQUIREMENTS FOR THE
DEGREE OF DOCTOR OF PHILOSOPHY

UNIVERSITY OF FLORIDA

1988

To my parents with love.

ACKNOWLEDGEMENTS

I wish to express my sincere appreciation to Dr. Richard A. Yost for his guidance and direction during the completion of this work. I would also like to acknowledge and thank the members of my graduate committee, Dr. John Eyler, Dr. Gar Hoflund, Dr. John Dorsey, and Dr. Cliff Johnston.

I acknowledge the U. S. Air Force Engineering and Services Center, at Tyndall, AFB, which provided the entire support for this work.

Many thanks go to the departmental machine, electronics, and glass shops, including Russ Pierce of the electronics shop who bailed me out several times with his insights, knowledge, and ability to explain electronics on my level; Steve Miles of the electronics shop who refined the design and oversaw construction of the corona discharge current-regulated power supply; Chester Eastman, Vern Cook, and Dailey Burch of the machine shop who constructed almost the entire source and took time out of their schedules for last minute changes during crunch-time; and Dr. Sam Colgate for his advice on vacuum system design.

I thank my fellow researchers, especially Mark Hail who helped extensively early on in this project, Dr. Jodie Johnson for his mass spectrometry advice, Mark Bolgar who assisted on the project, my fellow group members, especially Mike Lee, my roommates Bryan Hearn and Mike Cockman for putting up with me this past year, my friends here at UF,

especially Paul and Anne McCaslin, Regina Cheong, and my little bro' Jeff Keaffaber.

Sincere thanks go to my family, especially Mom and Dad, who have been so supportive, my friends back home in Chicago, and the members of St. Augustine Catholic Church and Inter-Varsity Christian Fellowship for uplifting me in their prayers.

My most special thanks go to the person who held me up here at the end, who wouldn't let me quit, who took care of me when I needed it, put up with me even when I was a jerk, made my days bright even when they were dark, and never ceased to shower me with love, my very soon-to-be wife, Laura Elizabeth Boudreaux (I love that name).

Last but not least, I thank the Lord Jesus Christ my Savior, because it was only by his grace that I had the ability and strength to finish.

TABLE OF CONTENTS

		PAGE
ACKNOWLEDGEMENTS		iii
ABSTRACT		vii
CHAPTER		
1	INTRODUCTION	1
	Analytical Scenario	1
	Overview of API/MS	2
	Overview of Thesis Organization	13
2	DESIGN OF THE API SOURCE	15
	Overall System Design	15
	Initial Source Design	18
	API Source Configuration for Finnigan 4500	25
	API Source Configuration for Finnigan TSQ 70	27
3	EXPERIMENTAL RESULTS AND SOURCE DEVELOPMENT	34
	Results with API Source Configuration for Finnigan 4500 Mass Spectrometer	34
	Adaptation of the API Source to the Finnigan TSQ 70 Mass Spectrometer	42
	Experimental Physical Parameters of API Source and Mass Spectrometer	58
	Clustering/Declustering	74
	Experimental Methods for Direct Atmospheric Monitoring	80
	Sampling Methodology	81
4	ANALYTICAL PERFORMANCE	82
	Characterization of the API/MS/MS Instrument	82
	Analytical Potential	94
5	CONCLUSIONS AND FUTURE WORK	104
	Summary of Results	104
	Evaluation as Direct Atmospheric Analyzer	106
	Suggestion for Future Work	107

LITERATURE CITED..... 114

BIOGRAPHICAL SKETCH..... 117

Abstract of Dissertation Presented to the Graduate School of the University of Florida in Partial Fulfillment of the Requirements for the Degree of Doctor of Philosophy

The Characterization of Atmospheric Pressure Ionization/Tandem Mass Spectrometry for Direct Atmospheric Analysis

by

Kenneth Paul Matuszak

April, 1988

Chairman: Richard A. Yost
Major Department: Chemistry

Atmospheric pressure ionization (API) has been shown to be very useful when combined with tandem mass spectrometry in performing direct atmospheric monitoring of trace compounds. The design and development of a new API source that has been developed to be compatible with a commercial, turbomolecularly-pumped triple stage quadrupole (TSQ) tandem mass spectrometer (MS/MS) is presented. This API/MS/MS instrument has been used to study (1) direct atmospheric sampling by mass spectrometry, (2) the production of ions in the atmosphere, (3) the effects of supersonic expansion on the clustering of these ions with neutral species, (4) the effectiveness of declustering of these ions by collisional means, and (5) the ability to qualitatively identify atmospheric gases. These studies will serve to lay the

groundwork for the development of an instrument capable of performing trace analysis while performing direct atmospheric monitoring.

This API source utilizes a corona discharge for the primary ionization of the atmospheric molecules and an orifice system to selectively leak the ions into the mass analysis region. It has been constructed so that it is interchangeable with a standard electron ionization (EI)/chemical ionization (CI) source on a Finnigan-MAT TSQ 70 triple quadrupole tandem mass spectrometer. In developing this source, a program to model the ion optics (SIMION) has been used to aid in the design of the post-orifice lens configuration.

The design of this source is such that memory effects have been essentially eliminated and the clustering of ions with molecules in the post-orifice region has been significantly reduced. Samples that have been studied include a variety of laboratory solvents. These solvents have been injected into streams of pure nitrogen carrier gas and have been analyzed under direct atmospheric conditions by bringing the caps of the solvent bottles near the sampling region of the API source.

Recommendations are made for overcoming the limitations of the present API source design and lens system. These include the consideration of supersonic jet expansion theory to redesign the post-orifice lens system and additional modifications to the discharge needle system.

CHAPTER 1

INTRODUCTION

The purpose of this work is twofold: first to design, construct, and develop, a new atmospheric pressure ionization (API) source for a turbomolecularly-pumped triple stage quadrupole (TSQ) tandem mass spectrometer (MS/MS), and second, to characterize and apply this new source to study (1) direct atmospheric sampling by mass spectrometry, (2) the production of ions in the atmosphere, (3) the effects of supersonic expansion on the clustering of these ions with neutral species, (4) the effectiveness of declustering of these ions by collisional means, and (5) the ability to qualitatively identify atmospheric gases. These studies will serve to lay the groundwork for the development of an instrument capable of performing trace analysis while performing direct atmospheric monitoring. Such an instrument could be used as an airport "sniffer" for drugs and explosives, or as an on-line vapor detector in the microchip, incineration, or chemical production industries. The major use of such an instrument, however, is anticipated as an environmental monitor for chemical waste spills and chemical dump sites or other forms of environmental contamination.

Analytical Scenario

Because this API source is interchangeable with the standard electron ionization (EI)/chemical ionization (CI) source for a

commercial tandem mass spectrometer, one such use would be as a preliminary pollution detection device, that is, to use this instrument to perform direct atmospheric analysis, sampling at various locations, and determining possible contamination of the air at each area of analysis. Thus, the instrument in that configuration would be able to perform preliminary identification of the pollutants present, as well as quantitation to determine the extent of the contamination. Once a site of contamination was found, the API source could be interchanged with the standard EI/CI source and the instrument in this configuration could be used to analyze soil and water samples in the surrounding area with ionization techniques which are already established and standardized for these two forms of sample matter. In this way, the extent of contamination could be mapped out in the full environmental scheme of air, water, and soil.

Overview of API/MS

Background and History of API/MS

To perform the analysis of atmospheric gases by mass spectrometry there are two basic approaches. Because a mass spectrometer operates under high vacuum, in the case of a quadrupole instrument at 10^{-5} to 10^{-7} torr, the pressure of the atmospheric sample must be vastly reduced. The first approach (Figure 1.1) is to bleed the atmospheric sample through an orifice or membrane and use high-vacuum pumps to reduce the pressure to that typically used in the ionization region for normal mass spectrometry. Unfortunately, while doing this, most of the

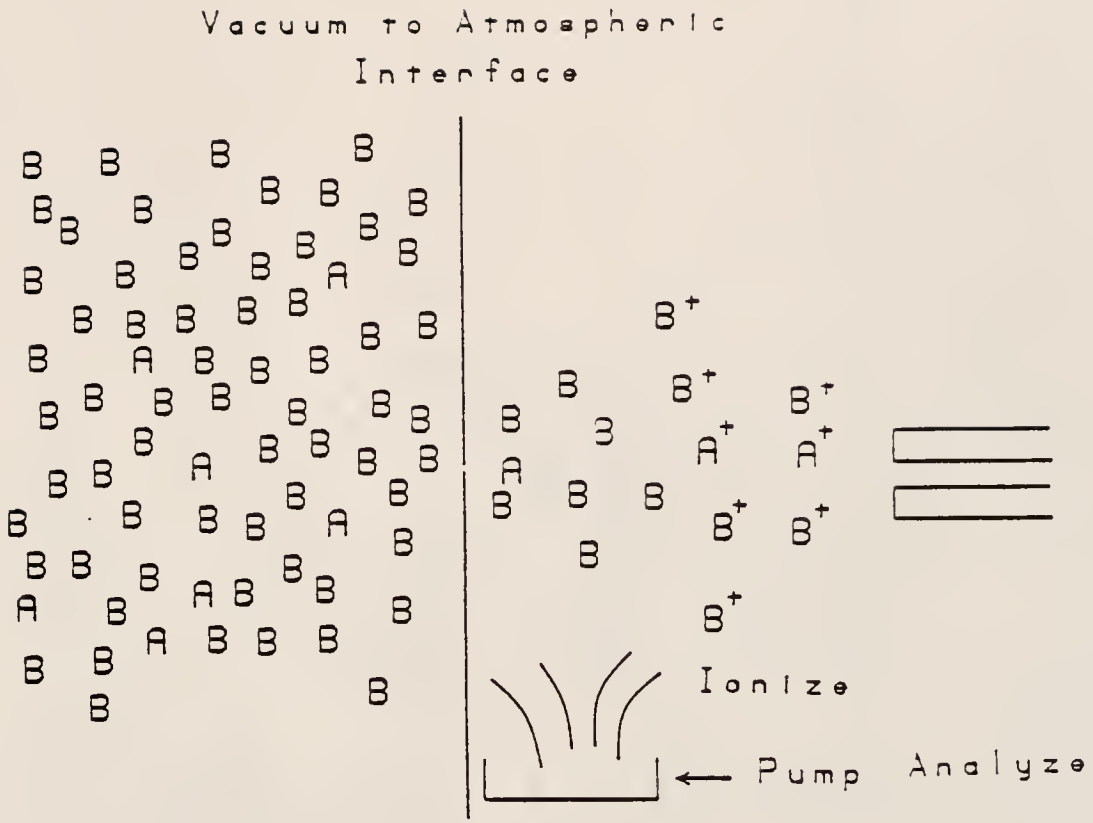

Figure 1.1

An atmospheric sampling methodology in which gas is reduced to normal mass spectrometric pressures and then ionized.

analyte is pumped away with the excess gas. For trace analysis this is obviously undesirable.

The second method (Figure 1.2) is to somehow ionize the analyte at atmospheric pressure and focus the ions through a small orifice into the mass analysis region by means of electrostatic fields, while pumping away the excess gas.

API is a unique ionization technique for mass spectrometry. Ionization occurs outside of the mass analysis (high vacuum) region of the mass spectrometer and the ions are permitted to enter the high vacuum region, usually via a sub-millimeter orifice in a thin diaphragm.

Molecules in an atmospheric pressure gas can be ionized by passing high energy electrons through the gas allowing, the gas molecules to collide with these electrons. This ionization process can produce both positive and negative ions. Positive ions are formed when an electron (e^-) collides with a gaseous molecule (G) and causes a second electron to be ejected, as in Equation 1.1.

$$G + e^- \rightarrow G^+ + 2e^- \qquad (1.1)$$

Negative ions are generated when a low energy (near thermal) electron is absorbed by a molecule of the gas, as in Equation 1.2. This is called electron capture ionization.

$$G + e_{th}^- \rightarrow G^- \qquad (1.2)$$

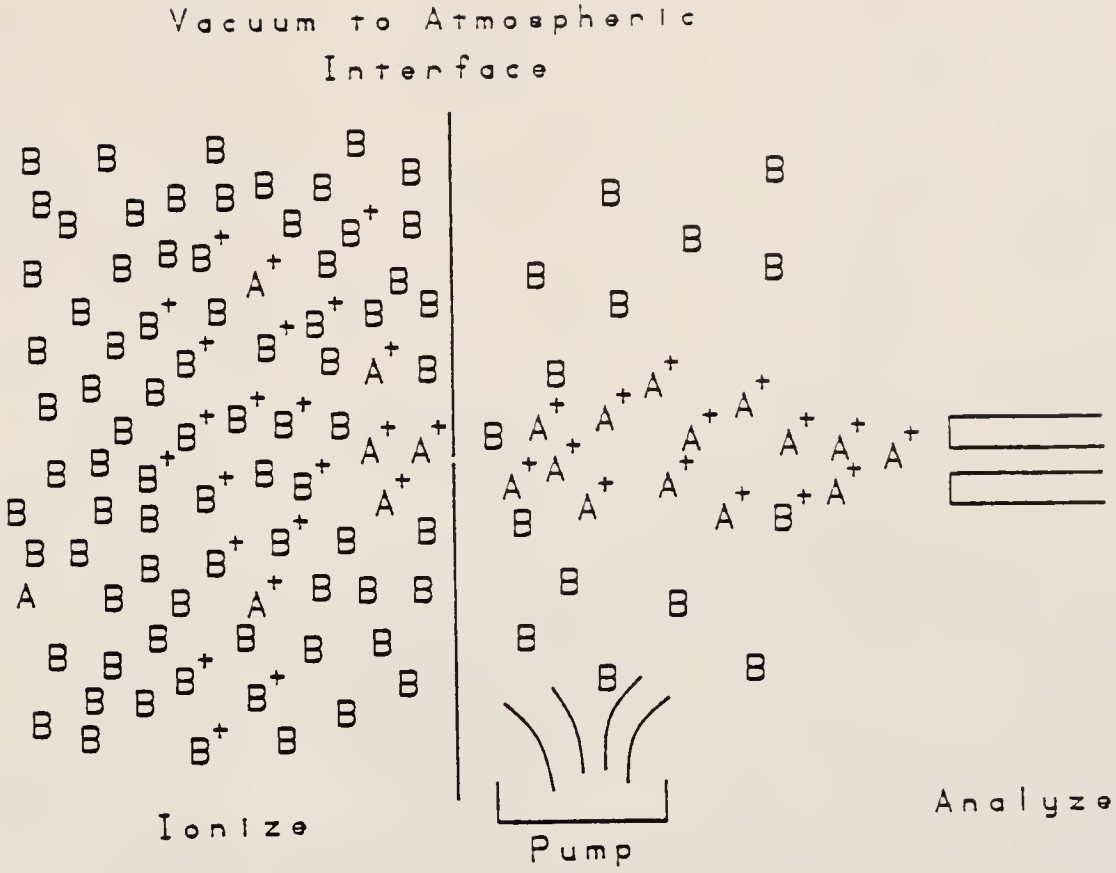

Figure 1.2

An atmospheric sampling methodology in which sample is ionized, sample ions are focused by electrostatic fields into mass analyzer, and gas is pumped away.

These ions can further react with background molecular species to form background reagent ions. In the case of direct atmospheric analysis, positive ions are formed when N_2 and H_2O molecules in the air react with the high energy electrons (Equations 1.3 and 1.4).

$$N_2 + e^- \rightarrow N_2^+ + 2e^- \quad (1.3)$$

$$H_2O + e^- \rightarrow H_2O^+ + 2e^- \quad (1.4)$$

These ions can further react by charge exchange and proton transfer reactions through collisions with other background molecules (Equations 1.5 and 1.6) to form reagent ions.

$$N_2^+ + H_2O \rightarrow N_2 + H_2O^+ \quad (1.5)$$

$$H_2O^+ + H_2O \rightarrow H_3O^+ + HO \quad (1.6)$$

Sample molecules (M) can react with these reagent ions by proton transfer or charge exchange to form molecular (M^+) or pseudo-molecular ($M+H^+$) ions (Equations 1.7 and 1.8).

$$M + H_2O^+ \rightarrow M^+ + H_2O \quad (1.7)$$

$$M + H_3O^+ \rightarrow M+H^+ + H_2O \quad (1.8)$$

Ion clusters can also be formed when ions associate with neutral species before the orifice or in the supersonic expansion in the post-orifice region. Low molecular weight molecules readily form clusters with ionized species. Thus sample and hydronium ions may cluster with either sample or water molecules (Equations 1.9-1.12).

$$M^+ + M \rightarrow M_2^+ \quad (1.9)$$

$$M^+ + H_2O \rightarrow M{+}H_2O^+ \quad (1.10)$$

$$M{+}H^+ + H_2O \rightarrow M{+}H_3O^+ \quad (1.11)$$

$$H_3O^+ + H_2O \rightarrow H(H_2O)_2^+ \quad (1.12)$$

In the preliminary studies with a commercially developed [1] but never marketed API source in an attempt to perform direct atmospheric monitoring, as many as 20 water molecules have been observed to cluster with a hydronium ion (Equation 1.13) to form a distribution of water cluster ions (Figure 1.3).

$$H_3O^+ + nH_2O \rightarrow H(H_2O)_{n+1}^+ \quad \text{where } n = 1\text{-}20 \quad (1.13)$$

At atmospheric pressure, molecules will undergo multiple collisions and those with the highest proton affinity (for positive ions) or highest electron affinity (for negative ions) will quickly become ionized by means of charge or proton transfer with the ions from the bulk gas. Because this is a collisional energy transfer, API is a low energy process and therefore little fragmentation of the molecular analyte ion will occur. Also, due to the multiple collisions, chemical and thermal equilibria will be established in the gas and thus there should be nearly a 100% ionization efficiency for analyte molecules that possess these characteristics. These factors should lead to a very high sensitivity. High selectivity is also obtained for certain classes of compounds because of this non-democratic process.

Sampling of Ions Formed at Atmospheric Pressure

Some of the earliest cases of performing mass spectrometric analyses upon ions formed at atmospheric pressure were performed by

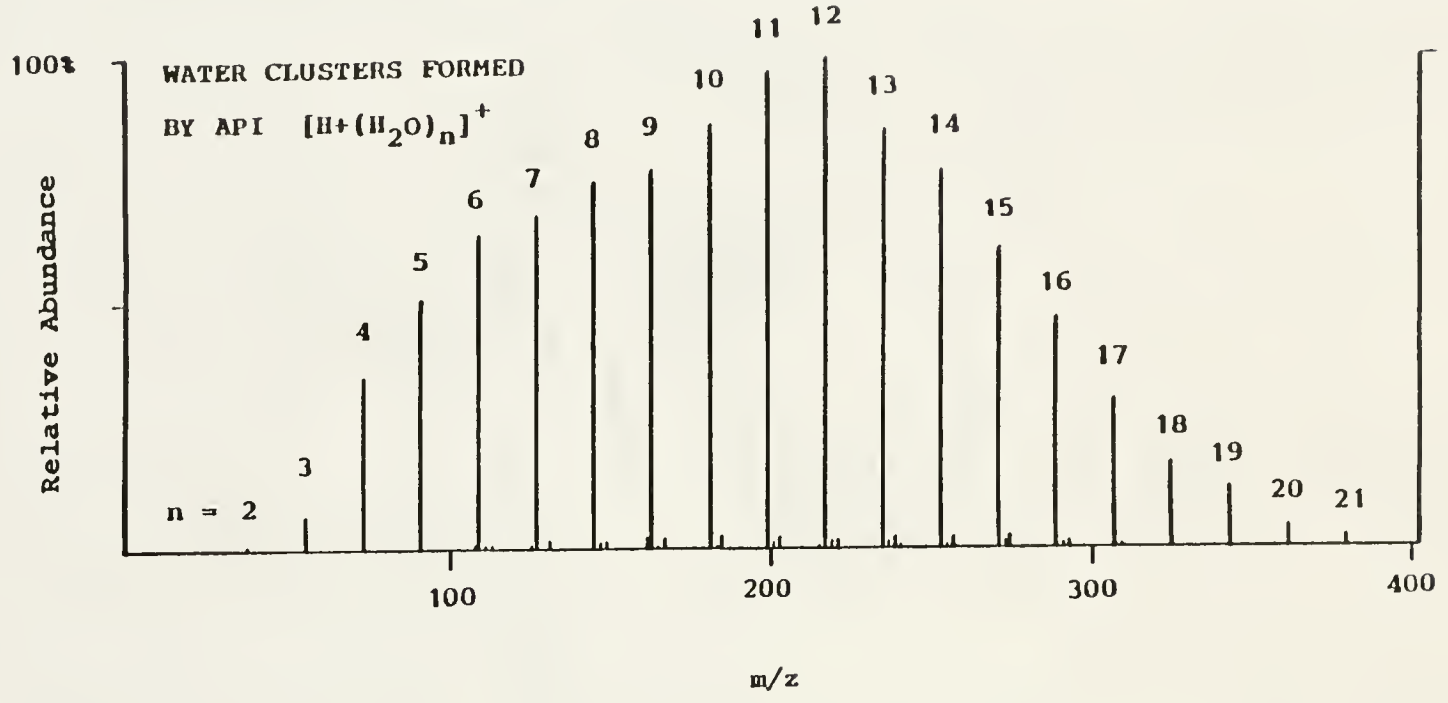

Figure 1.3

Mass spectrum of water cluster ions produced while performing direct atmospheric monitoring with Finnigan-MAT API source.

Knewstubb and Sudgen [2-5]. They used a 50 μm sampling orifice in a thin platinum foil attached to a water-cooled block, sampling ions produced in an atmospheric flame, to study the combustion chemistry of flames. Their system utilized three stages of differential pumping to reduce the pressure from atmospheric down to less than 10^{-6} torr in the analyzer region of their magnetic deflection mass spectrometer.

Kebarle and co-workers [6-8] used α-particle radiation to study the chemistry of the ionization processes for "spectroscopically pure" gases near atmospheric pressure. Their system utilized a 75 μm orifice to sample ions from these pure gases into a differentially pumped magnetic deflection mass spectrometer at pressures less than 10^{-6} torr, a similar instrument to that used by Knewstubb and Sudgen. They found that the spectra from the gases were dominated by ions from trace impurities in the gases, especially from water. Kebarle [9] used these findings to study the kinetics of the ionization process and the production of water cluster ions, of the form $(H_2O)_nH^+$, formed in the post-orifice adiabatic expansion from the atmospheric pressure source to the high vacuum of the mass spectrometer.

At about the same time, Shahin [10] developed a system for the mass spectrometric study of corona discharges in air at atmospheric pressures. Ion products were sampled using a 15 μm aperture into a differentially pumped region. This analyzer region (a quadrupole mass analyzer) was maintained at about 1 x 10^{-5} torr. The major positive ions that he observed were $(H_2O)_nH^+$ and $(H_2O)_nNO^+$ clusters in wet nitrogen. He also found that $(H_2O)_nH^+$ could be dissociated to H_3O^+ by collisional means in the post-orifice region by increasing the pressure and accelerating the ions through that region.

Analytical API/MS

Two excellent articles [11-12] review in detail the history of API/MS and the currently available API/MS technology. Because API is a "soft" ionization technique, the major positive ions formed and detected with mass spectrometry are the molecular ($(M)^+$), pseudo-molecular ($(M+H)^+$), and cluster ($(M_X)^+$, $(M_X+H)^+$, or $[M(H_2O)_X+H]^+$) ions. In the API source chemical and thermal equilibria are established owing to the large number of collisions occurring at atmospheric pressure. This leads to a nearly 100% ionization efficiency for compounds with either high proton or electron affinities [11]. The absolute ionization efficiency for a normal EI source is approximately 1 ion for every 10^4 molecules and a CI source may be 10 or 100 times greater than this [11]. Therefore an API source has a great potential as a very sensitive ionization source.

Many researchers have taken advantage of this and used API sources in conjunction with gas chromatography (GC), liquid chromatography (LC), and supercritical fluid chromatography (SFC). In a series of articles [13-15], Horning, et al., reported the development of an API/MS system for analysis of GC effluents. In 1973 they demonstrated the detection of 20 ng of nicotine, 20 ng of cocaine, 30 ng of methadone, and 500 ng of caffeine in 1 μL of chloroform by GC/API/MS using negative ions. Also analyzed were barbiturates, extracted from urine, in the 3-5 μg/mL concentration range. Mitchum et al. [16-17] used an Extranuclear API/MS instrument to detect 60 pg of 2,3,7,8-tetrachlorodibenzo-p-dioxin (TCDD) and 2,4,5-trichlorophenoxyacetic acid (20 ppm in 3 μL of whole blood and 30 ppb in urine and feces samples) with capillary column GC as the sample introduction method.

Tsuchiya and Taira [18], Carroll et al. [19], Scott et al. [20], and Arpino et al. [21] have all developed LC/API/MS systems and applied them to a variety of sample types.

Because of the design of the sources described above, cleanliness of the source and instrument was extremely important. Source regions for these instruments were characteristically very small (<1 cm^3) and this lead to contamination and memory effects. These sources also suffered from orifice clogging and clustering problems and these two problems would have been even more evident if these sources had been used as direct atmospheric monitors.

While performing direct atmospheric analyses, the low energy API method is likely to produce ions of the same mass-to-charge (m/z) values from components of the same molecular weight. In order to distinguish two such compounds it is therefore necessary to look at fragments of these compounds. However, if fragmentation is caused without first isolating the ion of interest, it would be impossible to tell which ions were fragments or merely ions formed from other compounds. Thus, to perform direct atmospheric analysis with an API source, a separation step is needed before mass analysis.

API/Tandem Mass Spectrometry

Much work has been performed showing that a mass spectrometer can be used as a mass separation technique followed by a second mass spectrometer for sample analysis [22]. Presently, only three examples have been reported of API sources being installed on tandem mass spectrometers, all triple stage quadrupole instruments. Caldecourt, Zackett, and Tou [23] constructed their own mass spectrometer and API source to analyze vapors from manufacturing processes. Extrel

Corporation [24] has reported installing its commercially available API source on a tandem mass spectrometer but as of this writing that system is not commercially available.

Sciex Inc. [25] has developed a API/MS/MS system with liquid helium cryogenic pumping. This API system has seen the most analytical usage of any system to date, although conventional mass spectrometric ionization techniques cannot be used with this mass spectrometer. This instrument has been shown by Bruins et al. to be applicable to LC [26-27] by means of an "ion spray" interface for the analysis of sulfonated azo dyes and to SFC [28] for the analysis of anabolic steroids at the 20-30 ppb concentration level. Snyder et al. have used the Sciex API/MS/MS instrument with a pyrolysis probe to analyze various pharmaceuticals in commercial polymer matrices [29]. The mobile Sciex TAGA 6000 has been applied to dioxin analysis [30] and for the detection of explosives and drugs in airports [31].

While the Sciex instrument has seen a wide spectrum of use, most of the analyses performed with it can be more easily performed with conventional, standardized methods utilizing EI/CI ionization. Its true advantage is its API source. However, because of the liquid helium cryopumping vacuum system, this instrument cannot be operated near any appreciable levels of hydrogen or helium gas, as the vacuum system has essentially no pumping speed for those gases.

One other tandem mass spectrometer system for direct atmospheric analysis that needs to be addressed is that built by Glish et al. at Oak Ridge National Laboratories [32]. This instrument uses an atmospheric sampling ionization (ASI) source in which glow discharge ionization occurs at sub-atmospheric pressures (0.1 to 1 torr), and a

tandem quadrupole/time-of-flight mass spectrometer for analysis. This source has been used to analyze the head space vapor of drinking water with 150 ppm trichloroethylene, and the head space vapor over trinitrotoluene (saturated head space vapor concentration for trinitrotoluene is approximately 6 ppb).

Overview of Thesis Organization

This thesis is divided into 5 chapters. This introductory chapter provides background material on atmospheric pressure ionization (API) and its marriage with mass spectrometry (MS) to help the reader understand the research described in succeeding chapters.

Chapter 2 describes the design of the API source which has been constructed for this work and its interfacing to two different mass spectrometers. Problems and characteristics of other early API sources are described to emphasize some of the features of this source.

The third chapter describes experimental results obtained during the development of the API/MS/MS instrument and the use of these results to guide the development of the API source to its final form. Included in this chapter are descriptions of computerized ion optic modeling which was used to help in source development and as an aid in gaining an understanding into some of the results that were obtained.

A description of the analytical performance of the API/MS/MS instrument as a direct atmospheric monitor can be found in Chapter 4.

The final chapter includes conclusions drawn from this work as to the potential for this API/MS/MS instrument to analytically perform

direct atmospheric analyses and proposes future work that should help attain that goal.

CHAPTER 2

DESIGN OF THE API SOURCE

In designing a new ion source of any type for a mass spectrometer, the design of the mass spectrometer and its component parts must be taken into consideration. The API source for this work was developed and modified to work with two different mass spectrometers.

Overall System Design

Even though the API source for this work was eventually modified to be compatible with a Finnigan-MAT TSQ 70 triple-stage quadrupole tandem mass spectrometer, at the inception of this work that instrument was itself, still in the design stages. Initial source design work was therefore performed on a Finnigan-MAT 4500 single quadrupole mass spectrometer with the goal of obtaining a functional API source that could later be adapted to the specifications of the mass spectrometer at hand.

Early attempts at developing API sources for performing direct atmospheric analyses suffered from many problems, not the least of which were severe memory effects from previously analyzed samples, clogging of the orifice, and clustering of the sample ions with neutral molecules of the bulk gas [11]. Stringent cleaning procedures were

required to clean these sources, including electropolishing of stainless steel surfaces, boiling in deionized water, washing with acetone or methanol, and baking at temperatures greater than 350 C. Indeed, an API source developed (but never marketed) by Finnigan [1] that generated the water cluster spectrum in Chapter 1 (Figure 1.3), demonstrated many of these problems. Figure 2.1 is a schematic drawing of this source, which is similar in design to many of the early API sources. The characteristics of this source include a small ion source region (approximately 0.25 cm^3 in volume), a discharge needle as the high energy electron supply, adjustable needle-to-orifice distance, sample inlet and outlet made out of 1/16" stainless steel tubing, and a single orifice interface between the atmospheric and vacuum regions. During operation the source was heated to ca. 200 C, in order to reduce memory effects. As can be surmised from viewing Figure 1.3, this source had little use as a direct atmospheric monitor because of the severe clustering problems. To be fair, this source was developed as a GC-detector and not an atmospheric monitor, but even as a GC-detector it suffered from memory effects (because of the small source region).

The goals of the development aspect of this work were to develop an API source that would be able to perform real-time atmospheric monitoring, minimize memory and interference effects, minimize the amount of clustering, and achieve a high sensitivity for compounds of interest.

Both the Finnigan-MAT [1] 4500 quadrupole and TSQ 70 triple quadrupole mass spectrometers utilize differential pumping (two 330 L/s turbomolecular pumps) to evacuate the separate ion source and analyzer

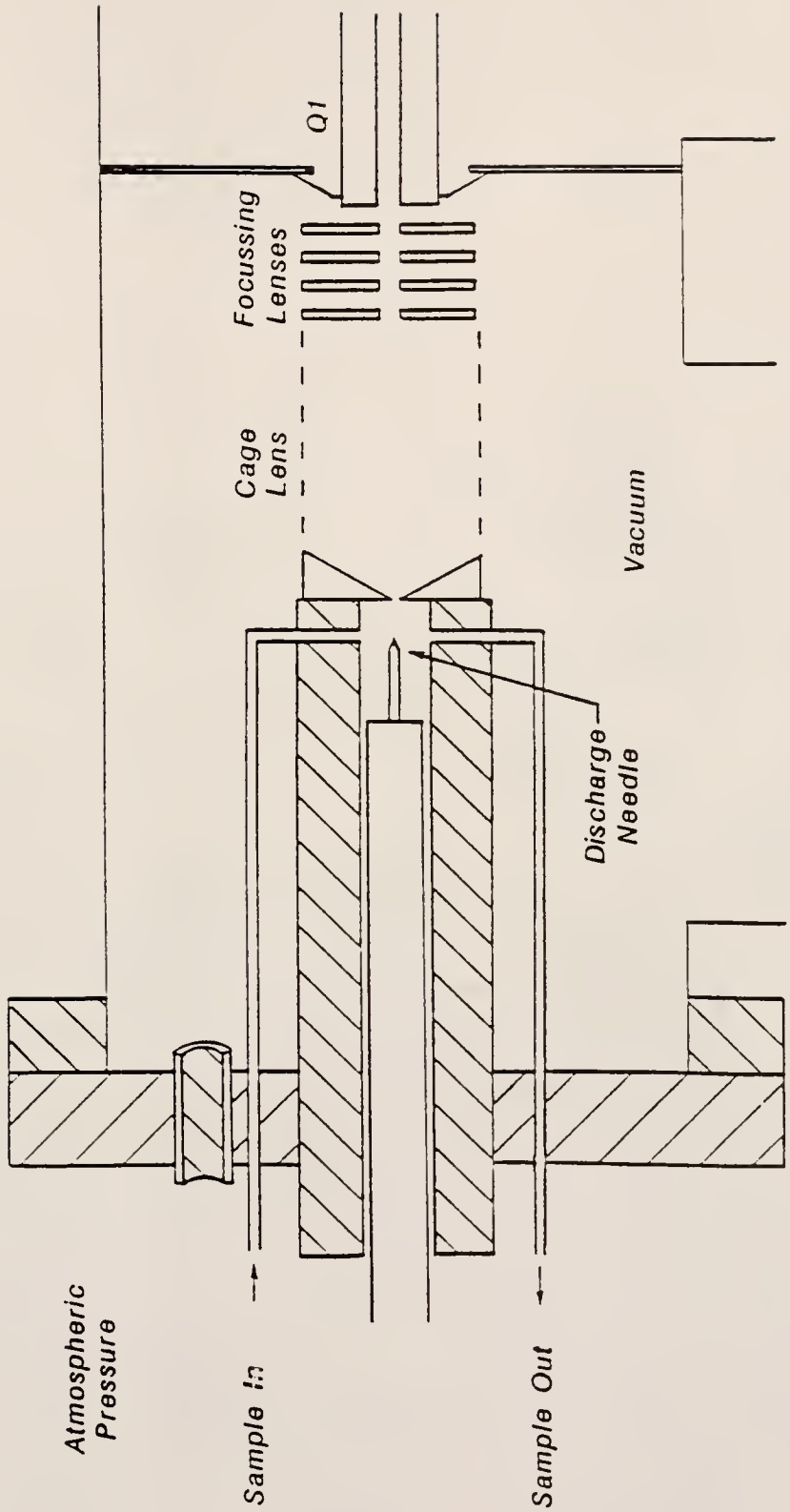

Figure 2.1

Schematic representation of experimental API source developed by Finnigan for a Finnigan 4500 quadrupole mass spectrometer.

regions. Because these instruments are pumped differentially, a much lower vacuum pumping speed is required (to maintain the analyzer regions at a sufficiently low pressure so that the performance of the analyzer is not degraded) than for a mass spectrometer which is pumped by normal means. These pumping speeds are significantly lower than those used by previously developed API/MS/MS instruments. Sciex has reported extremely high pumping speeds (as high as 60,000 L/s) [25] for its cryogenically pumped instrument. These pumping speeds allow for a much larger orifice diameter (>100 μm) than previously developed instruments (<20 μm) [33]. Sciex also claims that the large pumping speeds allow for a very quick, large drop in the pressure after the orifice to avoid the gas dynamics problem of shock waves at the end of the supersonic expansion of the gas in this region [34]. However, the differential pumping of the Finnigan instruments also allows for larger orifice diameters, on the order of 70 μm for this design. And since each of the two Finnigan instruments has easily interchangeable ion sources and lens assemblies, the potential for developing an interchangeable API source for these instruments was good.

Initial Source Design

Initial source design efforts began by developing an API source that was compatible with a Finnigan-MAT 4500 single quadrupole mass spectrometer while waiting for the new TSQ 70 tandem mass spectrometer. In order to make the API source compatible and interchangeable with the Finnigan EI/CI ion source assembly, it was built into a standard 6"

stainless steel conflat flange. The Finnigan EI/CI ion source assembly was mounted onto a similar flange, with associated electrical and gas feedthroughs also mounted in this flange.

In order to reduce the interference and sample memory effects, it was necessary to start with a much larger internal volume for the ionization region (Figure 2.2(a)) than used by the Finnigan API source. To minimize the number of lenses needed for focussing the ions from the orifice to the quadrupole entrance, it was desirable to have the orifice as close as possible to the pre-quadrupole focussing lenses. Because the distance between the face of the flange on the front of the instrument and the entrance to the quadrupoles was greater than 6", the API source canister was designed to be inserted through this flange, held in place by an o-ring. This limited the outside diameter of the flange to less than 3.7", which defined the inside diameter to be approximately 2.6", a significant increase over the 0.5" diameter source region of the old Finnigan API source.

The next step in designing a source for direct atmospheric monitoring was to develop a system to efficiently draw sample air into the source, past the discharge region, and then out of the source again. This was accomplished by drawing sample air through concentric glass tubes (Figure 2.2(b)), past the discharge region, and out a side port attached to the source canister, by means of a common laboratory blower fan that was modified to draw in sample air (≈100 mL/min) instead of blowing it out. The inner of the two concentric glass tubes can be removed for cleaning when necessary.

Figure 2.2

Development of an API source for direct atmospheric monitoring with (a) a large source region, (b) inlet system of concentric glass tubes, (c) corona discharge ionizer, (d) orifice system and associated electrostatic lenses.

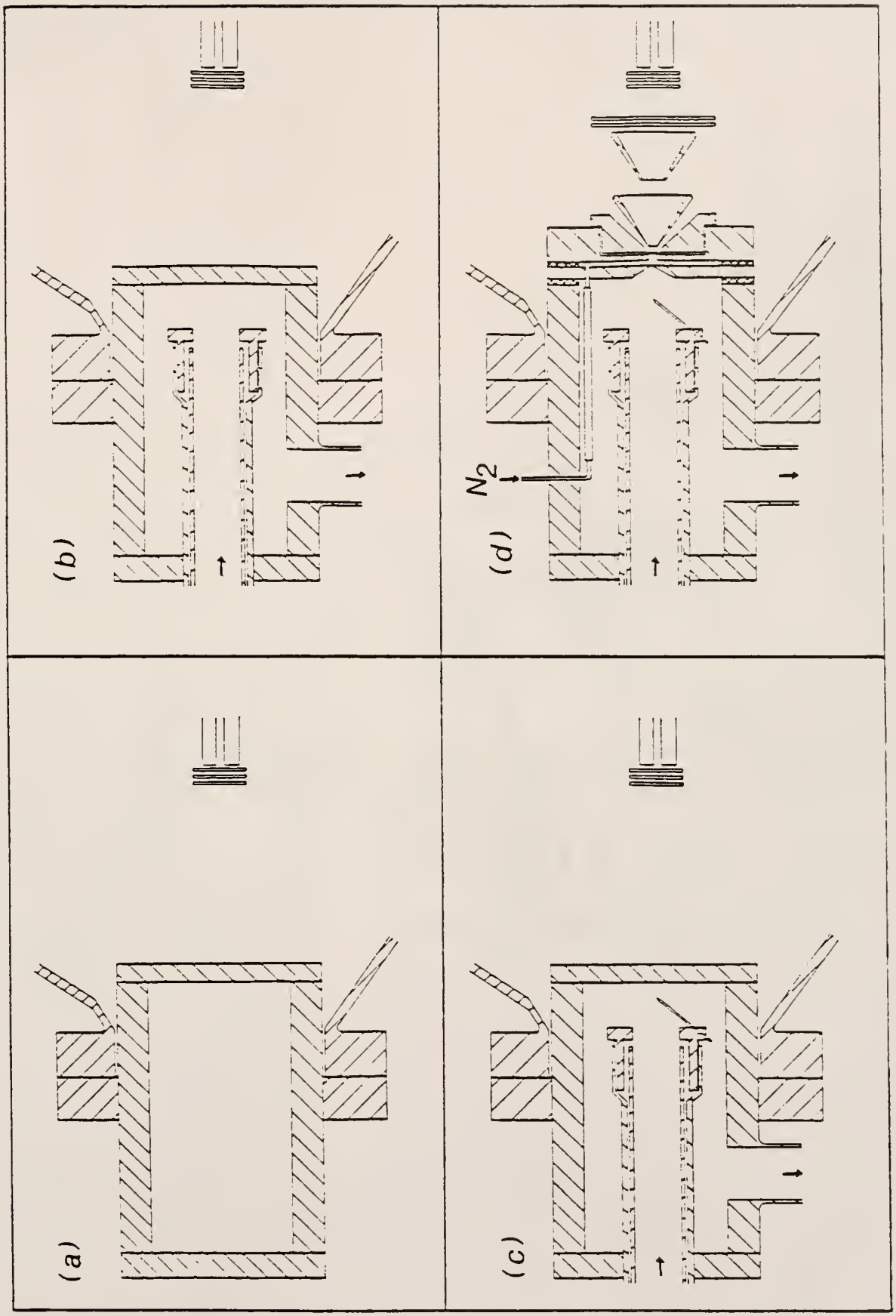
(a)
(b)
(c)
(d)
N_2

For a source of high energy electrons, the two most common methods in API have been a ^{63}Ni foil β^- emitter and a corona discharge. The radioactive foil has the advantages of using no external power and of continually emitting a steady flux of electrons. However, the electrons it emits have a wide energy distribution (the most probable energy being ca. 20 keV), and this energy distribution has a significant tail at high energies [11]. As a result, the spatial distribution of reactant ions is not well defined and the path length of the electrons and ions vary over a wide range [11].

The alternative source of high energy electrons in API is a corona discharge from the tip of a metal needle (often a common sewing needle) to a planar surface (usually the plate containing the diaphragm). This discharge provides a more well defined spatial distribution of electrons as well as a much higher electron flux. One other advantage is the ability to select the needle-to-orifice distance, which may be used to alter the relative intensity and distribution of ions produced in the source. However, it should be pointed out that, in order to obtain a true corona discharge, a current-regulated, high voltage (up to 10 kV), current limited (<20 μA) power supply is required. Later in this chapter, the design of such a power supply is discussed (there are presently no such supplies commercially available); however, all preliminary work was performed using a Bertan 205A-05R voltage-regulated power supply which provided 0 to ±5000 V [35]. Because this was a voltage-regulated supply, the discharge was unstable, and this contributed to not only clogging of the orifice and short needle

lifetimes (because of sputtering of the needle tip), but an ion signal which was extremely noisy.

To provide a supply of electrons for this source, a discharge needle was mounted in a teflon ring which threaded into the outer glass tube (Figure 2.2(c)). By attaching the needle to the tube in this way, rough control of the needle position and needle-to-orifice distance could be accomplished by rotating the glass tube or by sliding it in or out of the back plate of the source canister.

Finally, Figure 2.2(d) shows a proposed two-orifice and lens system to focus the ions to the quadrupoles. Because clustering was such a problem in the early sources, and because it is not clear what portion of the clustering was occurring in the thermodynamic cooling of the post-orifice supersonic jet expansion, it is therefore desirable to prevent water and sample molecules from entering into this region. Sciex uses a similar system [33,34] and pressurizes the region between the two apertures with a relatively inert gas such as carbon dioxide or nitrogen to act as an "ion window" which is transparent to ions (because of potential fields which pull the ions through this gas), but is restrictive to non-ionized species of the sample gas which might clog the orifice or cluster with the ions in the post orifice region. In ion mobility/mass spectrometry, it is common to have a backstream of a neutral nonreactive gas such as nitrogen or helium to prevent particulate matter from reaching the orifice [36], so this idea is not entirely unique to the Sciex instrument. Thus, it was felt that such a stream of dry nitrogen gas might serve both purposes for this instrument, that is, to keep particulate matter away from the orifice

and to keep all neutrals, except nitrogen molecules and small amounts of impurities from the nitrogen supply, from entering the post-orifice region.

Therefore, to provide this backstream of nitrogen gas, a two-orifice system was designed that could be pressurized with nitrogen gas. The gas would flow out into the atmospheric region of the source and also into the vacuum region of the mass spectrometer. The first orifice was a 500 μm aperture drilled into a stainless steel plate. This plate served to contain the nitrogen gas and possibly provide some focussing for the ions by electrically "floating" it relative to the ground. The major interface between the atmospheric pressure source region and the vacuum region of the mass analyzer was a thin, replaceable, stainless steel diaphragm with a laser-drilled orifice (20-100 μm diameter) obtained from Precision Aperture [37].

Two skimmer cone lenses were designed to focus ions and to divert excess gas away from the axis of the mass analysis system so that the gas could be more easily pumped by the turbomolecular pump in the normal ion source region. The region after the orifice and before the first conical lens (hereafter referred to as the post-orifice region) is at relatively high pressure. Shahin in 1965 [10] noted the ability to perform some declustering of the background water clusters by accelerating the ions through this region. Fite in 1971 [38] and Levy in 1984 [39] noted the effect of multiple collisions in a supersonic jet on thermodynamic cooling of molecules. Sciex applied similar knowledge to develop an ion lens and gas skimming system to focus ions in a supersonic jet expansion with little increase in their kinetic

energy spread [34]. This can be done by creating a potential difference between the diaphragm and the first conical lens. If this potential difference is sufficiently large, it can add enough kinetic energy to the ion clusters that have formed to cause collisional declustering with neutral molecules in the supersonic expansion. This ability should help reduce clustering in the mass spectra.

Potentials for additional lenses not in the Finnigan system were provided by a power supply designed and constructed by Mark Hail, a fellow research group member. The voltages for these lenses are adjustable by means of ten-turn potentiometers from 0 to ±225 V and are monitored by a 3-1/2 digit LED display.

API Source Configuration for Finnigan 4500

Unfortunately, discharging to the first orifice was not possible with that lens floated because the lens power supply described above did not provide a low output impedance. When a discharge is created between the needle and another surface, the current will seek to follow the lowest path of resistance to ground. Thus the power supply for this floated orifice would need a very low output impedance. If the power supply does not have a low output impedance, a destructive situation can occur in which the current passes through the electronic circuitry of the mass spectrometer seeking a path to ground, and this may result in the damage of circuit components. Since such a power supply was not immediately available, the source design was simplified (Figure 2.3) to include just one electrically grounded orifice

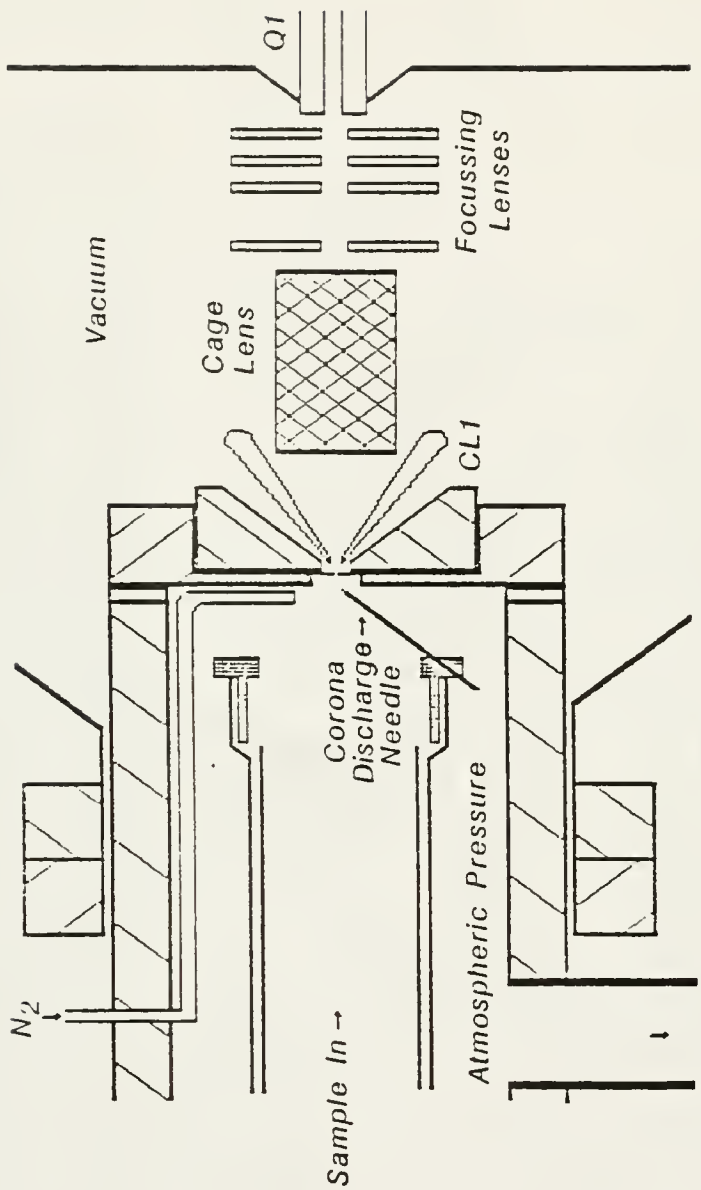

Figure 2.3

API source configuration developed for Finnigan 4500 quadrupole mass spectrometer.

(circumventing the need for the additional power supply). In early studies, a cage electrode was inserted in place of the second conical lens to mimic the lens system of the old Finnigan API source. To solve the problem of orifice clogging and cluster formation a flow of nitrogen gas was directed in a stream from a tube placed near the orifice parallel to the plane of the diaphragm. This design significantly reduced the frequency of orifice clogging when performing direct atmospheric monitoring.

API Source Configuration for Finnigan TSQ 70

To interface this source to the TSQ 70 system, several modifications were made. Figure 2.4 shows a schematic of the current API source design. This configuration again incorporates the less complicated one-orifice system. However, in this design, the seat for the diaphragm has been machined directly into a standard iso-K flange which is a standard vacuum flange for the instrument. This flange is divided into two sections with the inner section (which contains the diaphragm seat) having electrical and vacuum isolation from the outer ring. The outer ring clamps directly onto the TSQ 70 vacuum manifold and makes interchanging sources relatively easy. The first conical lens (CL1 in Figure 2.4) is mounted on the flange with the diaphragm seat. The second conical lens (CL2), a lens directly behind it (the back lens), a cylindrical lens, and three pre-quadrupole focussing lenses are all attached to a grounded mounting plate which replaces the

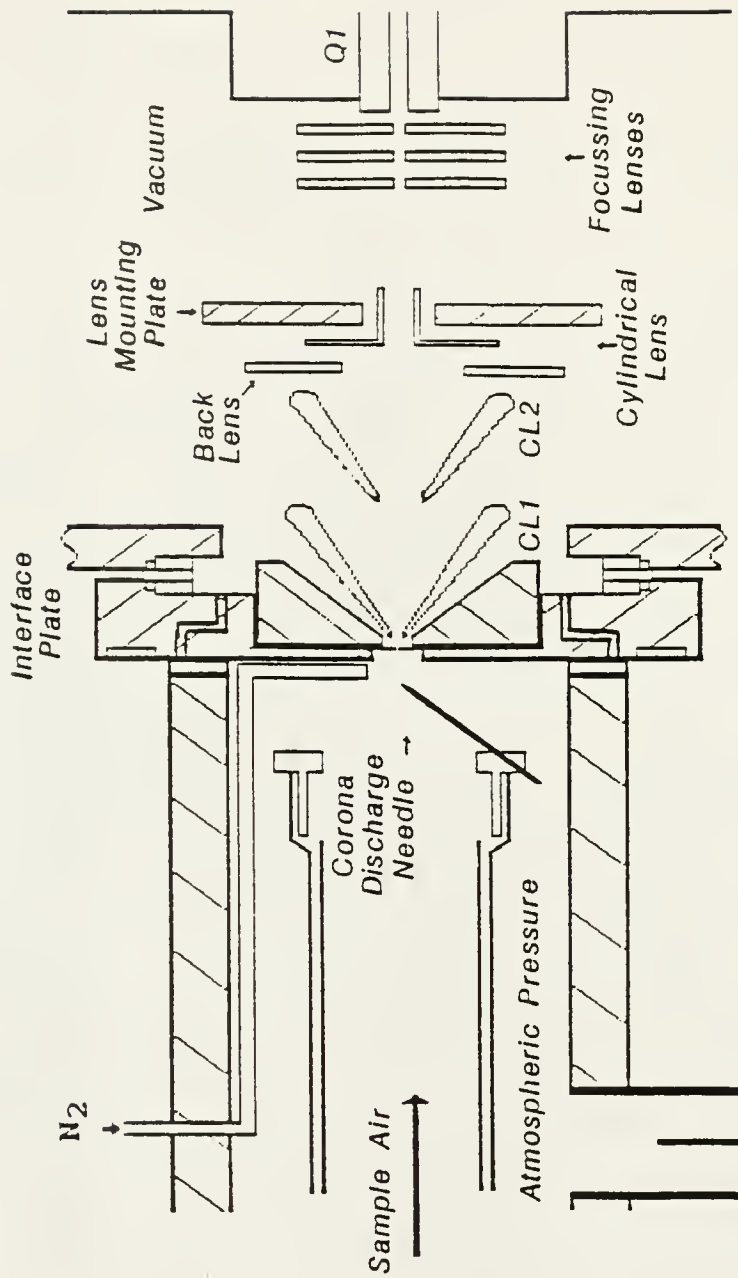

Figure 2.4

API source configuration developed for Finnigan TSQ 70 tandem mass spectrometer.

normal EI/CI source mounting plate and associated lenses. These lens assemblies can be switched by loosening two allen screws.

The API source canister and the associated lens system have been designed to be totally interchangeable with the related Finnigan components. Indeed, the instrument can be changed over from its normal EI/CI operating configuration to an API/MS/MS system, evacuated, and running in about 30 minutes. This increases the potential for the system to be later developed for possible field work.

The most recent addition to the source configuration was the development of a current-regulated, high voltage, low current, corona discharge power supply. This supply is capable of producing "true" (stable and invisible) corona discharges up to ±5000 V and with currents in the range of 0.5 to 5 μA. Figure 2.5 is a schematic for this power supply with the appropriate components labeled. The system is centered around an EMCO [40] 2 to 6 kV adjustable high voltage dc-dc converter. The current from the discharge is monitored and used in a feedback loop to regulate the input voltage into the dc-dc converter. Current and voltage are adjusted with two ten-turn potentiometers. The required voltage to generate a particular current depends upon different environmental factors such as the composition of the gas near the discharge needle, the flow rate of gas past the needle, and the needle-to-orifice distance. If the environment changes, the voltage changes so as to keep the current constant. However, if the dc-dc converter reaches its voltage limit, the system will become unregulated. In this case, the circuitry has been designed so that a

Figure 2.5

Electrical schematic of new current-regulated, high voltage, corona discharge power supply.

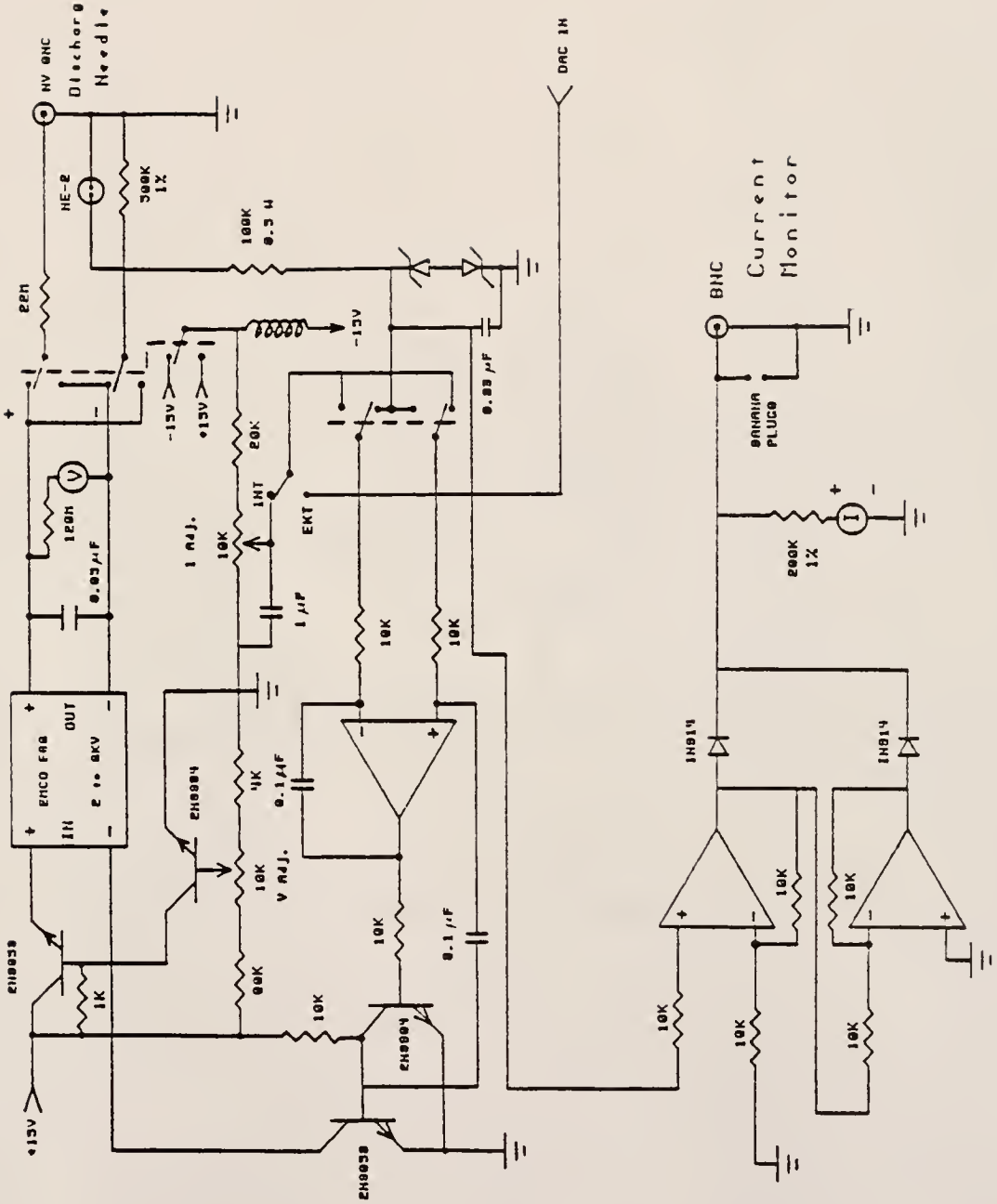
HV BNC
Discharge Needle
HE-2
300K 1%
100K 0.5 W
DAC IN
BNC
Current Monitor
BANANA PLUGS
200K 1%
EMCO F80
OUT
IN
2N3904
2N3053
1K
10K
V ADJ.
90K
0.1 µF
1 µF
I ADJ.
20K
INT
EXT
0.03 µF
0.33 µF
12M
2M
+15V
-15V
1N914
10K

large drop in current will occur to prevent an erratic and possibly dangerous discharge from ensuing.

Figure 2.6 is a schematic of the power supply for electrically floating the orifice from 0 to ±500 V based on an EMCO E05 dc-dc converter. This is a low output impedance power supply that is adjustable by means of a ten-turn potentiometer.

All parts of this source (except the normal Finnigan pre-quadrupole focussing lenses) including the power supplies for the corona discharge and the orifice potential were designed in this laboratory and constructed in the University of Florida Chemistry Department machine, electronics, and glass shops.

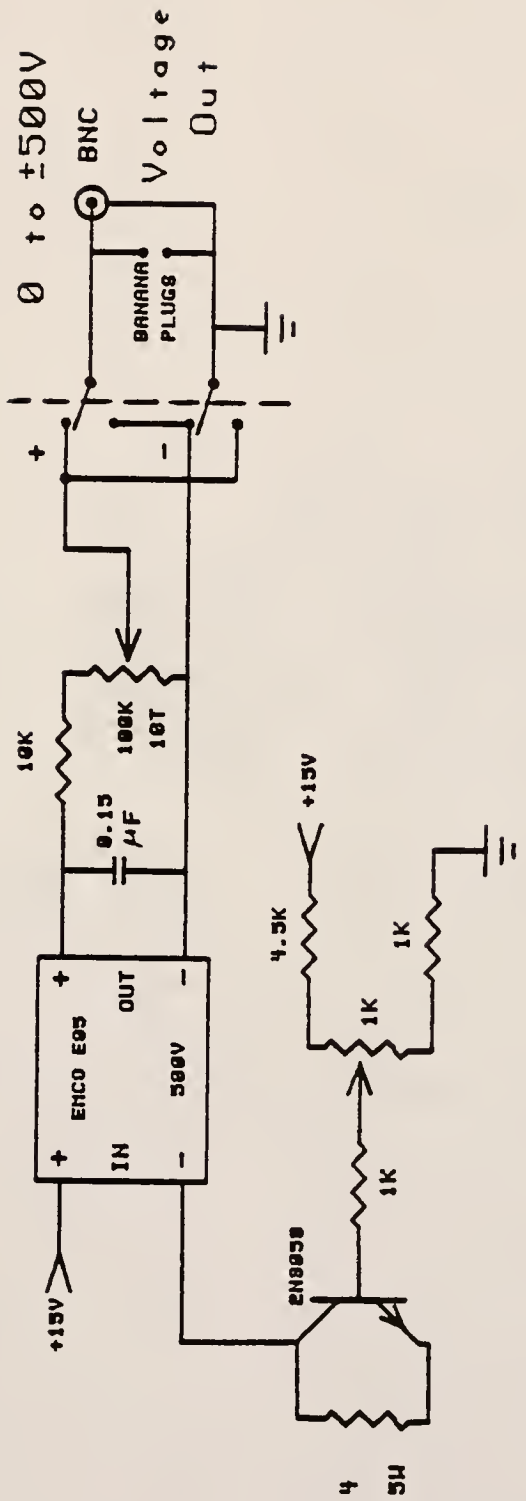

Figure 2.6

Electrical schematic of low impedance ±500V orifice power supply.

CHAPTER 3

EXPERIMENTAL RESULTS AND SOURCE DEVELOPMENT

Results with API Source Configuration for Finnigan 4500 Mass Spectrometer

As was stated in Chapter 2, the API source canister was designed to slide through a modified 6" conflat flange and into the vacuum region of the Finnigan 4500 single quadrupole mass spectrometer. While this design allowed the API source to be compatible with the Finnigan instrument, it caused several problems. The API source was designed to be modular in construction so that design changes could be made to selected parts of the assembly without the need to re-machine the entire API source for each modification made. Unfortunately, at each junction between individual parts of the source canister, there existed the potential for gas leaks from the atmospheric pressure source region, through the junctions in the assembly, into the vacuum region of the mass spectrometer. The source was designed so that the orifice plate was electrically isolated from the source canister (in the initial design, a second orifice flange was to be inserted between, and electrically isolated from, these two flanges). This concept was to be used later in electrically floating this flange. Electrical isolation was accomplished by means of placing am anodized aluminum, ring-shaped spacer between these two components. Vacuum integrity was maintained by two o-rings, one on either side of the aluminum spacer. The

assembly was to be held together with nylon screws. Because of the large force of atmospheric pressure pushing on the orifice flange, the nylon screws could not induce a sufficient counter pressure to maintain vacuum integrity. The nylon screws were replaced by metal screws to obtain vacuum integrity to some degree (although the metal screws did not allow for electrical isolation), and a pressure in the analyzer region of 1.2×10^{-5} torr was eventually obtained for a 20 μm diameter orifice. To calculate the expected pump-down pressure for an aperture of this size, fluid dynamics can be applied to treat each stage of differential pumping separately.

The conductance (C_{visc}) of a 20 μm diameter orifice at atmospheric pressure can be obtained from equation (1) below [41].

$$C_{visc} = 76.6 \times \delta^{0.712} \times (1-\delta^{0.258})^{0.5} \times \frac{A}{1-\delta}, \text{ in } Ls^{-1} \quad (1)$$

where $\delta = (P_2/P_1) < 1$ (where P_1 and P_2 are the respective pressures on either side of the orifice) and A is the surface area of the orifice (in cm^2). If $p_2 << p_1$, then C_{visc} approaches the limiting value for air in equation 2.

$$C_{visc} = 20 \times A, \text{ in } Ls^{-1}. \quad (2)$$

A 20 μm diameter orifice has a surface area of

$$S = \pi r^2 = \pi \times (1.0 \times 10^{-3} \text{ cm})^2 = 3.1 \times 10^{-6} \text{ cm}^2. \quad (3)$$

Thus, for this system,

$$C_{visc} = 20 \times (3.1 \times 10^{-6}\ cm^2) = 6.3 \times 10^{-5}\ Ls^{-1}. \quad (4)$$

The gas throughput, q_{pv}, can be defined as in Equation (5).

$$q_{pv} = C_{visc} \times (P_1 - P_2), \text{ in torr}\cdot Ls^{-1} \quad (5)$$

Substituting for C_{visc}, $P_1 = 760$ torr, and making the approximation that $P_1 - P_2 = P_1$, the gas throughput is found to be 4.8×10^{-2} torr$\cdot Ls^{-1}$. With q_{pv} as defined above and s as the pumping speed of the first turbomolecular pump (330 Ls^{-1}), P, the expected pump-down pressure for the first region of differential pumping, can be found from equation 6.

$$P = q_{pv}/s = (4.8 \times 10^{-2}\ \text{torr}\cdot Ls^{-1})/330\ Ls^{-1} = 1.5 \times 10^{-4}\ \text{torr}. \quad (6)$$

Applying this calculation again, now with $P_1 = 1.5 \times 10^{-4}$ torr, and with an aperture radius (for the aperture between the first and second vacuum chambers), r, of approximately 0.15 cm, the expected pressure in the second region of differential pumping is 6.0×10^{-7} torr. Although, in the calculations above, the nominal pumping speeds for the turbomolecular pumps were used and the effective pumping speeds are somewhat less (because of restrictions), the failure to get the analyzer pressure below 10^{-5} torr seems to indicate that the o-ring design was inefficient in its ability to maintain vacuum integrity.

Nevertheless, even though the vacuum integrity of the source was poor, these pressures were sufficient to perform mass spectrometry. The first ions generated with this source, in a one-orifice (at ground potential) system with no nitrogen jet, were cluster ions of the form $H(H_2O)_n^+$ (n = 5 (m/z 91) to n = 21 (m/z 109)), $(CH_3)_2COH(H_2O)_n^+$ [n = 3 (m/z 113) to n = 8 (m/z 203)], $[(CH_3)_2COH]_2(H_2O)_n^+$ [n = 2 (m/z 153) to n = 4 (m/z 189)], generated by inducing a flow of laboratory air past the discharge region (Figure 3.1). The acetone ions are from residual solvent left after source cleaning, which vaporizes off the source walls and diffuses to the discharge region because of the lack of a nitrogen jet. These ions were of very low intensity, and the lack of cluster ions with higher m/z values probably results from a lens tuning effect.

Without the nitrogen gas or an electrically floated orifice, this source configuration had only limited abilities for declustering. Figure 3.2 shows the resulting mass spectra (all normalized to the same intensity) when the potential difference between the grounded orifice and the first conical lens was changed from 2 to 8 V. While the effect is not dramatic, the slight decrease in the cluster ions with higher m/z values relative to those with lower m/z values is apparent.

However, even when analyzing vapor samples injected into a nitrogen stream (no direct atmospheric monitoring), clustering was still a problem. Figure 3.3 (a) - (c) shows mass spectra obtained for representative compounds which undergo charge exchange ionization in the API source, carbon disulfide (MW 76), benzene (MW 78), and toluene (MW 92), respectively. Carbon disulfide forms almost exclusively the

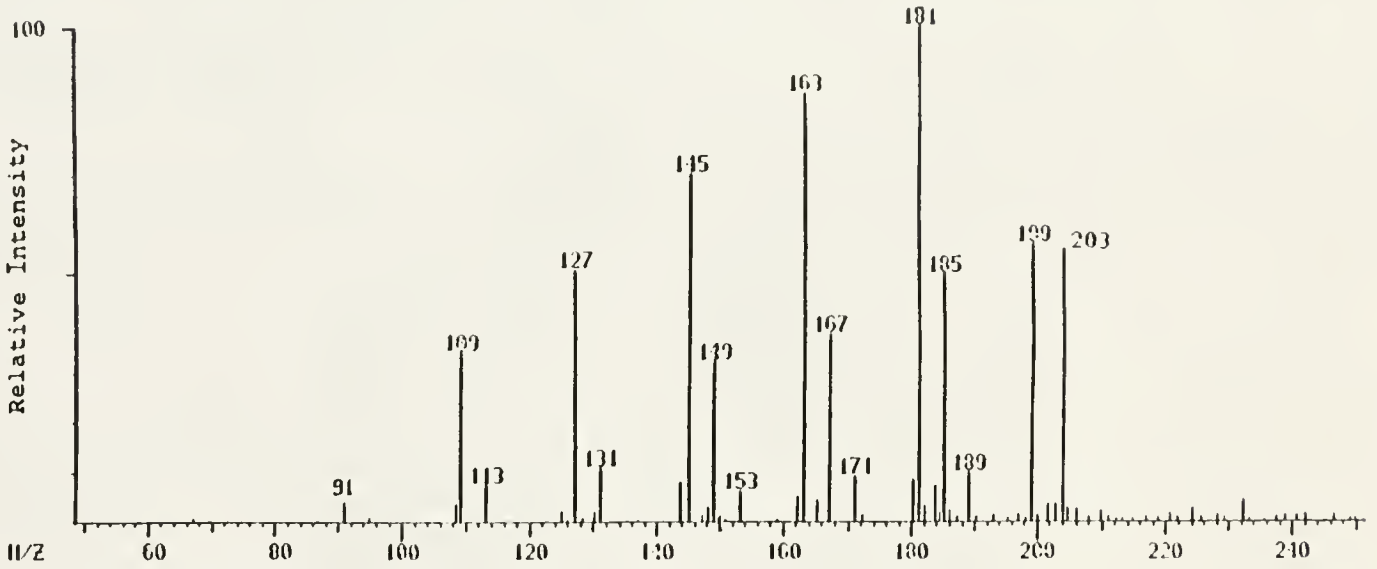

Figure 3.1

Mass spectrum of the first API ions generated with the new API source.

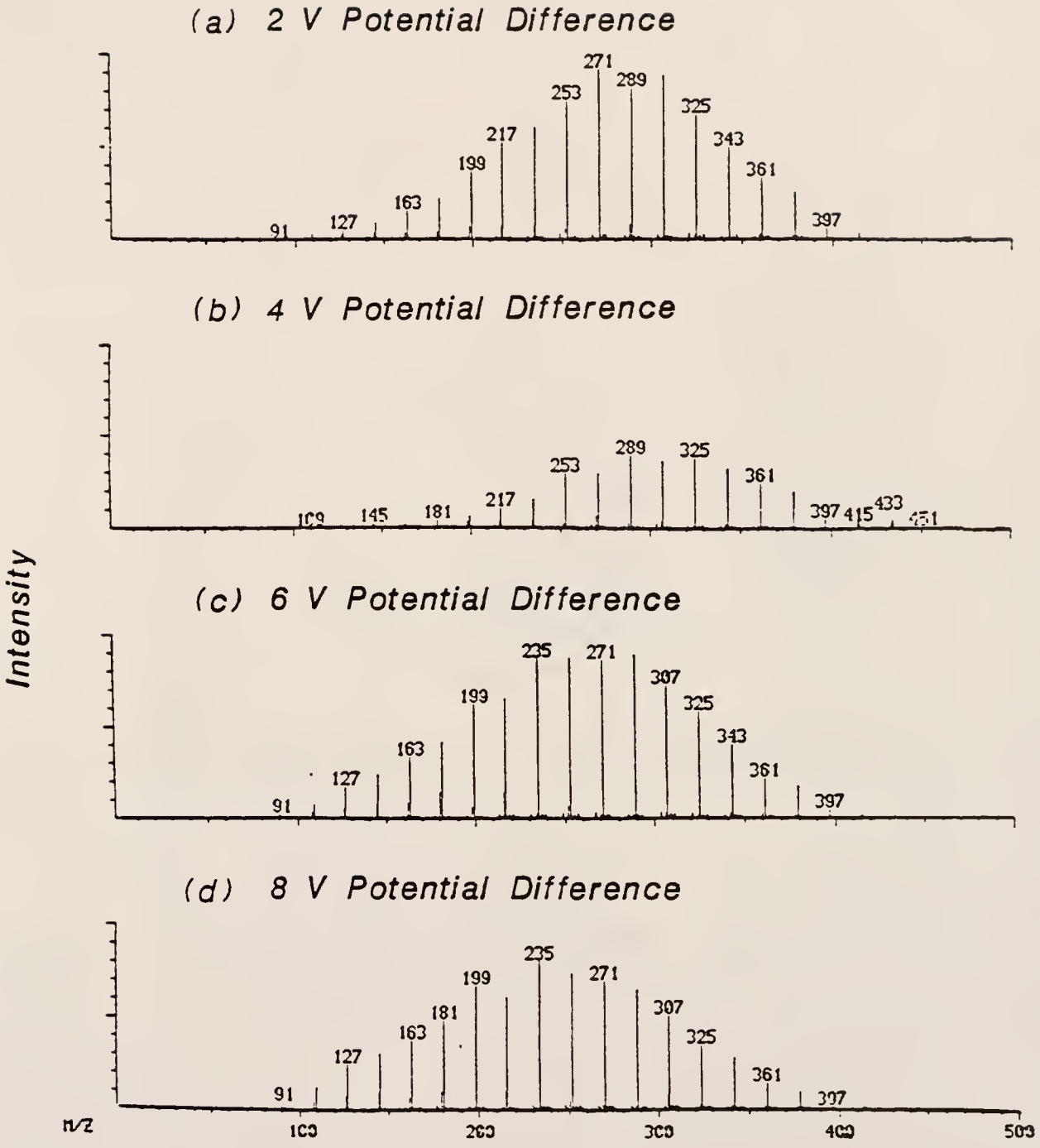

Figure 3.2

Declustering in post-orifice region with grounded orifice, no declustering gas, and with the potential of the first conical lens at (a) -2 V, (b) -4 V, (c) -6 V, and (d) -8 V.

Figure 3.3

API/MS of compounds that undergo charge exchange ionization in a pure nitrogen stream (a) carbon disulfide, (b) benzene, and (c) toluene.

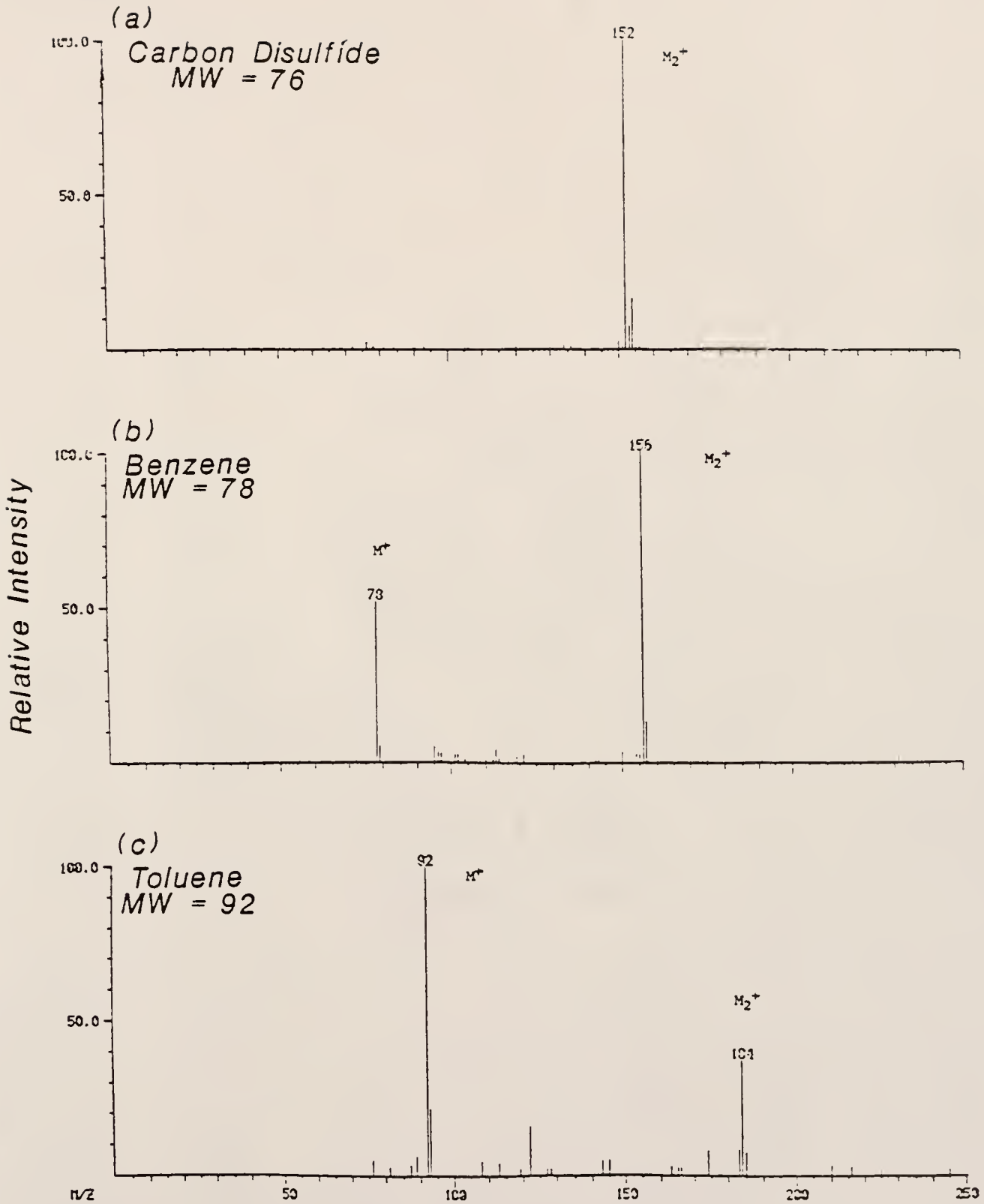
(a)
Carbon Disulfide
MW = 76
100.0
50.0
152
M_2^+
(b)
Benzene
MW = 78
100.0
50.0
156
M_2^+
M^+
78
(c)
Toluene
MW = 92
100.0
50.0
92
M^+
M_2^+
184
Relative Intensity
m/z
50
100
150
200
250

M_2^+ cluster ion. Benzene and toluene form both the M^+ molecular and the M_2^+ cluster ions. Figure 3.4 (a) - (c) shows mass spectra obtained for representative compounds which undergo proton transfer ionization in the API source, acetone (MW 58), ethyl acetate (MW 88), and methanol (MW 32), respectively. Acetone and ethyl acetate form both the $(M+H)^+$ pseudo-molecular and the $(M_2+H)^+$ cluster ions. The ions formed from methanol display severe clustering and are of the form $[M+H(H_2O)_n]^+$ (n = 2 - 5), $[M_2+H(H_2O)_n]^+$ (n = 0 - 2), $[M_3+H(H_2O)_n]^+$ (n = 0 and 1), and $(M_4+H)^+$.

Adaptation of the API Source to the Finnigan TSQ 70 Mass Spectrometer

TSQ 70 Characteristics

This mass spectrometer has some unique characteristics, most of which have proven beneficial to performing source development on it. This instrument is almost totally under microprocessor control. All valves, pumps, heaters, and most importantly lenses and quadrupoles can be controlled by "firmware" (program code stored on erasable, programable read-only memory (EPROM) chips) which accesses 5 single board minicomputers located on the instrument. This allows sophisticated tuning and optimization to be performed with relative ease. The instrument is differentially pumped by two 330 Ls^{-1} turbomolecular pumps, which can reach a vacuum suitable for mass spectrometry in less than 15 minutes (with no additional gas loads on the system). The vacuum manifold is shaped as a rectangular box, with a thick, glass lid, which presses down on two o-rings (one each for the

Figure 3.4

API/MS of compounds that undergo proton transfer ionization in a pure nitrogen stream (a) acetone, (b) ethyl acetate, and (c) methanol.

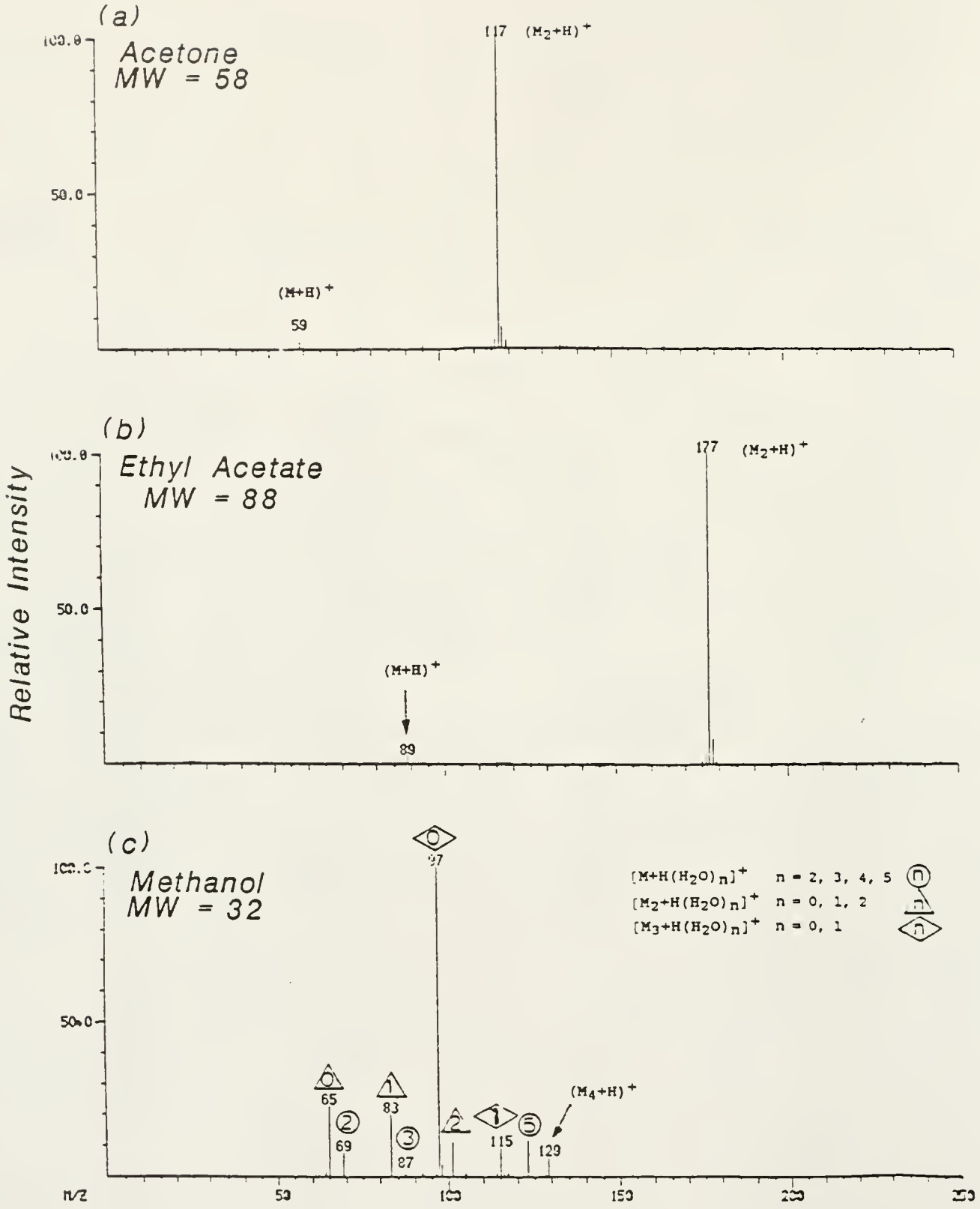
(a)
Acetone
MW = 58
117 (M2+H)+
(M+H)+
59
(b)
Ethyl Acetate
MW = 88
177 (M2+H)+
(M+H)+
89
Relative Intensity
(c)
Methanol
MW = 32
97
[M+H(H2O)n]+ n = 2, 3, 4, 5
[M2+H(H2O)n]+ n = 0, 1, 2
[M3+H(H2O)n]+ n = 0, 1
(M4+H)+
65
69
83
87
115
129
m/z
50
100
150
200

differentially pumped ion source and analyzer sections) to maintain a suitable vacuum. Vacuum flanges on the instrument are standard 6" diameter iso-K flanges which clamp onto the manifold using an o-ring between the flange and the manifold to maintain vacuum integrity. All lenses and quadrupoles are mounted on an optical rail for easy maintenance (and in this case easy modification) and are each held in place by only one or two screws. The normal EI/CI ion source and lens assembly mounts to this optical rail in the first differentially pumped chamber of the mass spectrometer, and is removable by loosening two allen screws.

Source Modifications and Ion Optical Modeling

In order to interface the source canister to the TSQ 70 vacuum manifold, a new adapter flange was needed to replace the conflat flange compatible with the Finnigan 4500. Since all the vacuum ports on the TSQ 70 vacuum manifold used iso-K type flanges, it was necessary to base the adapter flange on this standard. With the freedom to design a new flange, it was also decided to alter the design of the source to reduce the problems with vacuum integrity. This modified source design moves all the junctions between source parts outside of the vacuum manifold of the mass spectrometer by machining the diaphragm seat directly into the iso-K flange. Thus, the only possible locations for a gas leak are the knife-edge seal on the orifice and the o-ring between the iso-K flange and the vacuum manifold (which is in the normal instrument configuration). The rest of the canister attaches to the adapter flange by four bolts and can be easily removed without breaking vacuum. When the orifice gets clogged, a jet of high pressure

gas (such as that from a can of common laboratory freon, or from compressed nitrogen, or air) can be used to clear the blockage. Later, the flange was re-designed so that in the final configuration it was divided into two concentric sections, the inner section (containing the diaphragm seat) being electrically isolated from the outer section.

To test the vacuum integrity of this source, a diaphragm containing a 70 μm diameter orifice was installed. Using the equations found earlier in this chapter, the theoretical pump-down pressures, for the first and second differentially pumped-regions of the mass spectrometer are calculated to be 1.8 x 10-^{3} torr and 7.2 x 10^{-6} torr, respectively. The actual pump-down pressures were found to be 2.0 x 10^{-3} and 3.0 x 10^{-5}. Therefore it appears that this interface serves to maintain vacuum integrity.

An ion optical modeling program, SIMION [42], that has been modified to run on a PC/AT microcomputer [43], was used to model the lens system for the API/MS/MS instrument configuration. This approach has proven advantageous in the design and development of the lens system for interfacing the API source to the mass spectrometer. Two examples of the use of this program are given below, although it should be pointed out that this program does not take into consideration the multiple inelastic collisions that the ions incur in the relatively high pressure post-orifice region. Therefore, the actual lens voltages used for maximum ion transmission can be very different from the values that give the best transmission in the collision-force model used by the SIMION program. Despite this, the model is very useful for the

physical design of the lenses themselves, rather than predicting the actual lens potentials.

To simplify the system and facilitate testing, the source has been used in the one-orifice configuration. One characteristic of the TSQ 70 mass spectrometer which turned out to be a disadvantage to the adaptation of the API source to the mass spectrometer was the electrically grounded source mounting plate. Since the API source has been installed on the front of the mass spectrometer, this grounded plate resides between the API source and the mass analyzer. This plate holds the normal EI/CI ion source assembly, including the pre-quadrupole lenses. Since the positioning of these pre-quadrupole lenses is critical, it was desired to use this same mounting plate with a modified lens block which held only the pre-quadrupole lenses and had the excess metal removed. Unfortunately, there is only a 3/4" aperture in this mounting plate through which the API generated ions are to be focussed.

Figure 3.5 (a) shows the SIMION representation of the lens system for the API source interfaced to the TSQ 70 mass spectrometer. Figure 3.5 (b) shows the equipotential lines on each of the lenses and the lens mounting block. Because the TSQ 70 lens mounting plate is electrically grounded, relatively low energy positive ions which enter even slightly off-axis are repulsed by the associated field. Figure 3.5 (c) shows the ion trajectories for an ion with a m/z value of 181, an initial energy of 0.2 eV, and with initial angles of 0, 10, and 20 degrees off the center axis. Figure 3.6 (a) shows the addition of a cylindrical lens to penetrate the field produced by the grounded source

Figure 3.5

Ion optic modeling of lens configuration for API source on TSQ 70 mass spectrometer showing (a) the representation of this lens system with the SIMION program, (b) with potential contours (at values 10% more positive than lens voltages), and (c) with representative ion trajectories.

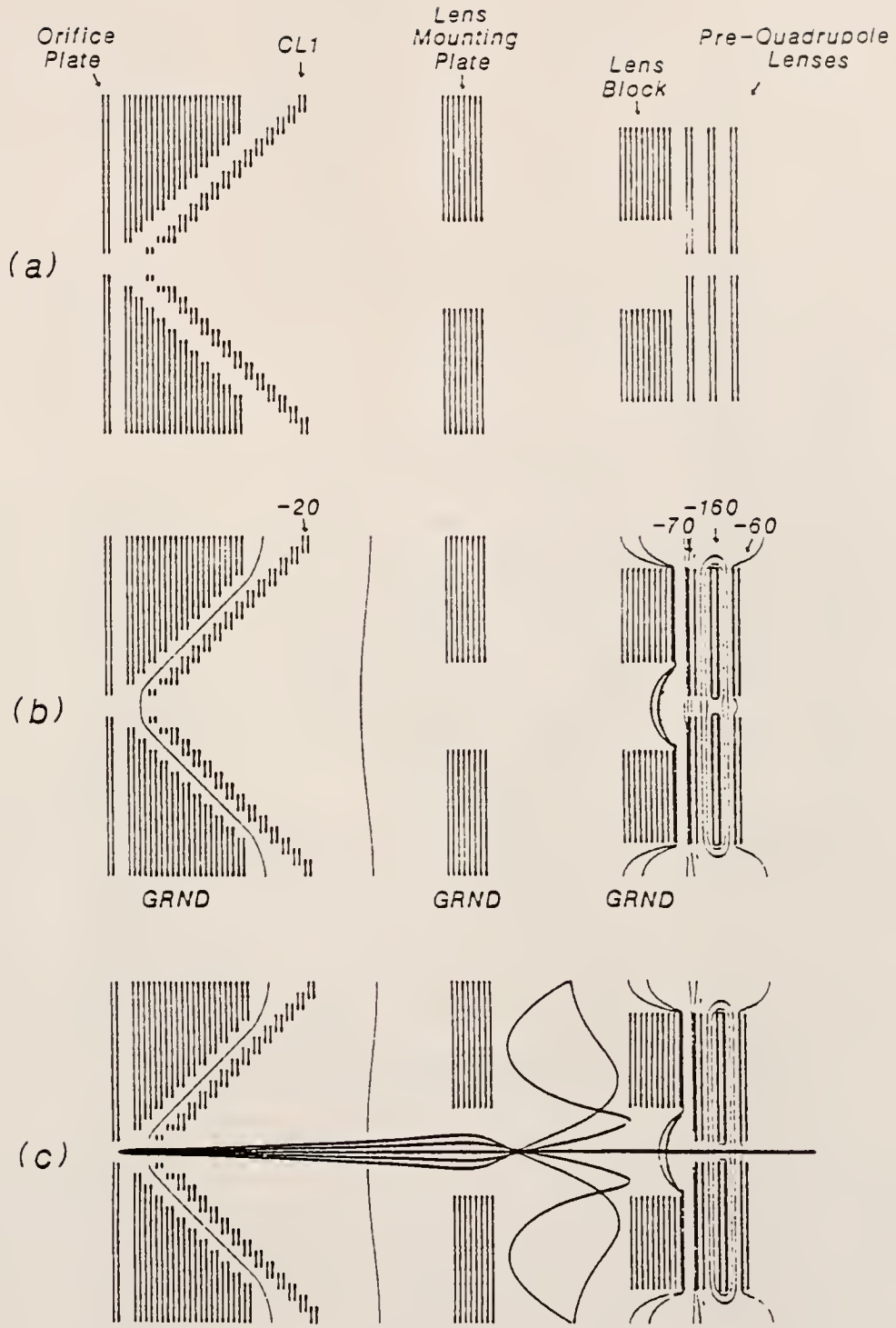
Orifice Plate
CL1
Lens Mounting Plate
Lens Block
Pre-Quadrupole Lenses
(a)
-20
-160
-70
-60
(b)
GRND
GRND
GRND
(c)

Figure 3.6

Ion optic modeling of lens configuration for API source on TSQ 70 mass spectrometer with the addition of a cylindrical lens showing (a) the representation of this lens system with the SIMION program, (b) with equipotential contours (for potentials of 10% more positive than the lens potential), (c) with representative ion trajectories for -5 V, and (d) with representative ion trajectories for -30V.

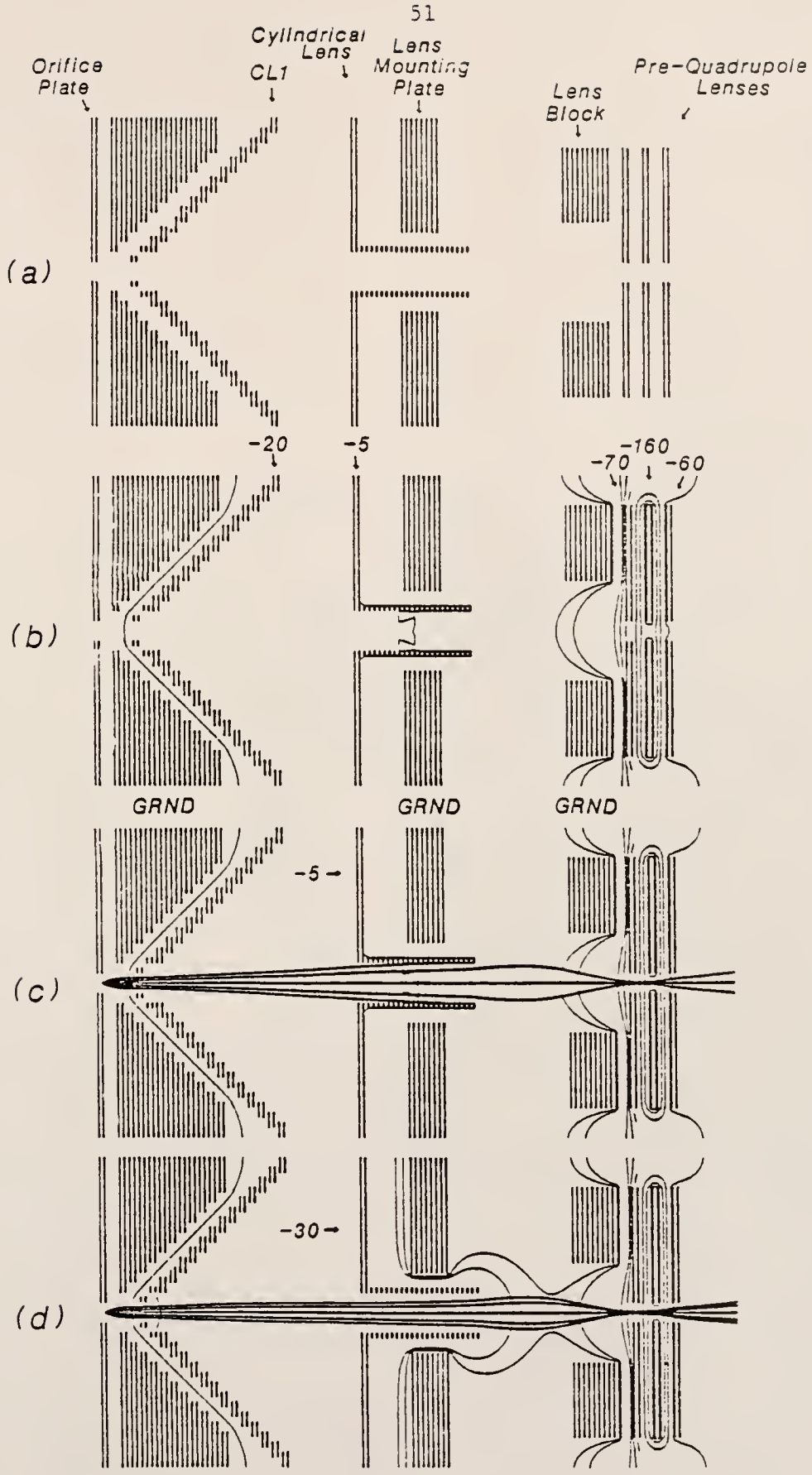
Orifice Plate
Cylindrical Lens
CL1
Lens Mounting Plate
Lens Block
Pre-Quadrupole Lenses
(a)
-20
-5
-160
-70
-60
(b)
GRND
GRND
GRND
-5
(c)
-30
(d)

mounting plate. Figure 3.6 (b) shows the equipotential contours for a cylindrical lens potential of -5 V. This improves the transmission of ions with m/z 181, initial ion energy of 0.2 eV, and initial angles of 0, 10, and 20 degrees off the center axis. With this potential, ions ≤10 degrees off the center axis are focussed through the lens system. In Figure 3.6 (d) the potential on the cylindrical has been increased to -30 V. By plotting the trajectories for ions with the same initial conditions as above, it can be seen that ions with initial angles of ≤20 degrees off the center axis are focussed through the lens system to the quadrupoles.

To aid in the focussing of ions and the pumping of the excess gas, a second conical lens (CL2) was added to the design. In order to implement this lens as a focussing lens element, a plate lens with a cylindrical hole is required directly behind the 2nd conical lens. The SIMION program was used to model the effect of the aperture size of a lens (the back lens), immediately behind CL2, on the focussing of ions (now with a higher energy (≈ 5 - 10 eV) after being accelerated through the first conical lens) through CL2 and into the cylindrical lens. Figure 3.7 (a) is the SIMION representation of a portion of the lens assembly consisting of CL2, and the back, and cylindrical lenses with potentials of -5 V, -50, and -150 V, respectively. Figure 3.7 (b)-(d) shows the effect of small (0.25" diameter), medium (0.50" diameter), and large (0.75" diameter) apertures on ion trajectories for ions with initial angles of 25, 20, 15, 10, and 5 degrees off the center axis. For a small aperture (b), ions with initial angles ≤10 degrees off axis are focussed through the cylindrical lens. For medium

Figure 3.7

Ion optic modeling of the effect of the aperture size of the back lens on ions passing through a conical lens showing (a) the SIMION representation of those lenses and the associated potential contours (10% more positive than the associated lens), and ion trajectories with (b) a small aperture, (c) a medium aperture, and (d) a large aperture.

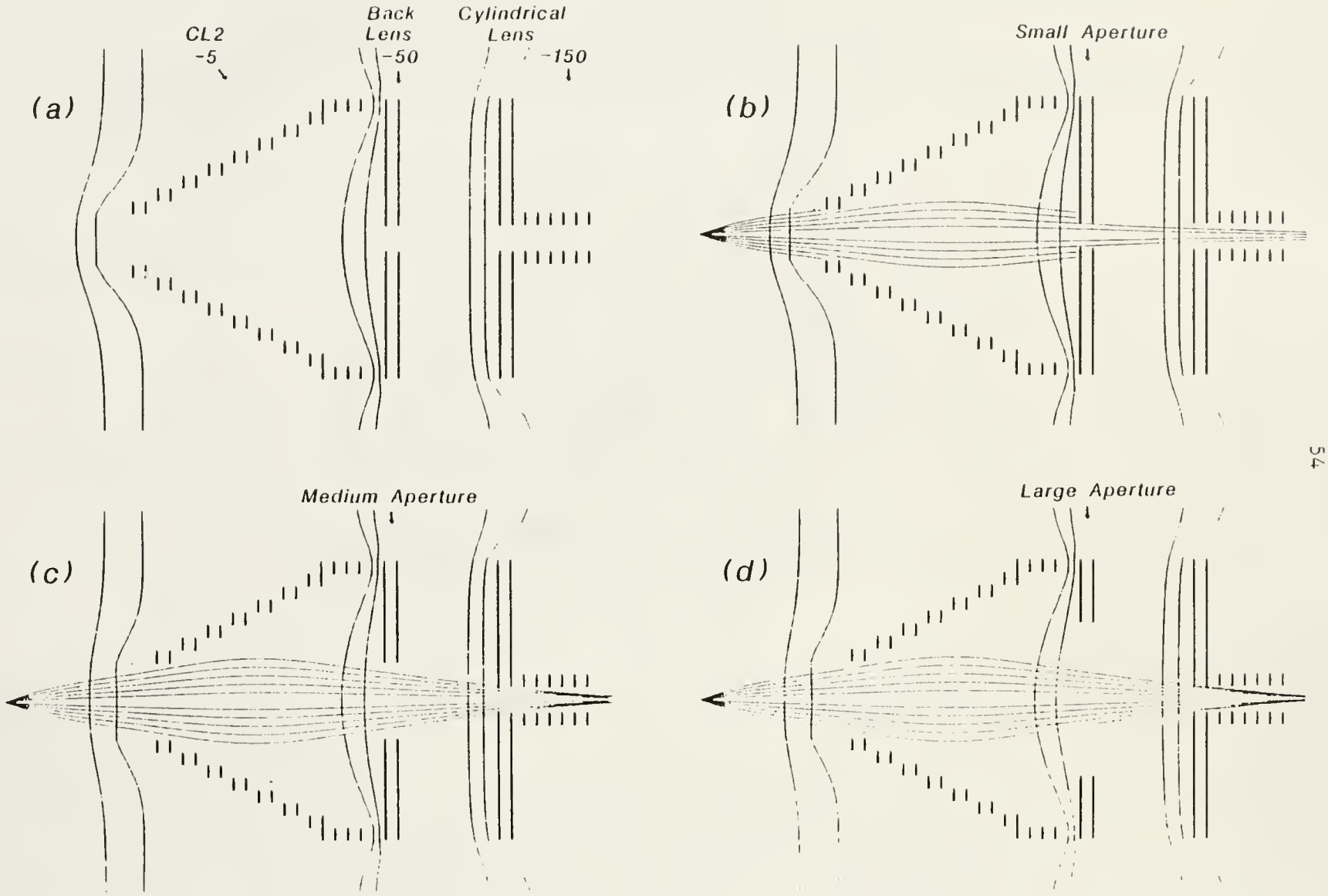
(a)
CL2
-5
Back
Lens
-50
Cylindrical
Lens
-150
(b)
Small Aperture
(c)
Medium Aperture
(d)
Large Aperture

(c) and large (d) apertures this value improves to 20 and 25 degrees, respectively. However, if this back lens is removed completely (not shown), the potential field of the cylindrical lens is not capable to cause sufficient convergence of the ions to allow transmission through the pre-quadrupole lenses.

The re-design of the source with a new adapter flange and the use of the SIMION program to model the lens system proved advantageous in developing an operable API source. By moving all junctions between source canister parts outside of the vacuum system, it became practical to use a 70 μm diameter orifice. Ion optical modeling saved much effort and time developing two new lenses for the system, a cylindrical lens to penetrate the potential field generated by the grounded source mounting plate and the optimum aperture size for the lens immediately following CL2.

Gas Flows

Using the equations presented earlier in this chapter, the conductance (C_{visc}) of a 70 μm diameter orifice is calculated to be 7.7×10^{-4} Ls^{-1} or 46.2 $mL \cdot min^{-1}$. To measure the rate of gas flow through the orifice a common laboratory bubble meter was hooked up to the exhaust port of the mechanical backing pump for the turbomolecular pumps. Since one mechanical pump serves as the backing pump for both turbomolecular pumps, any gas that enters the system must exit through this port. With the orifice (70 μm diameter) plugged, the flow rate, F_o, was $<<$ 1 $mL \cdot min^{-1}$. When the orifice was unplugged, this flow rate increased to 45.3 $mL \cdot min^{-1}$. This would indicate a flow rate through the orifice of 45.3 $mL \cdot min^{-1}$, which agrees within the experimental

error (the actual size of the orifice is 70 μm ±10%) for the calculated conductance.

For the measurement of the flow rate through the glass tube used for direct atmospheric sampling, the bubble meter was modified such that air was drawn through the bubble meter by attaching, with flexible tubing, the top of the bubble meter to the glass sampling tube. Both the orifice and the sampling fan served to draw air through the sampling tube. Because the flow rates through the orifice and through the sampling fan are fixed, any additional gas loads would reduce the flow through the sampling tube. With no flow of gas for the nitrogen jet, the sampling flow rate was found to be 77.4 $mL \cdot min^{-1}$. With the nitrogen gas jet on, the flow was found to be 74.8 $mL \cdot min^{-1}$. Therefore, the flow rate of the nitrogen jet (flowing out of a 1/16" tube) was 2.6 $mL \cdot min^{-1}$. This is the common configuration for the instrument while performing direct atmospheric analysis.

Discharge Power Supply

As was stated in the second chapter, the discharge power supply which was used for most of this work was a Bertan 205A-05R voltage-regulated power supply. The discharge from which ions were detected (with this power supply), was visible (violet in color), unstable to varying degrees, had a current >20 μA, and produced an ion signal which was extremely noisy. At times this discharge would become very unstable and erratic and would change to a bright white color. Since the power supply regulated the voltage, any change in resistance in the path of the discharge (such as those caused by changes in the gas flow rate or composition) would cause a change in the current and thus a

change in the ion intensity. Tuning was performed by scanning at a much slower rate (>1 s/scan) than is normally required for quadrupole mass spectrometry and still was, at best, difficult.

A true corona discharge is invisible, stable, and of much lower current than the discharge obtained above [34]. The second chapter discusses the power supply that was designed and built to generate such a discharge. The corona discharge obtained with this current-regulated power supply meets the aforementioned requirements, with a stable, selectable current of 0.5 to 4.5 μA. The voltage required to produce the corona discharge is dependent on the current desired, the flow rate and composition of gases in the discharge region, and the needle-to-orifice distance, but usually was on the order of 3 to 4.8 kV. With this stable discharge, the ion signal was significantly less noisy, and therefore, tuning could be performed with automated tuning procedures and at a much faster rate.

Orifice Potential

With the present design it is possible to have the orifice electrically grounded or floated by a ±500 V, low-impedance power supply (see Chapter 2). Initial experiments were performed with the orifice placed at instrument ground by connecting its electrical lead directly to the instrument manifold. Later, to improve sensitivity, the orifice was electrically floated at up to +150 V.

Experimental Physical Parameters of API Source and Mass Spectrometer

Initial Ion Energy and Energy Spread

An experiment was set up such that the intensity of the ions generated by the API source was monitored as the voltage on the second conical lens (CL2) was varied, while keeping the orifice at ground potential (0.0 V) and the first conical lens (CL1) at -4.4 V relative to ground.

Figure 3.8, a "stopping-potential curve", is a plot of the ion intensity (scale on left-hand y axis) vs. the potential of lens CL2 (with a potential of CL1 = -4.4 V), together with the first derivative of this curve (intensity scale on right-hand y axis). The first derivative provides (a) the potential that will stop an ion with the average kinetic energy (i.e. the peak of the first derivative curve) and (b) the kinetic energy spread of the ions (i.e. the peak width at half height). A simple numerical method was employed to find the first derivative, in which the difference of consecutive y axis values relative to the difference of consecutive x axis values ($\Delta y/\Delta x$) was plotted vs. the average of their corresponding pair of x axis values. The difference curve that was generated yielded values of -3.8 V and 0.8 eV for the potential required to stop an ion with the average ion kinetic energy and the ion kinetic energy spread, respectively.

Since the orifice is at 0.0 V (ground potential), the first conical lens is at -4.4 V, and positive ions were analyzed, the ions should be accelerated by 4.4 eV between those two components. If this were true, it should take a potential of 0.0 V on the second conical lens to

Figure 3.8

A stopping potential curve for the 2nd conical lens with a electrically grounded orifice and the superimposed associated differential curve showing the potential required to stop an ion with the average energy and the energy spread of the ions.

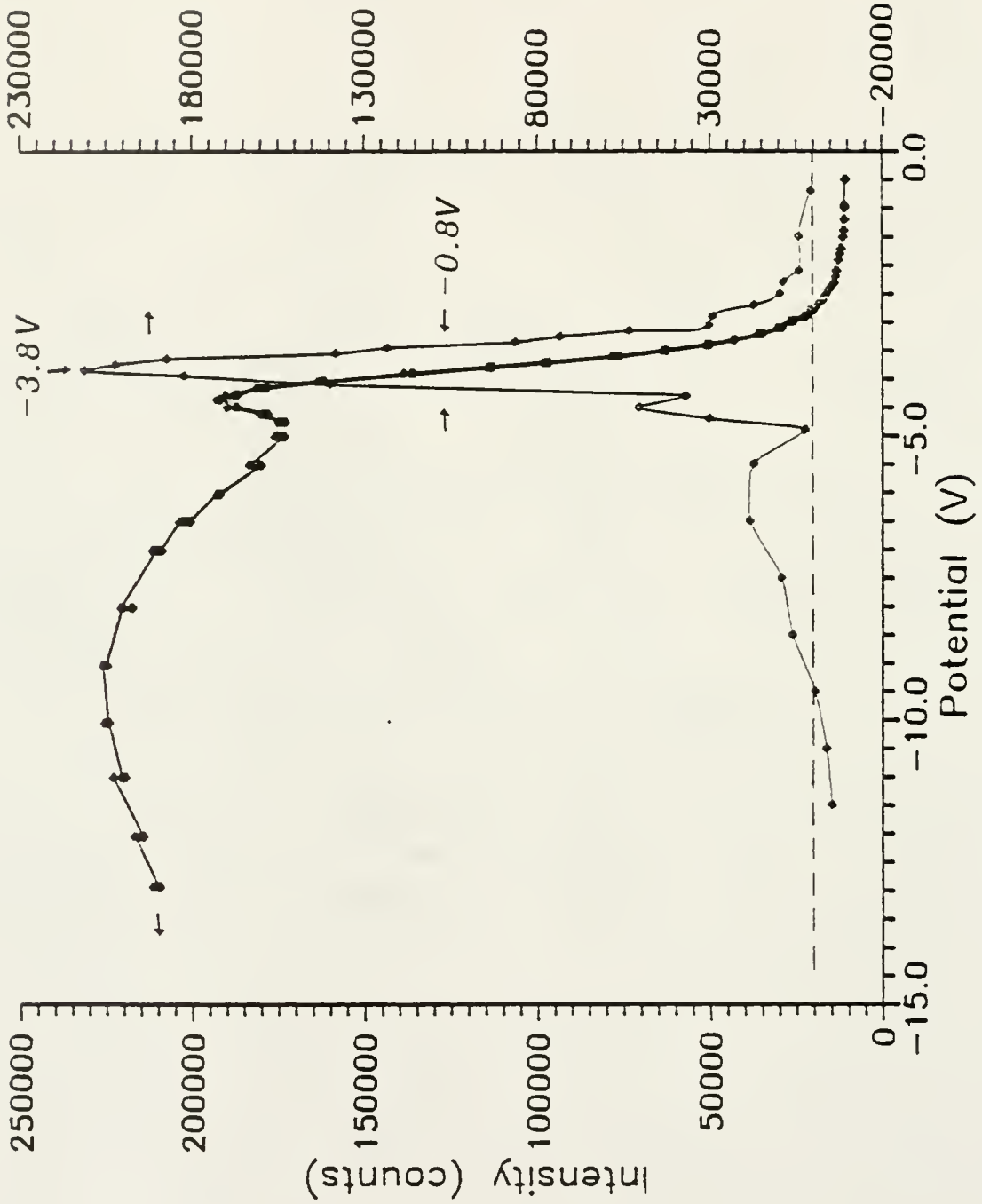
Intensity (counts)
250000
200000
150000
100000
50000
0
Differential (counts/V)
230000
180000
130000
80000
30000
−20000
−3.8V
−0.8V
0.0
−5.0
−10.0
−15.0
Potential (V)

"stop" the ions (i.e. decelerate the ions by 4.4 eV, to 0.0 eV of energy). A simplistic model for this system is displayed in Figure 3.9 (a). The ion, transversing the potential field, can be thought of as a ball rolling down a slope. If the ball is released down the slope from a resting position, it will be accelerated (i.e. gain in kinetic energy) due to gravity by falling some height, h, and therefore it will take a height equal to h to decelerate the ball (reduce its kinetic energy) until it stops again. The experimental results seem to indicate a situation more like Figure 3.9 (b), in which the ball is stopped by a slope that is only a fraction of the initial height; that is, it takes a smaller decelerating energy than expected to stop the ball. Barring other factors, if the ball were released from the same initial height as in Figure 3.9 (a) it should not be stopped on the opposite slope but should continue on out of the system (Figure 3.9 (c)). Likewise, barring other factors, the ion would be expected to pass through the decelerating field provided by CL2 instead of being stopped. The experimentally determined voltage needed to stop the ions was found to be -3.8 V (a deceleration of 0.6 eV from the CL1 to CL2 lenses); therefore, the ions must have been accelerated by only 0.6 eV on their way to the first conical lens. This could occur if the ions were generated at a potential field 0.6 V more positive than that of the first conical lens (i.e., at -3.8 V with respect to ground). This is analogous to the ball starting at a very low height. However, it is known that the ion is formed on the atmospheric side of the orifice (i.e. the ball is starting all the way up the slope). A second possible reason is that the ion's ability to increase its kinetic

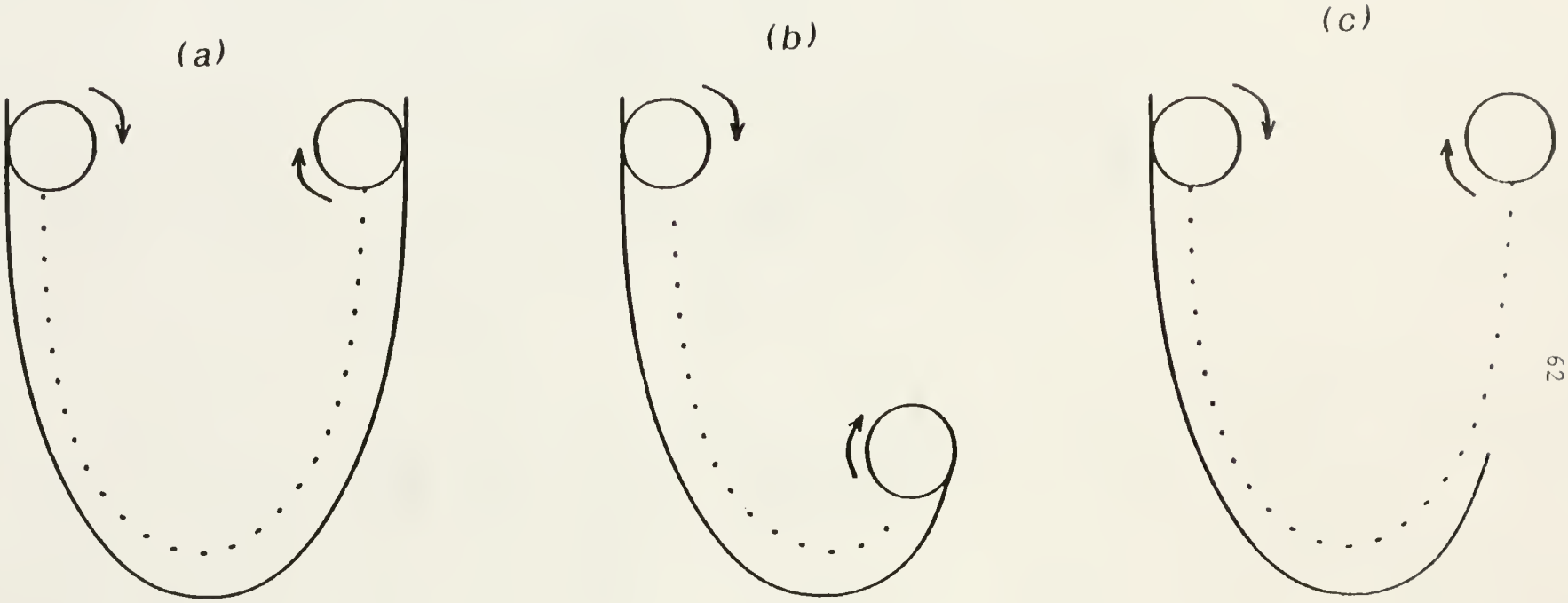

Figure 3.9

Schematic of a simplistic model to explain results of initial ion energy study. Response of ball (a) in a frictionless system, (b) experimentally observed, and (c) the expected response with the conditions in (b).

energy was being retarded. If the ball was rolling down a surface where the friction was large, the ball's acceleration would be slowed by the friction; that is, the friction would retard the ball from increasing its kinetic energy. In the post-orifice region, a supersonic jet expansion occurs as the ions and molecules go from the atmospheric side of the orifice to the vacuum side of the orifice. Since near the orifice the ions and molecules are still at a relatively high pressure (several mtorr), the bulk gas molecules undergo a lthermodynamic cooling of their translational energy through multiple collisions with each other in the supersonic jet expansion [39]. As the ions exit the orifice, they are translationally cooled along with the bulk gas molecules. The inelastic collisions the ions have with the translationally cool molecules also allows the rotational and vibrational motion of the ions to be transferred to the translationally cool molecules. Thus, the ions do not experience the full accelerating potential field because of collisional energy exchange with the more abundant neutral molecules which remain unaffected by the potential field. Further downstream in the jet, the number of collisions between the ions and the molecules decreases and this collisional cooling no longer occurs.

Figure 3.10 is stopping-potential curve (plotted on the left-hand y axis and its associated differential (plotted on the right-hand y axis) determined for CL2 with an electrically floated orifice with a potential of +120 V and with a potential for CL1 of +81.9 V. The potential of CL2 required to decelerate the average ion to rest orifice is approximately 89 V and the energy spread of the ions is

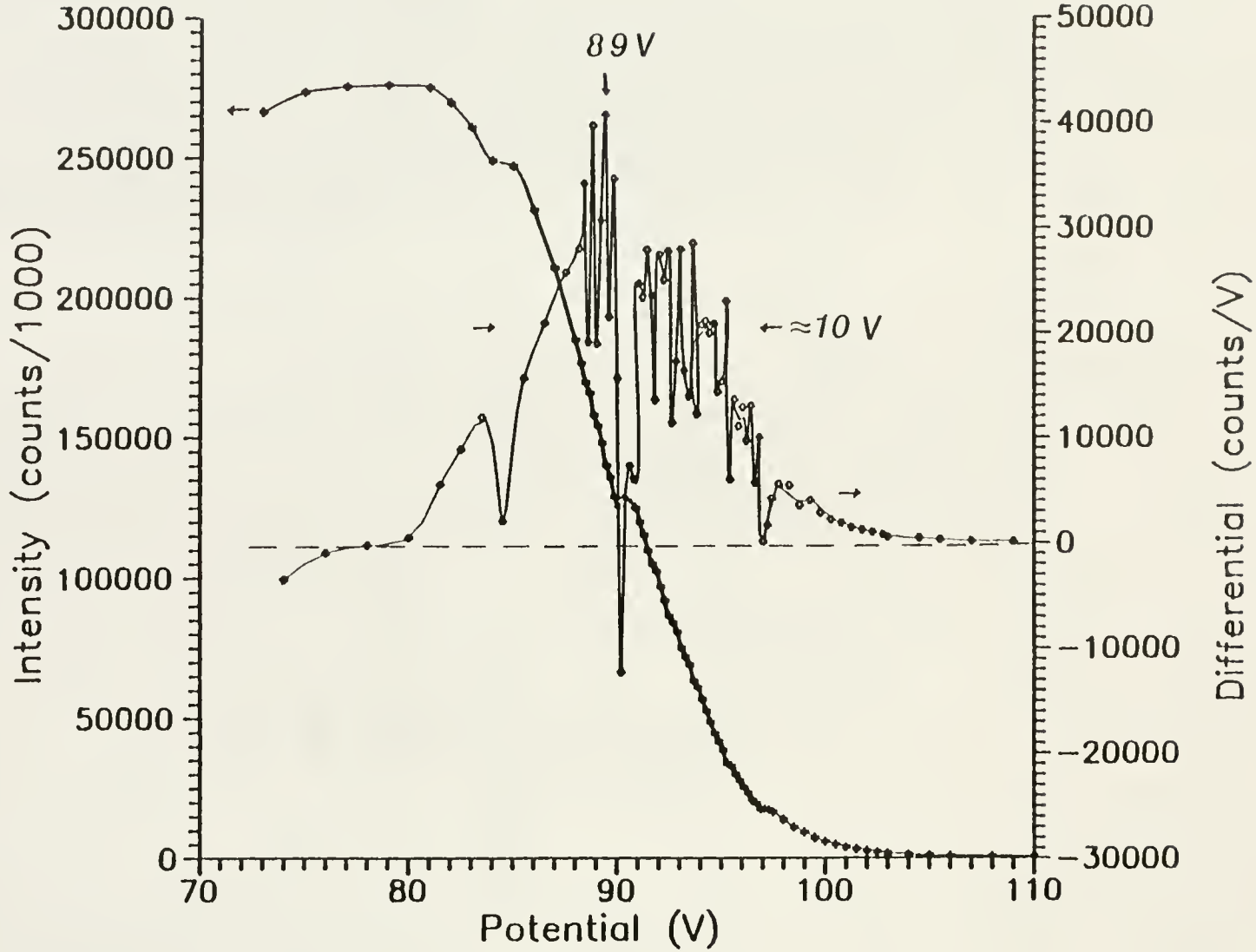

Figure 3.10

A stopping potential curve for the 2nd conical lens with a electrically floated orifice (+120 V) and the superimposed associated differential curve showing the potential required to stop an ion with the average energy and the energy spread of the ions.

approximately 10 eV. Because it required only 7.1 V to decelerate the average ion to rest, the ion therefore could only have been accelerated by 7.1 eV from the orifice to CL1 despite the 38.1 V potential difference between these components. At these higher voltages, however, there is a much greater spread in the ion energies.

Needle-to-orifice Positioning

For a discharge provided by a voltage-regulated power supply, the position of the needle was critical to the production of even a semi-stable discharge and to the number of ions which were detected by the mass spectrometer. Figure 3.11 (a) (all dimensions in inches) is a schematic representation of the needle position relative to the orifice and the orifice plate for which the greatest intensity of ions were obtained. Characteristically, the discharge was formed across the face of the orifice to the opposing sharp edge of the orifice plate. When the needle was moved across the face of the orifice towards the center axis of the orifice (Figure 3.11 (b)), the ion intensity decreased rapidly to zero. A semi-stable discharge was also obtained by moving the needle in towards the orifice (Figure 3.11 (c)); however, no ions were detected by the mass spectrometer for this needle-to-orifice position. Since the needle is at a large positive potential ($\approx$ 4000 V), positive ions will be repelled from it and accelerated towards whatever surface is serving as the counter electrode. When the needle is in the position in Figure 3.11 (a), ions that are created in the region between the needle tip and the center axis of the orifice can be directed through the orifice by the potential field. However, when the tip of the needle is towards the center of the orifice, ions will be

Figure 3.11

Schematic representation (not to scale, 1/8" = 1") of needle position relative to orifice. Position which generates (a) a discharge across face of orifice and from which ions are detected, (b) a discharge similar to (a) but shorter in length and for which no ions are detected, and (c) a discharge to the orifice.

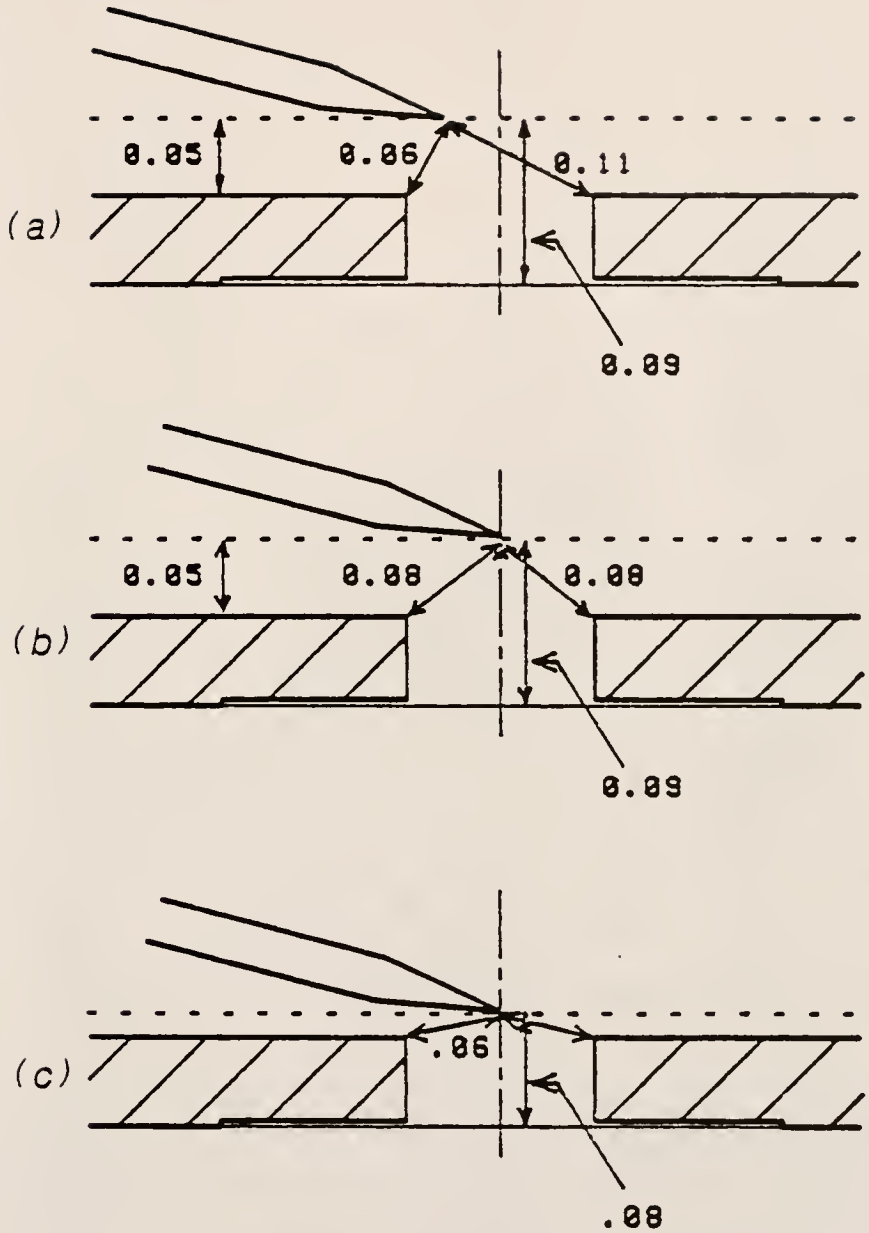
(a)
0.05
0.06
0.11
0.09
(b)
0.05
0.08
0.08
0.09
(c)
.06
.08

repelled into the diaphragm or into the source mounting plate and will not be directed through the orifice. Likewise, if the needle is moved in towards the orifice and discharges to the orifice, the potential field of the lens system will not be strong enough to direct ions through the orifice because the field generated by the discharge needle will be very strong in this region due to the close proximity of the needle to the grounded surface. For an electrically floated orifice, the position of the needle and the needle-to-orifice position are not as critical as in the case above for the production of a stable discharge and for the detection of ions. Factors that affect the discharge voltage required to produce a selected current include the gas flow rate and composition in the discharge region, the potential on the orifice, and the needle-to-orifice positions. Because of the limited output voltage (5 kV) of the dc-dc converter, the needle-to-orifice distance required to maintain a discharge is limited to only a few millimeters. However, within this range, this discharge was easily obtainable and always stable (unless the needle was shorted to the surface of the orifice plate).

Effect of Various Parameters on the Ethyl Acetate Ion Family

While the potential field from electrically floating the orifice to a positive potential causes a greater transmission of ions through the orifice, it also increases the energy spread of the ions. The ions with a very small amount of kinetic energy (<2 eV) can cluster in the post-orifice region. Ions with a large amount of kinetic energy (>7-10 eV) can undergo fragmentation through collision-induced dissociation (CID) with the bulk gas. Ions with an energy between these values can

be declustered to form molecular (M^+) or pseudo-molecular ($M+H^+$) ions [34].

When ethyl acetate ($M = CH_3CO_2CH_2CH_3$) is ionized in the API source, ions with m/z values of 177 (M_2+H^+), 125 [$M+H(H_2O)_2^+$], 107 ($M+H_3O^+$), 89 ($M+H^+$), 61 ($M+H^+ - C_2H_4$), and 29 ($C_2H_5^+$) are detected. Because of the kinetic energy spread, both cluster ions (m/z 177, 125, and 107) and fragment ions (m/z 61 and 29) are present with the pseudo-molecular ion (m/z 89). It is desirable to limit the production of both cluster and fragment ions to increase the amount of the pseudo-molecular ion that is detected. Therefore, the orifice potential and the potential of the first conical lens were varied and the intensities of members of the "ion family" of ethyl acetate (m/z 177, 107, 89, 61, and 29) were plotted vs. these values. Figure 3.12 shows the intensities of these ions plotted (m/z 125 and 61 not shown) vs. the orifice potential, while holding the potential of CL1 at +40 V. At approximately 100 V (a 60 V potential difference in the supersonic jet expansion region) the greatest intensity of m/z 89 relative to the intensities of the other ions is achieved. At lower values of the orifice potential (lower potential difference between the orifice and CL1) clustering increases, and at higher values (higher potential difference) fragmentation increases.

These same ions are plotted vs. the potential of the first conical lens, while holding the orifice at 100 V in Figure 3.13. The greatest intensity of m/z 89 relative to the intensities of the other ions occurred at ca. 36 V (approximately 2 to 1). Below this value the intensity drops off rapidly for all the ions. Above this value, all

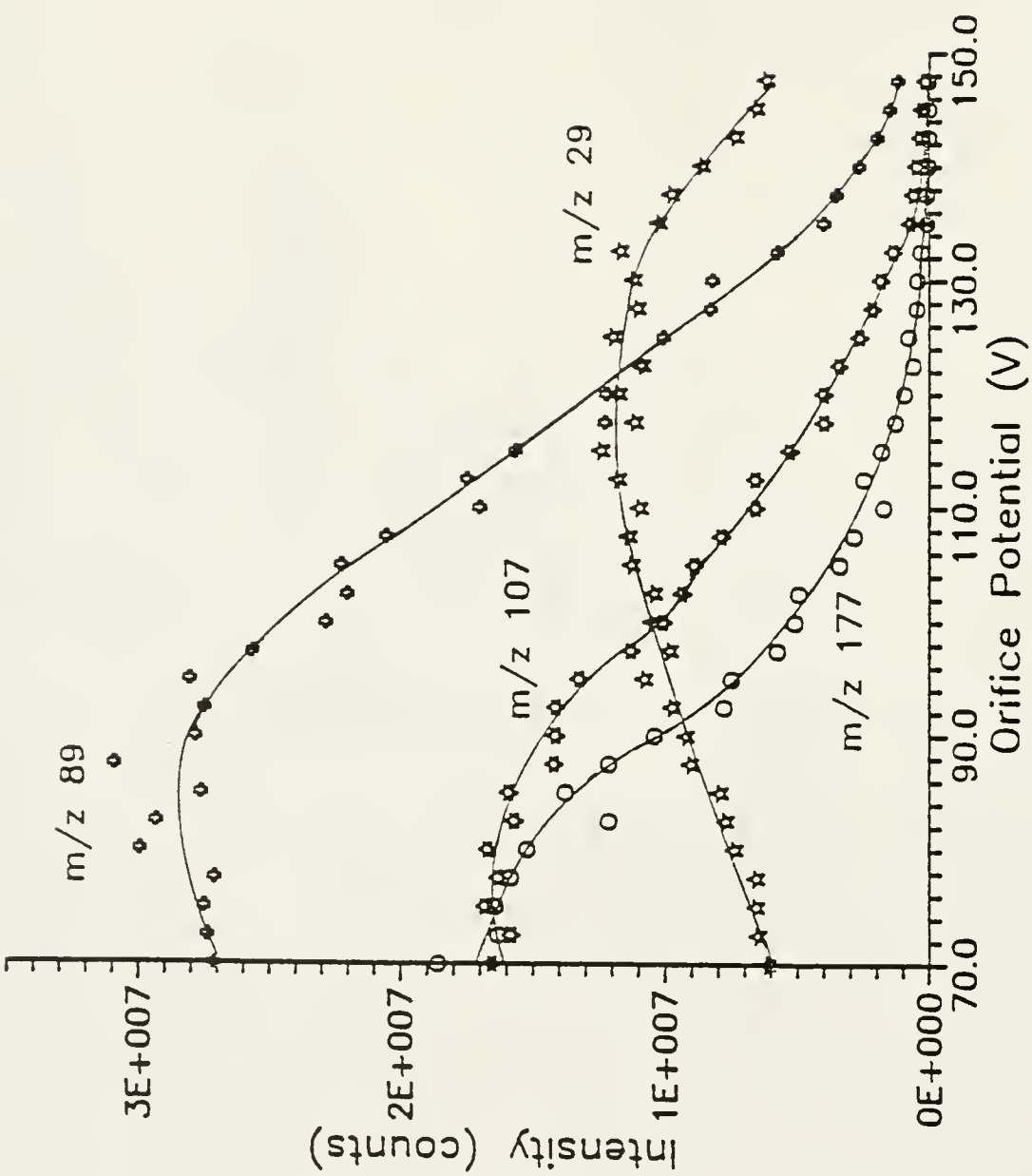

Figure 3.12

The intensities of members of the ion family of ethyl acetate (clusters, fragments, and the pseudo molecular ion) vs. the potential of the orifice with the potential of Cll = 140 V.

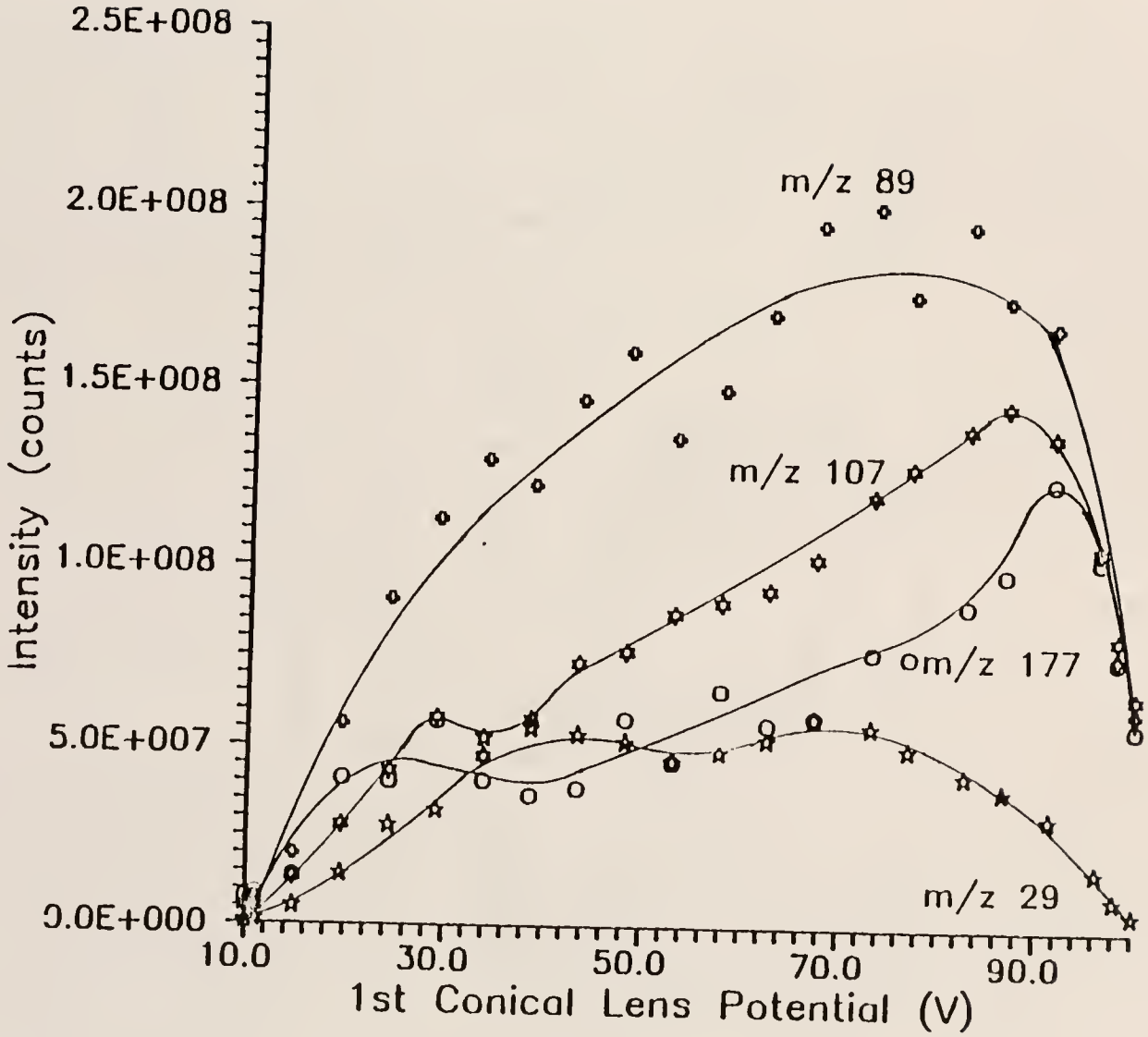

Figure 3.13

The intensities of members of the ion family of ethyl acetate (clusters, fragments, and the pseudo-molecular ion) vs. the potential of CL1 with the potential of the orifice = +120 V.

the ions increase steadily in intensity until a potential of about 70 V for the conical lens, at which time the intensity of the fragment ion, m/z 29, drops off. The other ions increase in intensity until approximately 85 V when the intensities for all the ions begins to decrease. It is apparent that, with the floated orifice, both clusters and fragments will be observed because of the kinetic energy spread; however, this seems to be a worthwhile tradeoff due to the increase in intensity that the floated orifice provides.

The intensities of members of the ion family of ethyl acetate (m/z 177, 107, 89, 29) were plotted relative to the discharge current (Figure 3.14) to determine what effect the current had upon the two processes of clustering and fragmentation, as well as on the intensities of all the ions. From these data, it appears that the highest intensities of the ions and the highest ratio of the pseudo-molecular ion intensity to that of the cluster and fragment ions occur in two regions, from 0.5 to 1.2 μA and from 2 to 3 μA. The lowest discharge current that can be set is 0.5 μA, because below this value it becomes very difficult to regulate the current. Between 1.2 and 2 μA the intensity of the protonated dimer increases significantly, while the intensities of the other ions decrease. Above about 3 μA the intensities of all the ions decrease rapidly. Currently, the effect of current on the relative intensities of these ions is not yet understood.

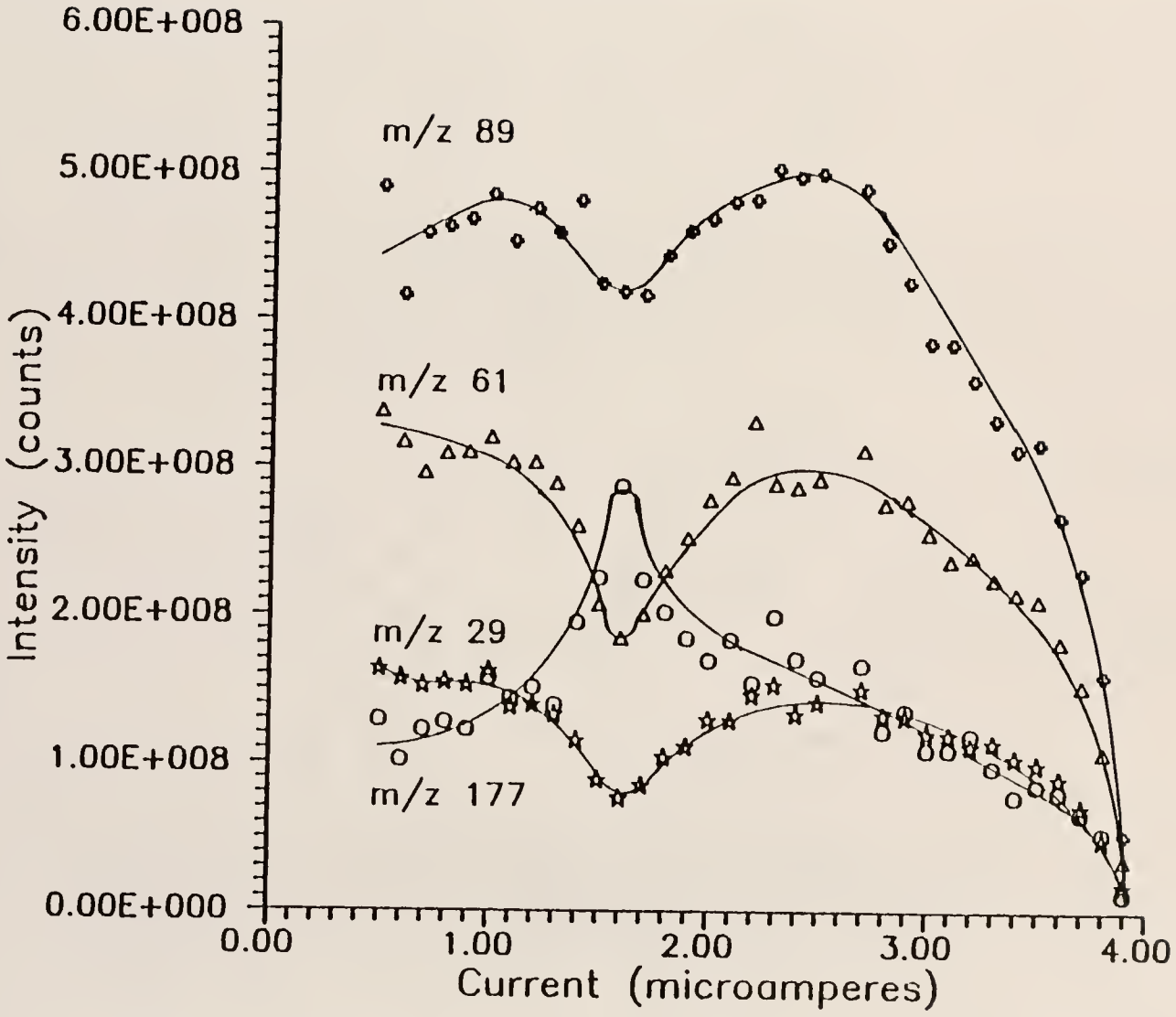

Figure 3.14

The intensities of members of the ion family of ethyl acetate (clusters, fragments, and the pseudo-molecular ion) vs. the discharge current.

Clustering/Declustering

The clustering of ions with molecules in the supersonic expansion of the post-orifice region has been one of the major problems in the development of an API source for direct atmospheric monitoring. Indeed, the only source that successfully overcomes this problem has been built by Sciex [25]. This problem can be minimized in one of three ways. The first is to start with a sample that contains no water vapor, such as the effluent from a GC. Unfortunately, in direct atmospheric monitoring removing the water vapor is nearly impossible.

A second method to reduce clustering is to prevent water molecules and other neutral impurities from entering the post-orifice region. Sciex accomplishes this by drawing the ions that are formed through a pre-orifice region (enclosed by an aperture plate, to which the discharge is struck, and the orifice plate) which has been pressurized (slightly > 1 atm) with a pure, relatively inert, cryopumpable gas such as carbon dioxide (for liquid nitrogen or liquid helium cryogenic pumping) or nitrogen (for liquid helium cryogenic pumping). Sciex has referred to this region as a "gas curtain" or "ion window" [33]. In this instrument, with a less complicated one-orifice system, a gas "jet" has been produced by introducing a gas through the aperture of a 1/16" tube positioned near the orifice. With an electrically grounded orifice, this gas jet has an appreciable effect on the amount of clustering that occurs. Figure 3.15 shows mass spectra of the water cluster ions obtained (with a grounded orifice) for direct atmospheric monitoring with (a) the nitrogen on and (b) the nitrogen off. With the

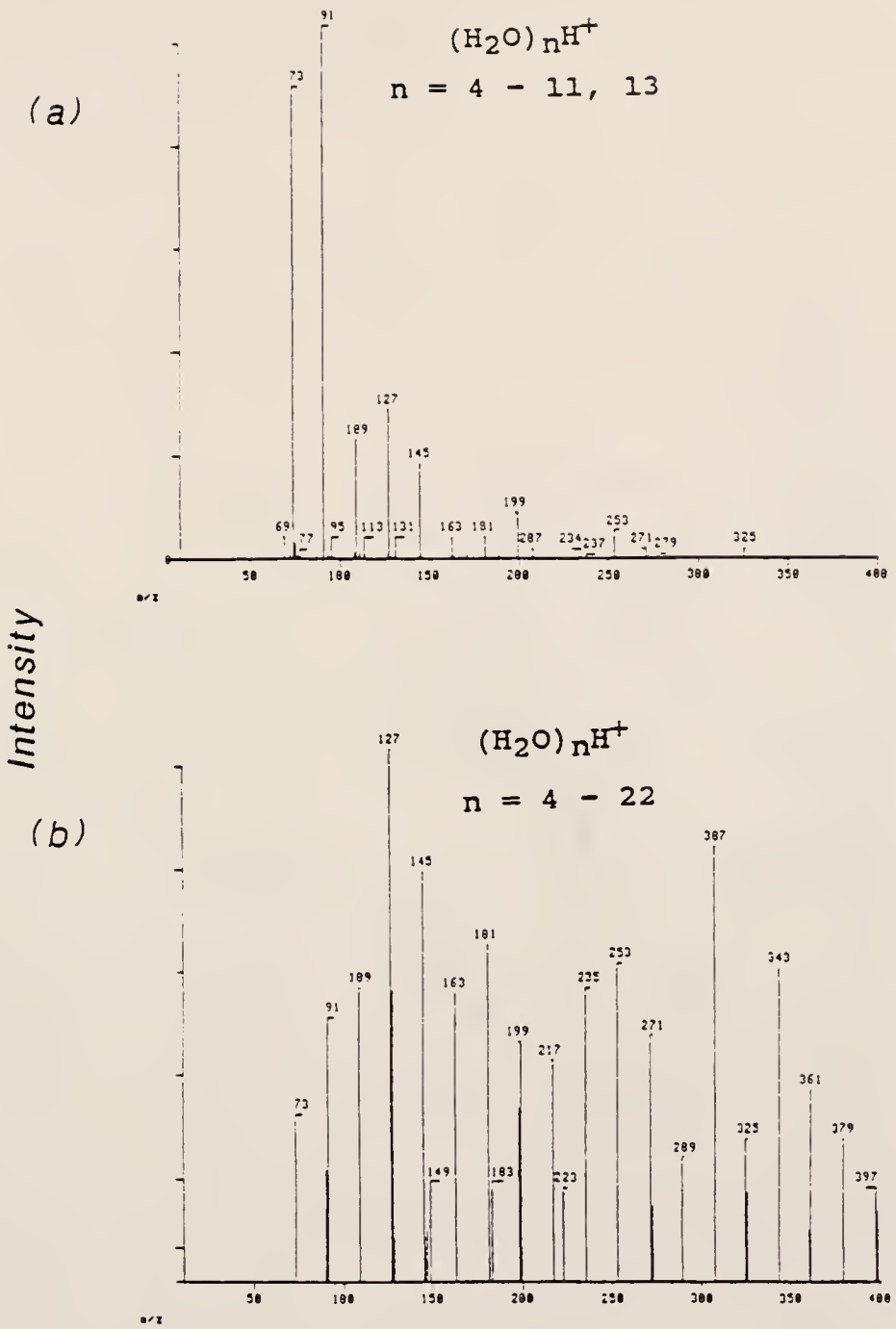

Figure 3.15

Mass spectra of background water cluster ions generated from direct atmospheric monitoring of laboratory air with nitrogen jet (a) on and (b) off.

nitrogen on, the intensities of the large cluster ions are reduced, while the intensities of the small cluster ions are increased by ≈2 orders of magnitude relative to their intensities with the nitrogen jet off.

The third method to reduce clustering is to perform collision-induced declustering in the post-orifice region. Sciex has performed this by applying a potential field in this region to impart enough kinetic energy to allow CID of the cluster ions to occur [34]. In theinstrument developed in this lab, this same effect can be observed. Figure 3.16 shows mass spectra obtained (orifice potential = +100 V and a dry compressed air jet flow rate of approximately 1 $mL \cdot min^{-1}$) for (a) a potential difference between the orifice and the first conical lens of 17 V and (b) a potential difference of 66 V (both mass spectra plotted on the same intensity scale). While the cluster ions with large m/z values are reduced, the cluster ion with small m/z values are increased (by a factor of ≈2 for m/z 37 and ≈7 for m/z 19). Furthermore, with a floated orifice (at a potential difference high enough to cause CID declustering), the gas jet appears to have no effect. Figure 3.17 (a) and (b) show the mass spectra attained with a floated orifice (potential difference = 50 V) and a nitrogen jet on and off, respectively. This same effect is observed for sample cluster ions. Figure 3.18 shows that having the gas jet (a) on or (b) off has little or no effect on the spectra obtained when ethyl acetate is analyzed by direct atmospheric monitoring by this source with a floated orifice (potential difference = 50 V). While with a floated orifice the gas jet has little effect on clustering, it may still be worthwhile

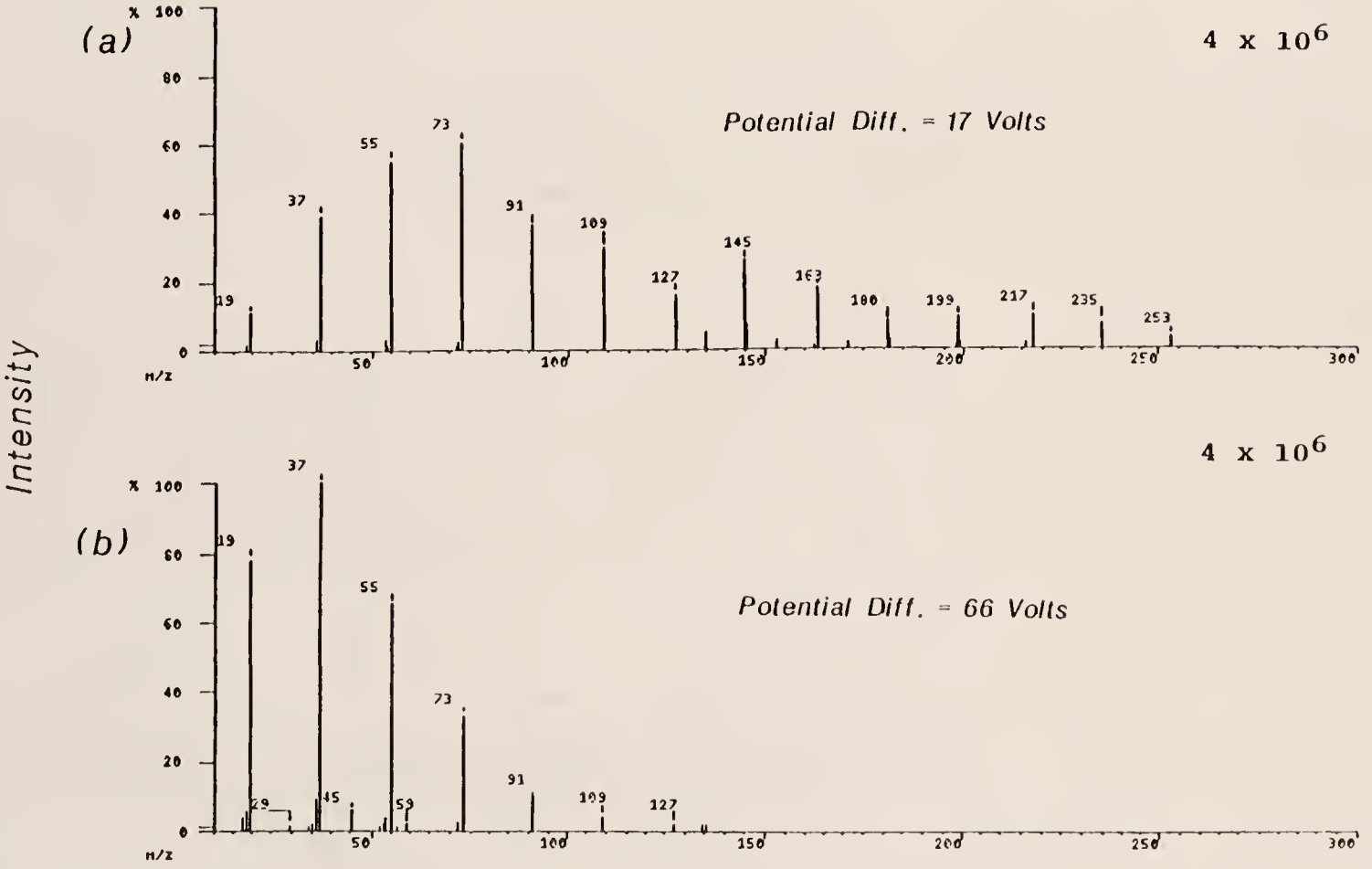

Figure 3.16

Mass spectra of background water cluster ions generated from direct atmospheric monitoring of laboratory air with the orifice potential at +100 V and a potential difference in the post-orifice region of (a) 17 V and (b) 66 V.

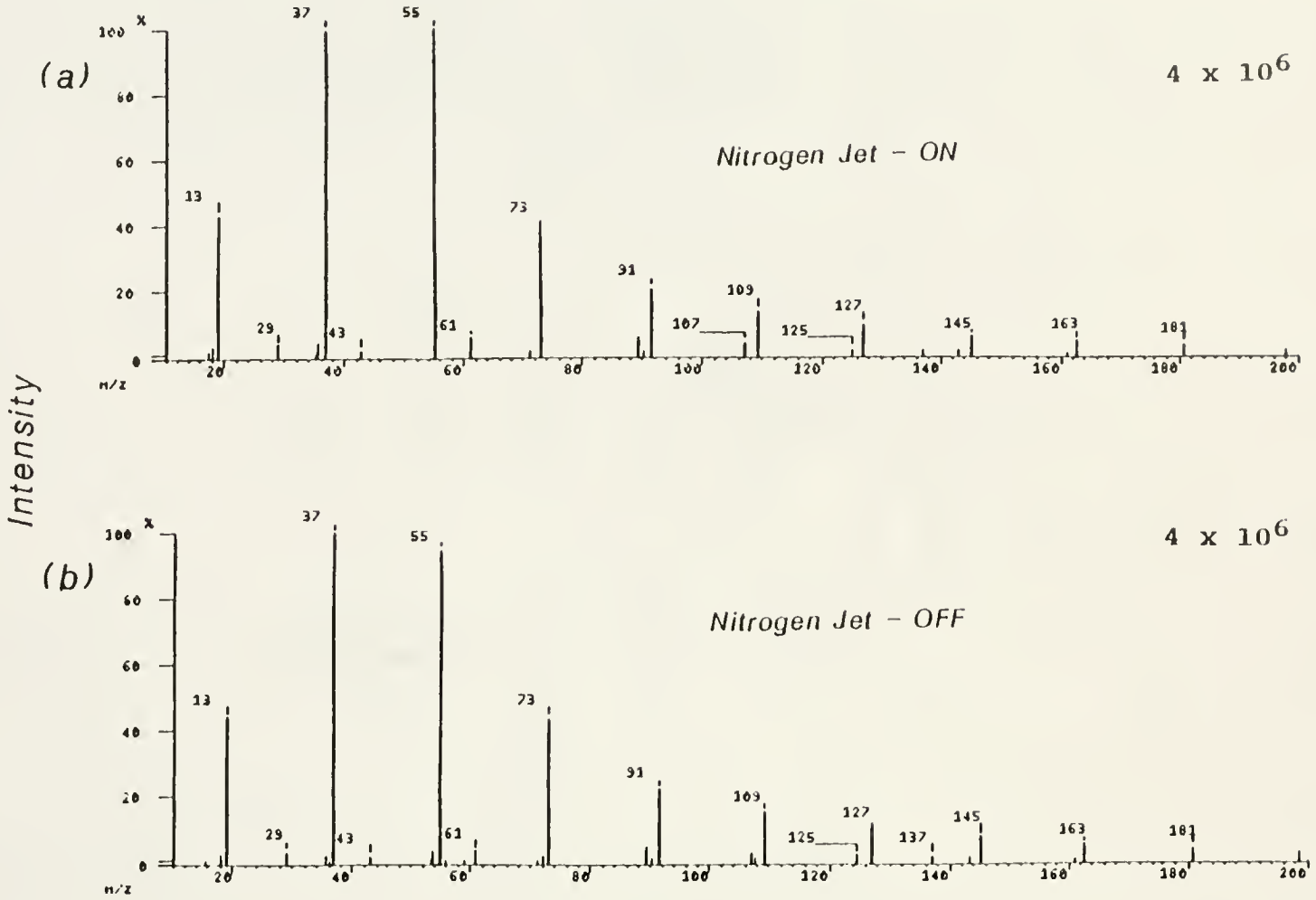

Figure 3.17

Mass spectra of backgrounnd water cluster ions generated from direct atmospheric monitoring of laboratory air with a potential difference in the post-orifice region of 50 V and with the gas jet (a) on and (b) off.

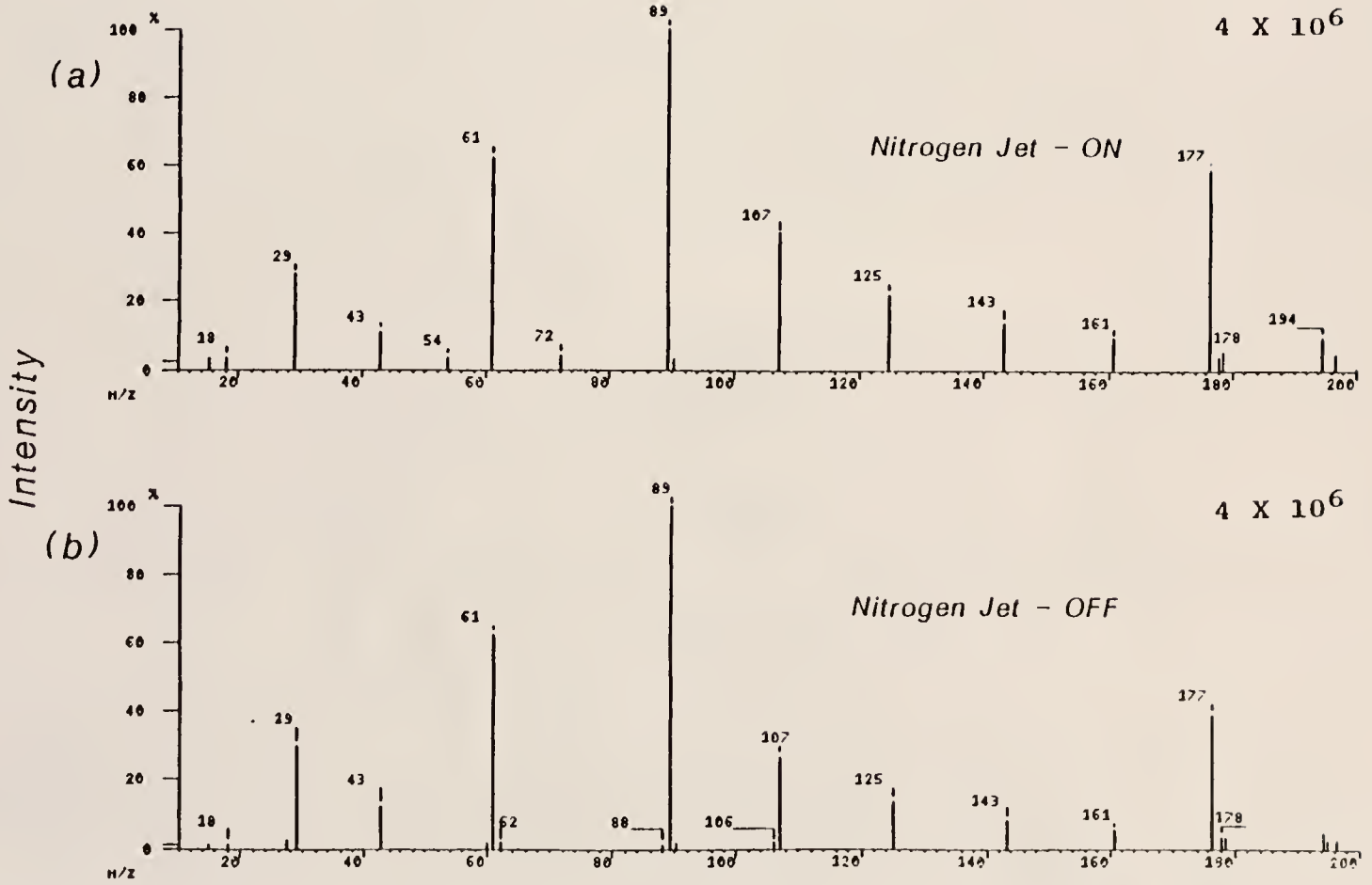

Figure 3.18

Mass spectra for direct atmospheric monitoring of ethyl acetate with the gas jet (a) on and (b) off.

to employ the gas jet to prevent orifice clogging and to reduce memory effects.

Experimental Methods for Direct Atmospheric Monitoring

Mass Calibration of API/MS/MS Instrument

In order to employ any mass spectrometer for mass analysis, the instrument must have a way to accurately assign m/z values to the signals it is obtaining. This process is called mass calibration. The tuning of a mass spectrometer usually refers to the adjustment of lens and quadrupole offset voltages so that the maximum ion intensity is obtained. In the case of a quadrupole mass spectrometer, a calibration compound which produces ions of known m/z values is analyzed (for EI/CI this is typically perflurotributylamine (FC43)). A calibration table is then generated which relates the scanning voltage of the quadrupole to the correct m/z value. These values can be compared to the voltages needed to pass ions, of otherwise unknown mass, from other samples to calculate their m/z values. Although mass calibration for this instrument does not change while switching between EI and CI, the installation of this source requires a new lens system which results in the need to re-calibrate and re-tune for API. Since background ions are abundant in API/MS, water cluster ions (no API ions were detected for FC43) are used to calibrate the instrument and perform lens tuning, after which sample gases may be analyzed. As can be ascertained from the spectra shown in this thesis, this method for tuning and mass

calibration proved efficient at the unit mass resolution of the quadrupole mass analyzers.

Sampling Methodology

All vapors analyzed by direct atmospheric monitoring were generated by drawing air across the caps from bottles of liquid compounds. For studies which required a steady concentration of sample for long periods of time (such as calibration and tuning), a few drops of compound were placed in the bottle cap and the cap was placed in front of the 1" diameter glass sampling tube of the API source. Although the vapor pressure of the liquid samples can be estimated, the amount of sample introduced is not accurately known, and absolute determination of the API/MS/MS instrumental sensitivity or LOD is therefore not possible.

CHAPTER 4

ANALYTICAL PERFORMANCE

To evaluate the performance of an analytical instrument, several factors may be considered; however, not all factors are necessarily important for all types instruments. For an instrument which performs direct atmospheric analysis, these factors include the ability of the instrument to identify the sample it is analyzing, the ability of the instrument to detect trace amounts of the sample, the ability of the instrument to distinguish between compounds in the same sample, memory and interference effects in the analysis, ease of use of the instrument, and the time required for sample analysis (including equilibration time between samples).

Characterization of an API/MS/MS Instrument

Analyses of Pure Compounds

With the source configuration for the Finnigan 4500 quadrupole mass spectrometer, clustering proved such a large problem that direct atmospheric monitoring was nearly impossible. Indeed, even solvent vapors injected into a pure nitrogen stream displayed cluster ions as the predominant ions detected (Figures 3.3 and 3.4). In the source design for the TSQ 70 with a nitrogen jet, the instrument can be tuned to significantly minimize the clustering, even while performing direct atmospheric analyses. Figure 4.1 (a) - (c) shows mass spectra obtained

Figure 4.1

Direct atmospheric monitoring/API/MS of compounds that undergo charge exchange ionization (a) carbon disulfide, (b) benzene, and (c) toluene.

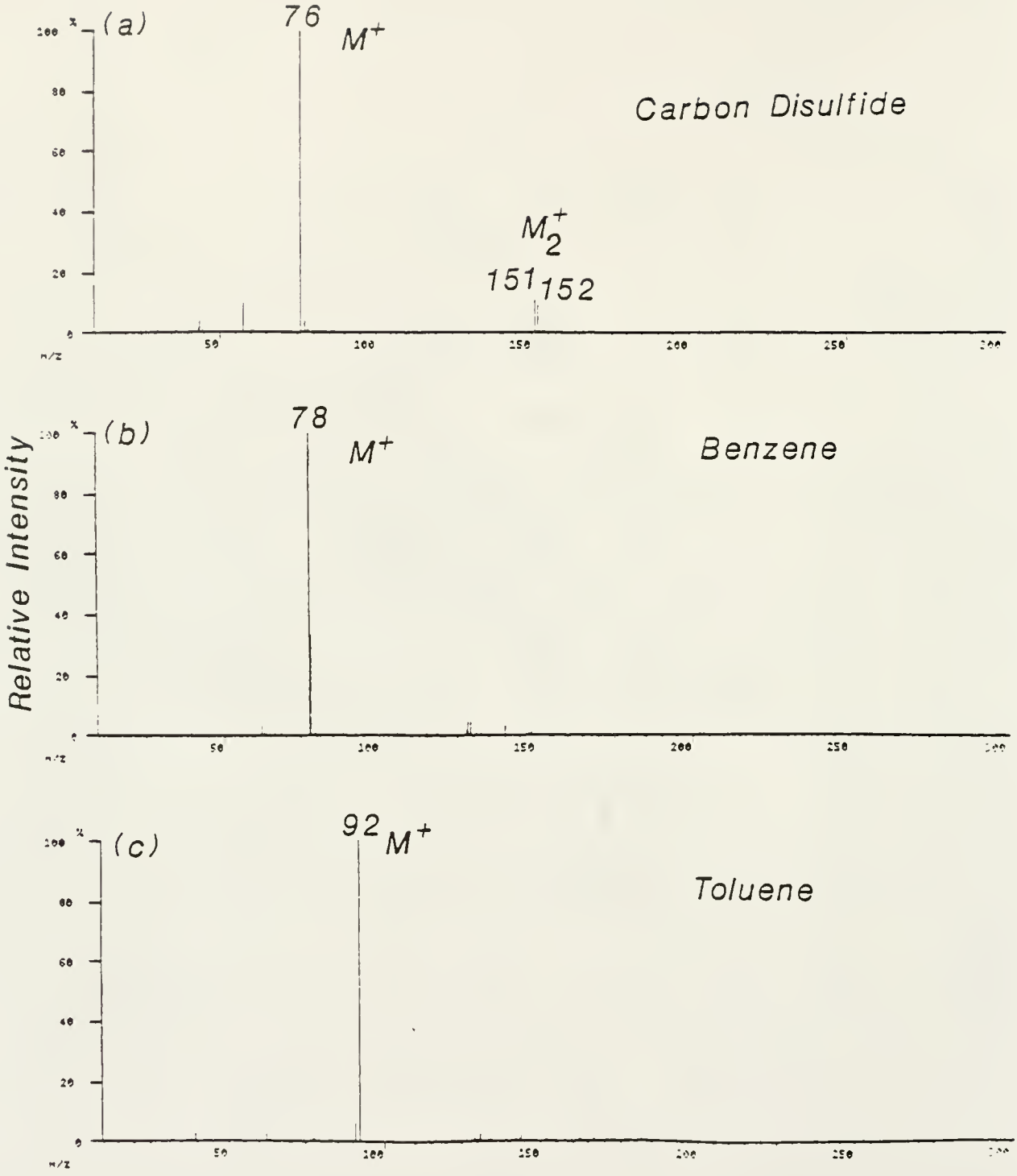
(a)
76
M+
Carbon Disulfide
M2+
151 152
(b)
78
M+
Benzene
Relative Intensity
(c)
92 M+
Toluene
m/z

(with a grounded orifice and a voltage-regulated power supply) while performing direct atmospheric monitoring of representative compounds which undergo charge exchange ionization in the API source, carbon disulfide (MW 76), benzene (MW 78), and toluene (MW 92), respectively. These compounds each form almost exclusively the M^+ molecular ion, with carbon disulfide forming a small amount of the M_2^+ dimer ion. Figure 4.2 (a) - (c) shows mass spectra obtained (with a grounded orifice) while performing direct atmospheric monitoring of representative compounds which undergo proton transfer ionization in the API source, acetone (MW 58), ethyl acetate (MW 88), and methanol (MW 32), respectively. Acetone and ethyl acetate both form almost exclusively the $(M+H)^+$ pseudo-molecular ion. The most predominant ion for methanol is the $(M_2+H)^+$ protonated dimer ion. While the signal obtained under these conditions for these samples was not sufficient to perform tandem mass spectrometry (MS/MS), these results demonstrate that this API source can reduce clustering significantly.

Figure 4.3 shows the reconstructed ion current (RIC) traces for the two most predominant background ions (when the instrument is tuned for large amounts of declustering and analysis is performed by bringing caps of solvent bottles near sampling tube of API source) (a) $(H_2O)_2H^+$ (m/z 37) and (b) $(H_2O)_3H^+$ (m/z 55), two representative sample ions (c) $C_6H_6^+$ and (d) $(CH_3CO_2C_2H_5)H^+$, and (e) all the ions. In normal EI mass spectrometry, sample ionization occurs by the bombardment of the sample molecules with electrons from a filament. In positive CI mass spectrometry, ionization occurs through charge exchange or proton transfer with ions created from a reagent gas. Usually, however, these

Figure 4.2

Direct atmospheric monitoring/API/MS of compounds that undergo proton transfer ionization (a) acetone, (b) ethyl acetate, and (c) methanol.

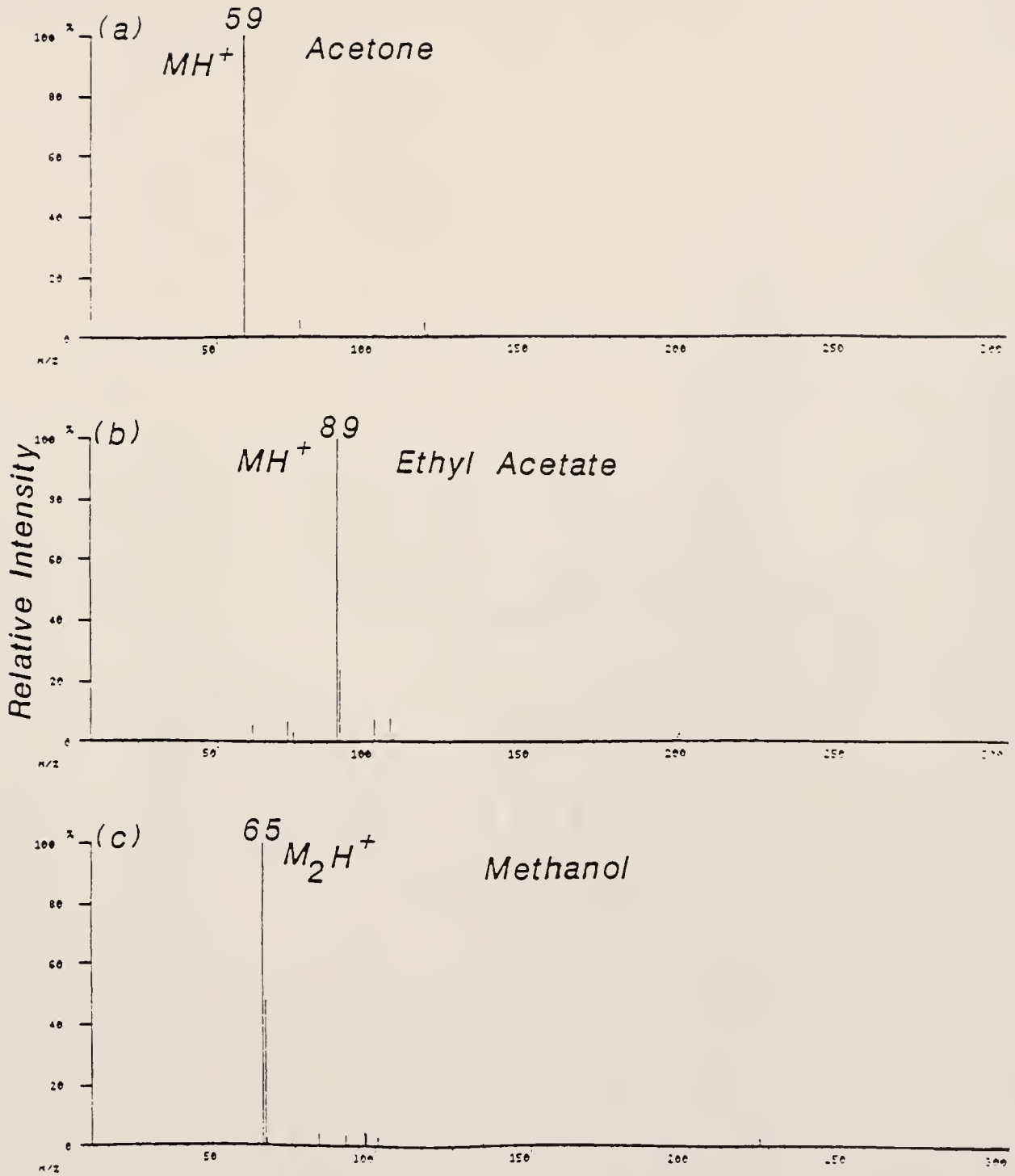
(a)
59
MH+
Acetone
(b)
89
MH+
Ethyl Acetate
(c)
65
M2H+
Methanol
Relative Intensity
m/z

Figure 4.3

RIC traces for the two most predominant background ions (a) $(H_2O)_2H^+$ and (b) $(H_2O)_3H^+$, two representative sample ions (c) $C_6H_6^+$ and (d) $(CH_3CO_2C_2H_5)H^+$, and (e) all the ions.

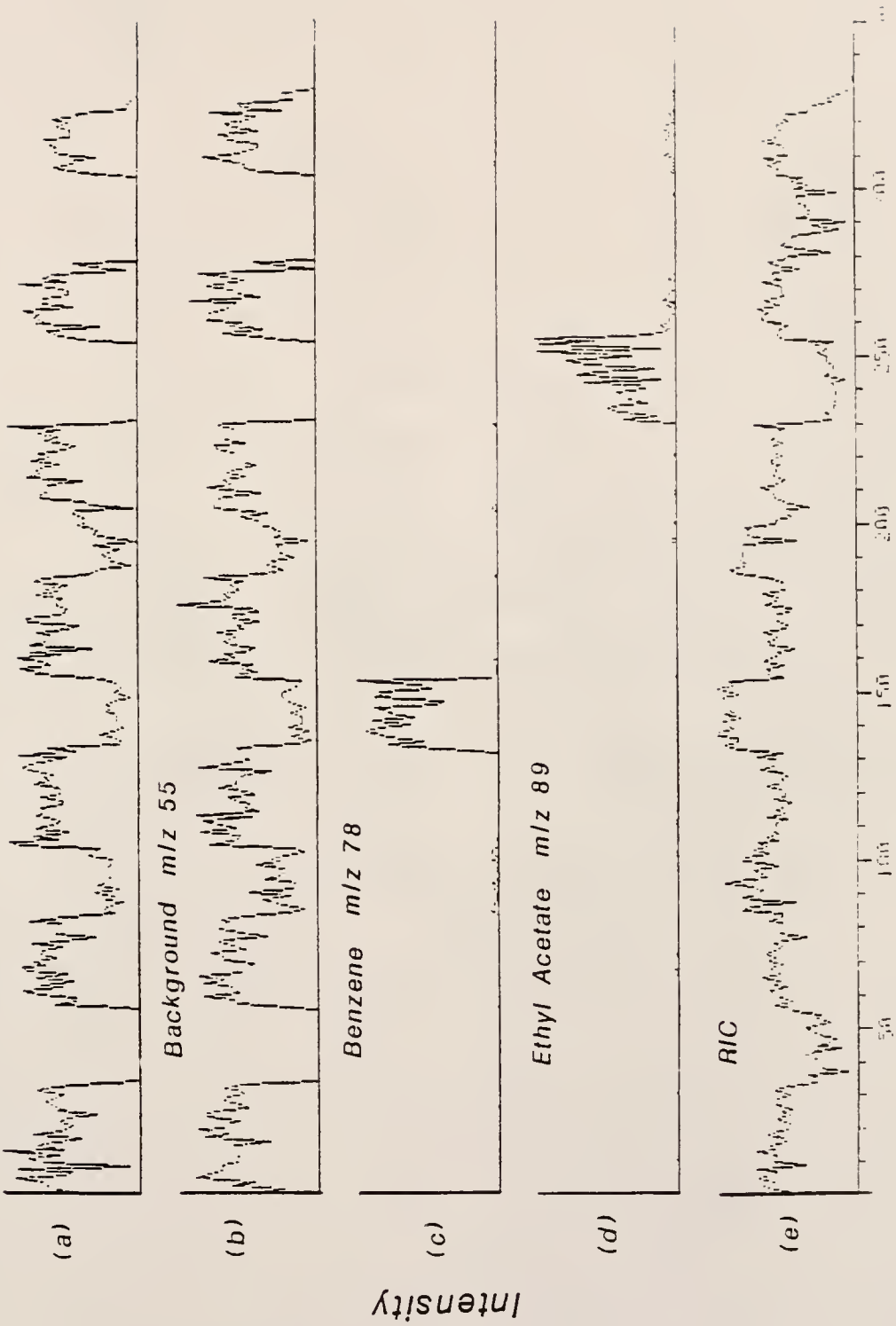
(a)
Background m/z 37
(b)
Background m/z 55
(c)
Benzene m/z 78
(d)
Ethyl Acetate m/z 89
(e)
RIC
Intensity
Scan #

reagent ions are low in m/z value and the mass spectrometer can be set up to pass only ions of a greater mass. Ionization in API mass spectrometry occurs in a similar fashion to CI mass spectrometry (see Chapter 1). In direct atmospheric monitoring mass spectrometry, air serves as the reagent gas, generating N_2^+, H_2O^+, and H_3O^+ ions (equations 1.2 - 1.5). Sample molecules (M) can react with the reagent ions through charge exchange or proton transfer reactions to form M^+ molecular or $M+H^+$ pseudo-molecular ions. The kinetics of the production of ions in discharges at atmospheric pressures has been studied by Shahin [10] and Kebarle [44]. Shahin stated that for direct atmospheric sampling (or for any samples with even a small quantity of water vapor) the production of H_2O^+ (by charge exchange with the initial N_2^+ ions) and H_3O^+ ions would be the dominant reactions. In the case of either charge or proton transfer ionization reactions, the intensity of the reagent ions is reduced as the sample is ionized. Samples that undergo proton transfer ionization may totally deplete the population of the background ions, while samples that undergo charge transfer ionization reduce but do not deplete that population. Figure 4.4 shows the relationship between the intensity of the reagent ions with respect to the time allowed for reaction. Equations 4.1 - 4.3 [44] give the rate constants for the production of H_2O^+, H_3O^+, and $H(H_2O)_n^+$.

$$N_2^+ + H_2O \rightarrow N_2 + H_2O^+ \quad k = 1.9 \times 10^{-9}\ cm^3 \cdot molecule^{-2} \cdot s^{-1} \qquad (4.1)$$

$$H_2O^+ + H_2O \rightarrow H_3O^+ + HO \quad k = 1.8 \times 10^{-9}\ cm^3 \cdot molecule^{-2} \cdot s^{-1} \qquad (4.2)$$

$$H_3O^+ + nH_2O \rightarrow H(H_2O)_{n+1}^+ \quad k \approx 10^{-27}\ cm^3 \cdot molecule^{-2} \cdot s^{-1} \qquad (4.3)$$

Figure 4.4

The kinetics of the production of ions in corona discharges at atmospheric pressure. Generated with the results from a BASIC program utilizing the kinetics of the reactions in Equations 4.1 - 4.3. Study limited to generation of termolecular water cluster.

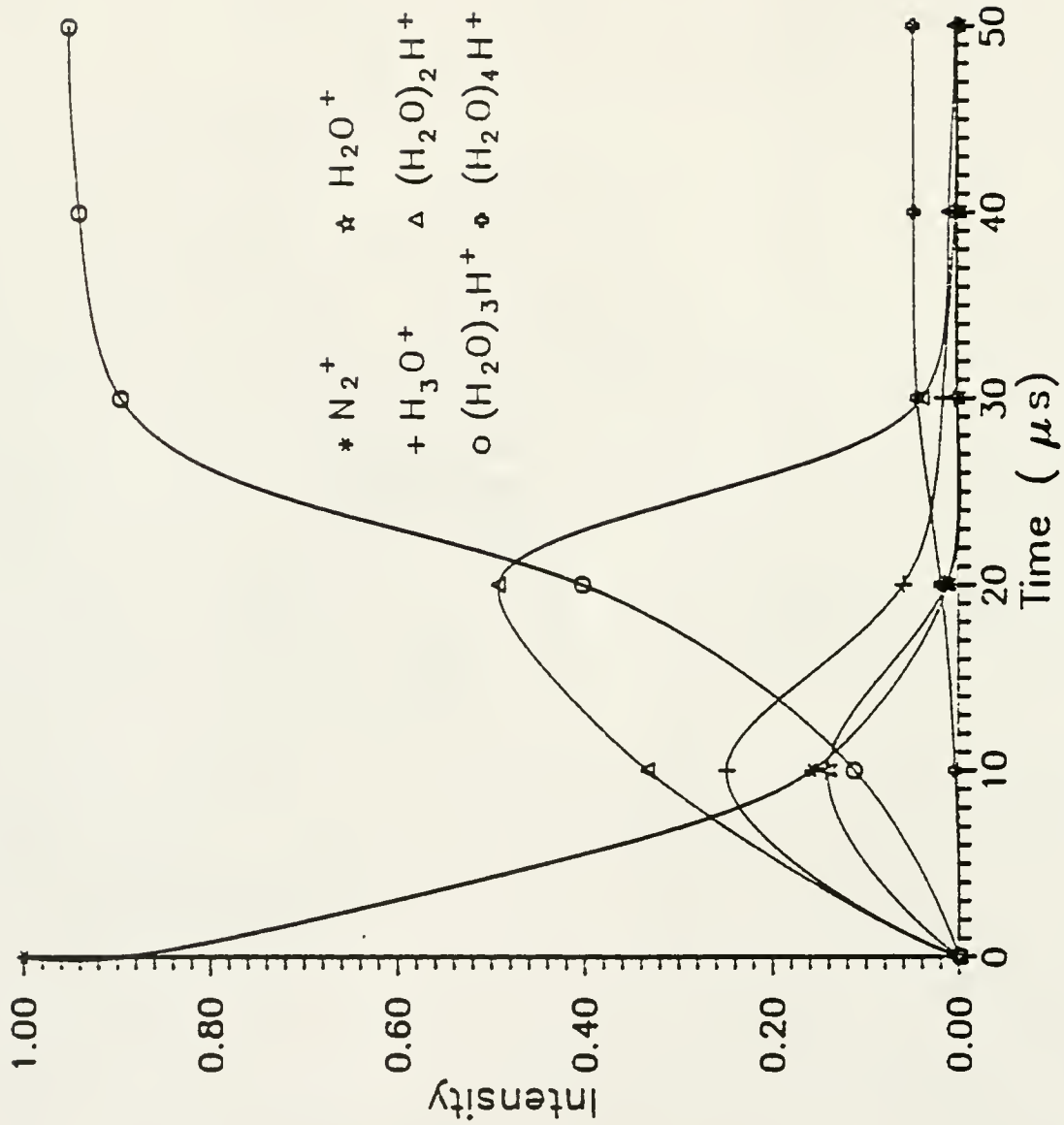
1.00
0.80
0.60
0.40
0.20
0.00
Intensity
0
10
20
30
40
50
Time (μs)
* N_2^+
☆ H_2O^+
+ H_3O^+
△ $(H_2O)_2H^+$
○ $(H_2O)_3H^+$
◇ $(H_2O)_4H^+$

sample molecules with H_2O^+ and H_3O^+ are on the order of 3×10^{-9} $cm^3 \cdot molecule^{-2} \cdot s^{-1}$ [45]. Proton transfer reactions with sample molecules will thus consume H_3O^+ before it can further react to form $(H_2O)_2H^+$ (m/z 37) and $(H_2O)_3H^+$ (m/z 55). Charge transfer reactions with sample molecules cannot consume all the H_2O^+ before some of it can be converted to H_3O^+ and therefore, the population of $(H_2O)_2H^+$ (m/z 37) and $(H_2O)_3H^+$ (m/z 55) will be reduced but not depleted.

Memory effects

The RIC traces for the benzene molecular and ethyl acetate pseudo-molecular ions (Figure 4.4) show that, as the sample is brought to the sampling tube, the signal immediately increases and as it is removed, the signal decreases rapidly to zero. This would indicate that memory effects have been minimized with this source; however, it should be pointed out that this source has yet to be applied to trace analysis, and this application would give a much better indication of memory effects.

Orifice Clogging

Orifice clogging proved to be a severe problem with both the Finnigan developed API source and the one developed in this work for the Finnigan 4500 quadrupole mass spectrometer. The major reasons for this problem was that there was no way to prevent particulate matter in the sample gas stream from reaching the orifice. With the addition of the gas jet near the orifice, this problem has been almost eliminated. When the orifice does become clogged (maybe once or twice a day), a gas jet of relative high pressure ($\approx$ 20 - 40 psi) may be directed at the orifice to dislodge any matter. Occasionally, when all else has

failed, the instrument has needed to be vented to atmospheric pressure and the orifice removed and cleaned with an appropriate solvent (methylene chloride). The diaphragms are surprisingly rugged and a single diaphragm has been used for several months of source development and sample analysis while the API source has been installed on the TSQ 70.

Analytical Potential

Compound Identification

An instrument must be able to distinguish between different compounds to be of analytical use. This may be done by separating compounds in time and using a universal detector, by analyzing all compounds at the same time with a detector that provides a different response for each compound, or by some combination of both of these techniques. A single stage of mass analysis can be used with low energy ionization techniques (such as CI, fast atom bombardment, or API) to determine the molecular weight of a compound, or with high energy ionization techniques (such as EI) to provide fragment ions which can be used for structure elucidation. Therefore, mass spectrometers are commonly used with some type of pre-separation step before mass analysis, such as GC, LC, or MS. When API/mass spectrometry is used for direct atmospheric monitoring, by definition there is no opportunity for any pre-ionization separation.

Methyl benzoate (MW 136) and methoxy benzaldehyde (MW 136) are examples of compounds with the same empirical formula and the same

molecular weight that form ions with the same m/z value. Both of these compounds produce an intense $M+H^+$ pseudo-molecular ion (m/z 137), as well as some less intense fragmentation ions when ionized by this API source with the potential difference of the supersonic jet expansion region set at ≈ 50 V (Figure 4.5 (a) and (b)). In a normal API/MS system, it would be difficult to determine the presence of one or both of these compounds and distinguish between them (or other compounds that have MW 136 and form ions through proton transfer reactions). However, because the TSQ 70 is an MS/MS instrument, the pseudo-molecular ion can be fragmented in the center quadrupole to obtain a daughter spectrum (spectrum of fragment ions from a parent ion) of the m/z 137 ion. Figure 4.6 (a) and (b) show the daughter spectra (each under the same conditions of collision energy = 15 eV and pressure of nitrogen collision gas = 2 torr) for methyl benzoate and methoxy benzaldehyde, respectively. Major daughter ions observed for the API-generated $M+H^+$ ion from methyl benzoate are m/z 59 $[(M+H)-C_6H_6]^+$, 77 $[(M+H)-CH_3COOH]^+$, 91 $[(M+H)-HCOOH]^+$, 93 $[(M+H)-CH_3CHO]^+$, 105 $[(M+H)-CH_3OH]^+$, and 109 $[(M+H)-CO]^+$. Major ions observed for the $M+H^+$ ion from methoxy benzaldehyde are m/z 77 $[(M+H)-CO-CH_3OH]^+$, 94 $[(M+H)-CO-CH_3]^+$, and 109 $[(M+H)-CO]^+$. There is a clear difference in these daughter spectra, and thus the compounds can be distinguished.

A concern about API has been its ability to analyze mixtures of samples. Figure 4.7 shows a spectrum of a solvent mixture composed of benzene (MW 78), ethyl acetate (MW 88), benzaldehyde (MW 106), and methoxy benzaldehyde (MW 136), obtained when the API source was used with a floated orifice (potential difference of supersonic jet

Figure 4.5

Direct atmospheric monitoring/API/MS spectra of (a) methyl benzoate and (b) methoxy benzaldehyde.

(a) Methyl Benzoate
M+H+
137
59
77
105
(b) Methoxy Benzaldehyde
M+H+
137
59
77
94
109
Relative Intensity
m/z

Figure 4.6

Direct atmospheric monitoring/API/MS/MS spectra of (a) methyl benzoate and (b) methoxy benzaldehyde with collision energy = 20 eV and collision pressure = 2 torr N_2.

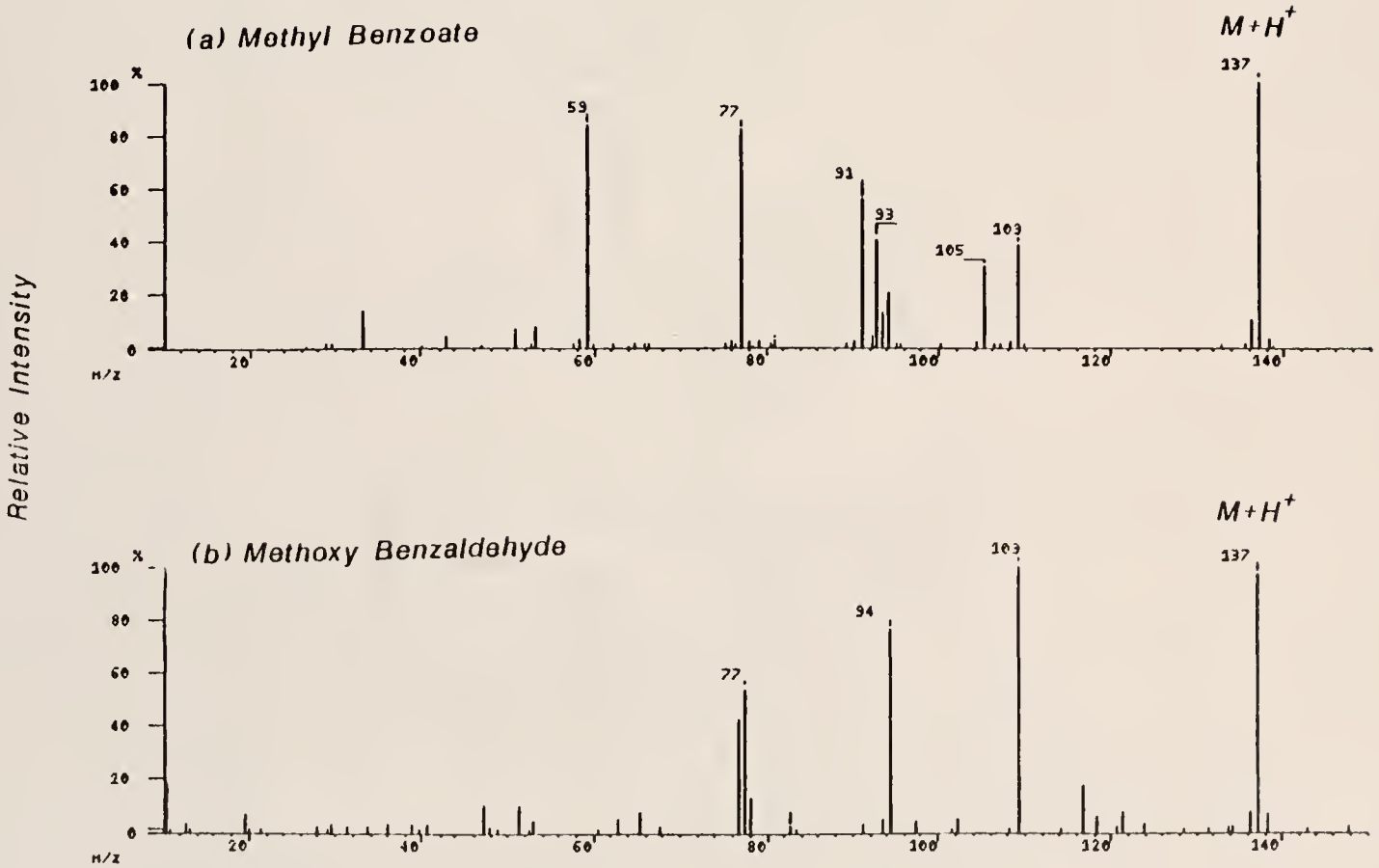
(a) Methyl Benzoate
M+H+
137
59
77
91
93
103
105
100
80
60
40
20
0
%
m/z
20
40
60
80
100
120
140
(b) Methoxy Benzaldehyde
M+H+
137
103
94
77
Relative Intensity

Figure 4.7

Direct atmospheric monitoring/API/MS spectra a solvent mixture composed of benzene (MW 78), ethyl acetate (MW 88), benzaldehyde (MW 106), and methoxy benzaldehyde (MW 136).

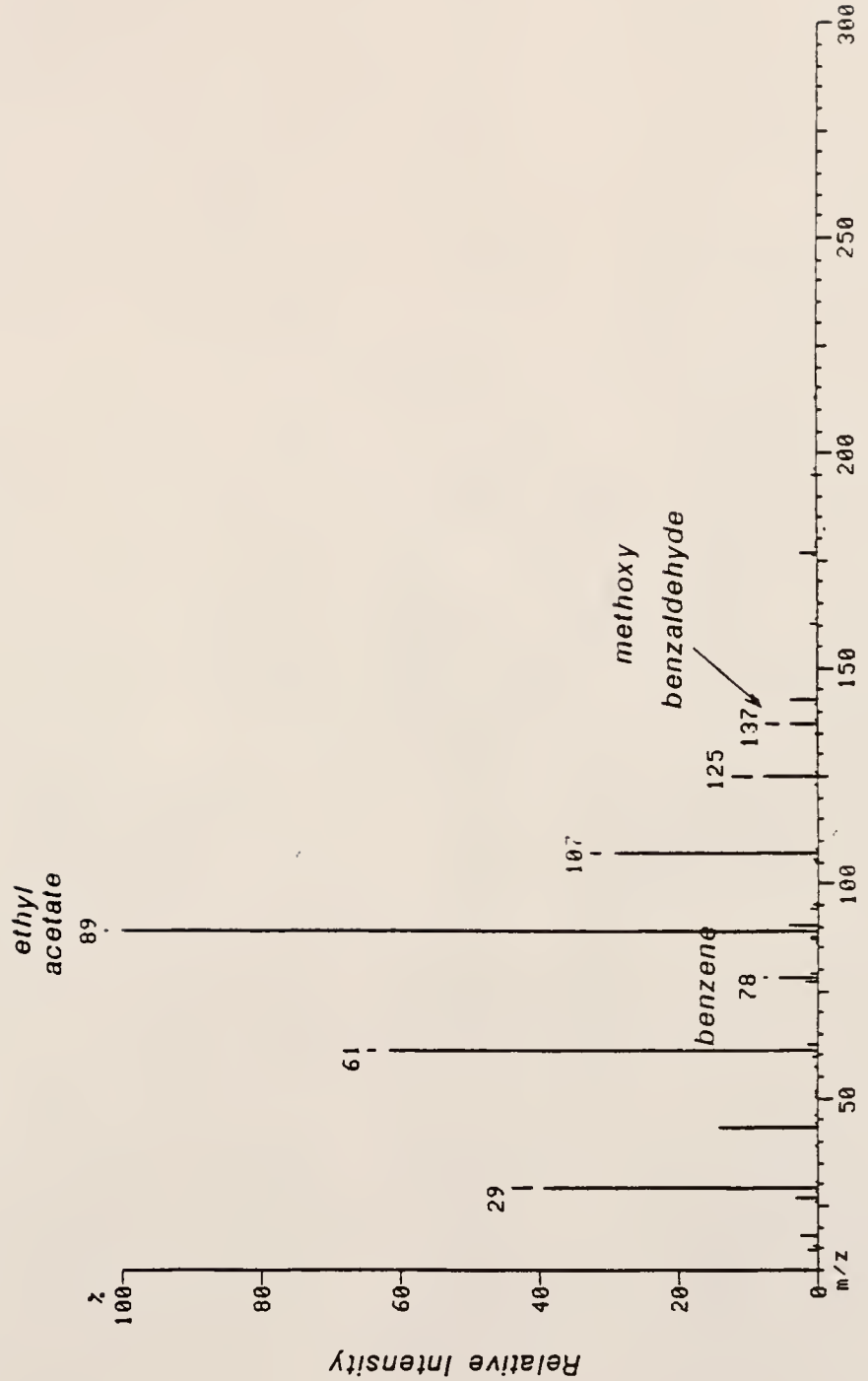
Relative Intensity
%
100
80
60
40
20
0
m/z
50
100
150
200
250
300
ethyl acetate
89
61
29
benzene
78
107
methoxy benzaldehyde
125
137

expansion region ≈ 50 V) and tuned for a high degree of declustering. The pseudo-molecular ion (m/z 89) from ethyl acetate clearly dominates the spectrum and a small quantity of the protonated dimer (m/z 177) is present. Fragment ions of ethyl acetate are also observed at m/z 29 ($C_2H_5^+$) and m/z 61 ($CH_3COOH_2^+$). However, ions from benzene (m/z 78) and methoxy benzaldehyde (m/z 137) are clearly present. There is some confusion as to the identities of m/z 107 and m/z 125. Because of the large intensity of ethyl acetate it is possible that these ions are cluster ions of ethyl acetate ($M+(H_2O)H^+$ and $M+(H_2O)_2^+$) or that they are related to benzaldehyde ($M+H^+$ and $M+(H_2O)H^+$). Unfortunately, the low intensity of these ions made it difficult to obtain their daughter spectra, and therefore, this uncertainty was left unresolved.

Sensitivity

The sensitivity of this API/MS/MS instrument can be roughly estimated from the daughter spectrum of methoxy benzaldehyde, which has a vapor pressure at room temperature and atmospheric pressure conditions of ≈ 0.2 torr [46]. The concentration (mol/mol) of methoxy benzaldehyde in air above a bottle cap can be approximated to be,

$$0.2 \text{ torr}/760 \text{ torr} = 0.0003. \qquad (4.3)$$

Neglecting the slightly reduced pressure near the entrance to the glass tube (this occurs because air is being drawn through the tube) and the dilution of the concentration with the air flowing through the system, the API source has detected and positively identified by a full-scan daughter spectrum methoxy benzaldehyde at a concentration of 300 parts

per million (ppm) in room air. Given an air sampling rate of 100 mL/min and an MS/MS acquisition time for the daughter spectrum of 5 s, this corresponds to 15 μg of methoxy benzaldehyde. Clearly, the resultant daughter spectrum has a high enough signal-to-noise ratio that one or two orders of magnitude less of the compound could still be identified. Furthermore, selected reaction monitoring of one or more parent ion-daughter ion pairs, would provide even lower detection limits.

CHAPTER 5

CONCLUSIONS AND FUTURE WORK

Summary of Results

The original purpose of this work was to design and develop a new atmospheric pressure ionization (API) source for a turbomolecularly-pumped triple stage quadrupole (TSQ) tandem mass spectrometer (MS/MS). This API source could be used to study API and direct atmospheric monitoring by mass spectrometry. To accomplish this, the work initially evaluated a commercially developed [1], but never marketed API source, which was developed as a GC-detector. This API source was characterized on a Finnigan 4500 single quadrupole mass spectrometer. Even as a GC-detector, the Finnigan-developed source suffered from memory effects (because of a small source region) and severe clustering of ions with molecules in the supersonic jet expansion of the post-orifice region. Because of these effects, direct atmospheric monitoring with this source was essentially impossible.

Therefore, a new API source was designed, which would be compatible with a commercial turbomolecularly-pumped mass spectrometer, and which would reduce or eliminate the problems of clustering and memory effects. This source was at first developed to be compatible and interchangeable with the Finnigan 4500 mass spectrometer used to

evaluate the Finnigan-developed API source; however, because of its design, this API source suffered from vacuum integrity problems. Even with these problems, ions were obtained with reduced, but not eliminated, clustering. Because of this clustering effect, this source was not viable for use as a direct atmospheric monitor.

This API source was redesigned to be compatible and interchangeable with a state-of-the-art triple stage quadrupole (TSQ) tandem mass spectrometer (MS/MS), the Finnigan TSQ 70. The modifications included moving all junctions between parts of the source canister outside of the vacuum chamber of the mass spectrometer, thus reducing some of the vacuum integrity problems. A new interfacing flange was designed to mate the source with the mass spectrometer. This flange contained the diaphragm seat, which now became the only interface between the atmospheric pressure source region and the vacuum of the mass spectrometer, and allowed the orifice to be electrically floated. Replaceable diaphragms were obtained with laser-drilled orifices, and a diaphragm with a 70 μm diameter orifice was installed in the interface place. This interface flange maintained vacuum integrity to near theoretical levels calculated from fluid-flow theory.

Unfortunately, moving all source components outside of the vacuum chamber resulted in a greater distance between the orifice and the first quadrupole. An ion optical modeling program (SIMION) was employed to model the region between the orifice and the first quadrupole. Although the model, which the program utilized, did not take into consideration the inelastic collisions of ions in the supersonic jet expansion in the post-orifice region, it proved

invaluable in the actual design of two lenses. These lenses increased the fraction of ions which were transmitted to the quadrupoles.

This new version of the API source employed a small tube near the orifice to provide a gas jet in the discharge region. This gas jet served to keep particulate matter away from the orifice (to prevent orifice clogging) and reduced the amount of water vapor which entered the post-orifice region (to reduce clustering).

A new current-regulated power supply, which was adjustable between 0.5 and 4.5 μA with a discharge voltage between 3 and 4.8 kV, was developed that generated a stable corona discharge. Along with this power supply, a ±500 V low output impedance power supply was developed to electrically float the orifice. The ability to electrically float the orifice allowed for an increased sensitivity and a strong declustering capability by creating a potential difference between the orifice and the first conical lens. The combination of these effects provided the ability to minimize clustering with or without the gas jet. The gas jet still served, however, to prevent orifice clogging.

Direct atmospheric monitoring was accomplished for various common laboratory solvents by sampling vapors from the caps of the solvent bottles. The orifice and lens potentials could be tuned such that the molecular or pseudo-molecular ion was the predominant ion in the mass spectrum for each solvent (methanol being the only exception).

Evaluation as Direct Atmospheric Analyzer

The API/MS/MS instrument was applied to differentiating a pair of

solvents with the same molecular weight which generated pseudo-molecular ions of the same m/z value. MS/MS was used to fragment each of the pseudo-molecular ions and generate daughter spectra which were easily distinguishable.

Electrical floating of the orifice caused a larger spread in the kinetic energy of the ions generated. Clustering and fragmentation occurred simultaneously, which in true mixture analysis would make the interpretation of mass spectra more difficult. While the API source was shown to detect compounds directly in the atmosphere at the ppm concentration range (≈15 μg of methoxy benzaldehyde), the potential of the sensitivity of the API source remains to be evaluated.

Suggestions for Future Work

Consideration of Supersonic Expansion Theory

The large body of work which has been performed to study the effects of a supersonic jet expansion of gases for the production of molecular beams has been reviewed by Bossel [47]. Most of the associated theory has been derived for systems with an "effusion source". An effusion source is one in which the diameter of the orifice is less than or equal to one mean-free-path of the species on the high pressure side of the orifice. This assures that no more than one molecule passes through the orifice at a given time. The mean-free-path for nitrogen (the major constituent of air) is 6.56×10^{-2} μm [48] or 656 nm. Clearly, an orifice of this size would reduce sensitivity and suffer from frequent clogging. However, this theory

can be used to calculate the velocity which the ions and molecules obtain in the supersonic jet expansion when they reach the plane of the aperture of the first conical lens. Equation 5.1 [38] can be used to calculate Mach number (the velocity of the molecule or ion relative to the speed of sound) at that point in the supersonic jet expansion.

$$M \approx \left[\frac{\tau+1}{\tau-1}\right]^{(\tau+1)/4} \times \left[\frac{z}{d}\right]^{(\tau-1)} \qquad (5.1)$$

For nitrogen τ (C_p/C_v) = 1.4 [38], and for this system the diameter of the orifice, d, is 0.00276" (70 μm) and the orifice-to-first conical lens (CL1) distance, z, is 0.075" (1900 μm). Using these values, M can be calculated to be 11.0. The ions and molecules are therefore moving at 8360 mph (3740 m/s). For a molecule of mass 100 g/mole, accelerated to 8360 mph, with a charge of 1, the kinetic energy can be calculated from equation 5.2.

$$K.E. = 0.5 \cdot m \cdot v^2 \qquad (5.2)$$

Applying the values above ($m = 1.66 \times 10^{-25}$ kg/molecule and $v = 3.40 \times 10^{-2}$ m/s), the kinetic energy can be calculated to be 7.2 eV. As the gas expands from the orifice, fluid dynamics predicts that the thickness of the beam of gas will be equal to one orifice diameter for a distance of approximately one orifice diameter [38]. To efficiently sample the beam of gas, CL1 should then have the location of its projected apex within one orifice diameter of the orifice. Figure 5.1

shows the relationship between the Mach number M, the orifice-to-CL1 distance z, and the required diameter of the aperture on CL1 D (see below). Sciex has stated [34] that if z is less than 50D then a potential field may be applied between the lens and the orifice to focus the ions while increasing the kinetic energy spread of the ions by less than 2 eV (for an electrically grounded orifice). Figure 3.8 shows a kinetic energy spread of less than 1 eV with this system for z ≈ 27D. However, for a floated orifice, the kinetic energy spread is much greater (Figure 3.10 shows a value of ≈ 10 eV). Therefore, by applying the knowledge of supersonic jet expansion theory, it may be possible to reduce this energy spread by reducing the size of the conical lens aperture and reducing z.

Bossel also reviews the need for finely machined conical lenses [47]. The front of the cone should come to as sharp an edge as possible. This reduces the production of a shock wave at the plane of cone aperture, termed a "mach disk", which can reduce the transmission of ions through the cone. The conical lenses used in this work lack this precise machining. Therefore, new conical lenses should be obtained. Several companies specialize in the production of molecular beam skimmers for supersonic expansion, two of which are Beam Dynamics [49] and Custom Service Technologies [50].

Requirements for Future Work

For the future development of this source, several components should be modified or replaced. Sciex has shown [34] that varying the needle-to-orifice distance can affect the relative intensities of the ions produced. This may be useful for providing additional selectivity

Figure 5.1

Relationship between the Mach number, M, the distance between the orifice and the plane of the aperture of the first conical lens, z, and the diameter of the aperture, D, required to allow efficient sampling of the ions exiting a 70 μm diameter orifice.

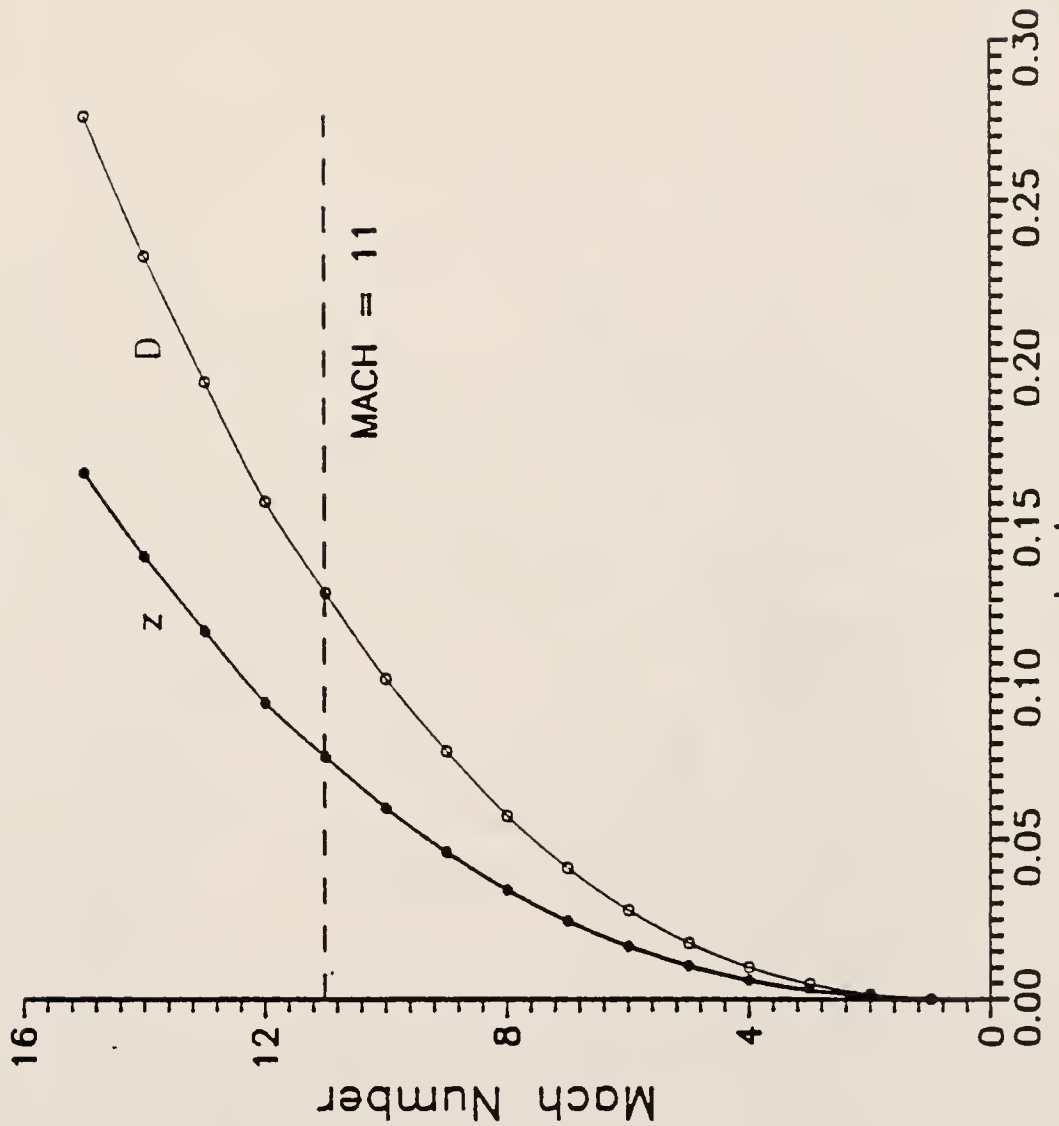
Mach Number
16
12
8
4
0
0.00
0.05
0.10
0.15
0.20
0.25
0.30
Inches
MACH = 11
D
Z

for the ionization process. Although the new corona discharge power supply has served to generate a stable corona discharge, the needle-to-orifice separation has been limited. For a given current, a larger needle-to-orifice distance requires a larger voltage from the power supply. The current power supply is limited to 5 kV. This has limited the needle-to-orifice separation to a few millimeters, and therefore it is proposed that a new discharge power supply be constructed based on a 10 kV power supply.

The vacuum system has proved inefficient in handling the large gas loads provided by the API source. When a normal gas load is put on the system, the forepump pressure (the pressure at the entrance to the mechanical pumps) is a few mtorr. With the API source installed, this pressure increases to approximately 400 mtorr. On the TSQ 70, one mechanical pump serves as the backing-pump for both turbomolecular vacuum pumps. For future work, the turbomolecular pump for the analyzer region should be provided with an independent backing-pump. This may allow for pressures closer to the theoretical value for the analyzer region and may allow the size of the orifice to be increased, increasing the sensitivity of the instrument.

The API source canister for this work was designed to allow flexibility in its configuration. Since the one-orifice system has been shown to perform adequately, a new, second-generation source canister should be built that has a larger diameter source region, is shorter, and provides micrometer control over the needle position. The walls of the original canister are approximately 0.5" thick stainless steel. This makes the source heavy and cumbersome. Therefore, the

canister should be built out of a lighter material such as aluminum, or the wall thickness should be reduced where possible.

To achieve total computer control of the API/MS/MS instrument, digital-to-analog (DAC) converters should be implemented to control the corona discharge current, the ±500 V orifice potential, and the potentials for the additional lenses that the API lens system has added to the mass spectrometer.

To sample gases, the sample must currently be brought near the entrance to the glass sampling tube. A larger capacity gas sampling fan should provide the ability to sample from greater distances.

Applications

Finally, the applications of API/MS/MS with this instrument should be extended. While this instrument has been applied to simple mixtures, it has not be applied to any "real" samples. With improvements listed above, the sensitivity of the instrument should be significantly increased. Also, this instrument has yet to be applied to samples which are more amenable to negative ionization.

The research presented in this thesis has demonstrated the ability to develop a functional API source for a commercial, turbomolecularly-pumped tandem mass spectrometer. The future research proposed here should prove this combination to be a viable method for the direct atmospheric monitoring of trace compounds.

LITERATURE CITED

1. Finnigan-MAT Corporation, 355 River Oaks Parkway, San Jose, CA 95134-1991.

2. Knewstubb, P. F.; Sugden, T.M. Nature 1958, 181, 474.

3. Knewstubb, P. F.; Sugden, T.M. Ibid. 1958, 181, 1261.

4. Knewstubb, P. F.; Sugden, T.M. 7th International Symposium on Combustion (Oxford, 1958) Butterworth, London, 1959, 247.

5. Knewstubb, P. F.; Sugden, T.M. Proc. R. Soc. London 1960, A255, 1920.

6. Kebarle, P.; Hogg, A. M. J. Chem. Phys. 1965, 42, 688.

7. Hogg, A. M.; Kebarle, P. Ibid. 1965, 43, 449.

8. Hogg, A. M.; Haynes, R. N.; Kebarle, P. J. Am. Chem. Soc. 1966, 88, 28.

9. Kebarle, P.; Searles, S. K.; Zolla, A.; Scarborough, J.; Arshadi, M. Ibid. 1967, 89, 6393.

10. Shahin, M. M. J. Chem. Phys. 1965, 45, 2600.

11. Carroll, D. I.; Dzidic, I.; Horning, E. C.; Stillwell, R. N. Appl. Spectrosc. Rev. 1981, 17(3), 337-406.

12. Mitchum, R. K.; Korfmacher, W. A. Anal. Chem. 1983, 55, 1485A-1499A.

13. Horning, E. C.; Horning, M. G.; Carroll; D. I., Dzidic, I.; Stillwell, R. N. Anal. Chem. 1973, 45, 936-943.

14. Dzidic, I.; Carroll, D. I.; Horning, E. C. Anal. Chem. 1976, 48, 1763-1768.

15. Carroll, D. I.; Dzidic, I.; Horning, M. G.; Horning, E. C. Anal. Chem. 1974, 46, 706-710.

16. Mitchum, R. K.; Althaus, J. R.; Korfmacher, W. A.; Moler, G. F. Advances in Mass Spectrom. 1980, 8B, 415-421.

17. Mitchum, R. K.; Althaus, J. R.; Korfmacher, W. A.; Rowland, K. L.; Nam, K.; Young, J. F. Biomed. Mass Spectrom. 1981, 8, 539-545.

18. Tsuchiya, M.; Taira, T. Int. J. Mass Spectrom. Ion Phys. 1980, 34, 351-359.

19. Carroll, D. I.; Dzidic, I.; Stillwell, R. N.; Haegele, K. D.; Horning, E. C. Anal. Chem. 1975, 47, 2369-2273.

20. Scott, R. P.; Scott, C. G.; Munroe, M.; Hess, J. J. Chromatogr. 1974, 99, 395.

21. Arpino, P. J.; Dawkins, B. G.; McLafferty, F. W. J. Chromatogr. Sci. 1974, 12, 574.

22. Yost, R. A.; Fetterolf, D. D. Mass Spectrom. Rev. 1983, 2, 1-45.

23. Caldecourt, V. J.; Zackett, D.; Tou, J. C. Int. J. Mass. Spectom. Ion Phys. 1983, 49, 233-251.

24. Extrel Corporation, P.O. Box 11512, Pittsburgh, PA 15238.

25. Sciex Inc., 55 Glen Cameron Rd, Thornhill, Ontario, L3T 1P2 Canada.

26. Bruins, A. P.; Covey, T. R.; Henion, J. D. Anal. Chem. 1987, 59, 2642-2646.

27. Bruins, A. P.; Weidolf, L. O.; Henion, J. D. Anal. Chem. 1987, 59, 2647-2652.

28. Henion, J.D.; Weidolf, L. O.; Lee, E. D.; Covey, R. C. 35th Annual Conference on Mass Spectrometry and Allied Topics 1987, 15-16.

29. Snyder, A. P.; Kremer, J. H.; Liebman, S. A.; Yost, R. A. 35th Annual Conference on Mass Spectrometry and Allied Topics 1987, 181-182.

30. Davidson, W. R.; Shusan, B. I.; Fulford, J. E.; Thomson; B. A.; Tanner, S. D.; Ngo, A. 32nd Annual Conference on Mass Spectrometry and Allied Topics 1984, 7.

31. Thomson, B. A.; Davidson, W. R.; Lovett, A. M. Environ. Health Perspectives 1980, 36, 77.

32. Glish, G. L.; McLuckey, S. A. 35th Annual Conference on Mass Spectrometry and Allied Topics 1987, 290-291.

33. French, J. B.; Reid, N. M.; Buckley, J. A. U. S. Patent No. 4,023,398, May 17, 1977.

34. French, J. B.; Reid, N. M.; Buckley, J. A. U. S. Patent No. 4,121,099, October 17, 1978.

35. Bertan Associates, 121 New South Road, Hicksville, NY 11801.

36. Karasek, F. W. Anal. Chem. 1974, 46, 710A-720A.

37. Precision Aperture, P.O. Box 10863, Fort Wayne, IN 46803.

38. Fite, W. L. Research note #1, Extranuclear Laboratories, Inc. January, 1971.

39. Levy, D. L. Sci. Amer. 1984, 250, 96-109.

40. Emco High Voltage Co., 11126 Ridge Rd., Sutter Creek, CA 95685.

41. Product and Vacuum Technology Handbook; Leybold-Heraeus, Inc.: San Jose, CA 1986.

42. McGilvery, D. D. Latrobe University, Department of Physics and Chemistry, Bundoora Victoria, Australia, 1977.

43. Dahl, D. A.; Delmore, J. E. Idaho National Engineering Laboratory, EG&G Idaho, Inc., P.O. Box 1625, Idaho Falls, ID 83415.

44. Good, A.; Durden, D. A.; Kebarle, P. J. Chem. Phy. 1970, 52, 212-221.

45. Harrison, A. G. Chemical Ionization Mass Spectrometry; CRC Press Inc.: Boca Raton, FL, 1982.

46. Jordan, T. E. Vapor Pressure of Organic Compounds; Interscience Publishers, Inc.: New York, NY, 1954.

47. Bossel, U. "Investigation of Skimmer Interaction Influences on the Production of Aerodynamically Intensified Molecular Beams", thesis, University of California-Berkeley, 1968.

48. Barrow, G. M. Physical Chemistry; McGraw-Hill Book Company: New York, NY, 1979.

49. Beam Dynamics, Inc., 708 E. 56th St., Minneapolis, MN 55417.

50. Custom Service Technologies, 4300 N. W. 23rd Ave, Suite 289, Gainesville, FL 32602.

BIOGRAPHICAL SKETCH

Kenneth Paul Matuszak was born on March 21, 1961, at Cook County Hospital, in Chicago, Illinois. He attended St. Robert Bellarmine Grammar School for grades 1-8 and graduated from Albert G. Lane Technical High School in Chicago, IL, while earning athletic letters in three sports and was one of ten students selected by the faculty to receive the Wabeno award (the school's most prestigious award, for scholarship, citizenship, and leadership).

After high school he attended Coe College in Cedar Rapids, Iowa, earning a Bachelor of Arts degree in 1983 for completing the requirements for both the chemistry and mathematics degrees in 4 years. At Coe, he also earned 5 varsity athletic letters in track and cross-country. He completed a semester of senior research at Argonne National Laboratories, in Argonne, IL, where he studied electron transfer reactions in frozen glass matrices.

In August, 1983, he entered the University of Florida to begin work on a Ph.D. in chemistry. Following graduation, Dr. Matuszak will be working as an applications chemist at the Finnigan-MAT Corporation in San Jose, CA, a corporation which specializes in the research, development, and production of mass spectrometers.

He is newly married.

I certify that I have read this study and that in my opinion it conforms to acceptable standards of scholarly presentation and is fully adequate, in scope and quality, as a dissertation for the degree of Doctor of Philosophy.

Richard A. Yost, Chairman
Associate Professor of Chemistry

I certify that I have read this study and that in my opinion it conforms to acceptable standards of scholarly presentation and is fully adequate, in scope and quality, as a dissertation for the degree of Doctor of Philosophy.

John R. Eyler
Professor of Chemistry

I certify that I have read this study and that in my opinion it conforms to acceptable standards of scholarly presentation and is fully adequate, in scope and quality, as a dissertation for the degree of Doctor of Philosophy.

Gar B. Hoflund
Professor of Chemical Engineering

I certify that I have read this study and that in my opinion it conforms to acceptable standards of scholarly presentation and is fully adequate, in scope and quality, as a dissertation for the degree of Doctor of Philosophy.

John G. Dorsey
Associate Professor of Chemistry

I certify that I have read this study and that in my opinion it conforms to acceptable standards of scholarly presentation and is fully adequate, in scope and quality, as a dissertation for the degree of Doctor of Philosophy.

Clifford T. Johnston
Assistant Professor of Soil Science

This dissertation was submitted to the Graduate Faculty of the Department of Chemistry in the College of Liberal Arts and Sciences and to the Graduate School and was accepted as partial fulfillment of the requirements for the degree of Doctor of Philosophy.

April, 1988

Dean, Graduate School

UNIVERSITY OF FLORIDA
3 1262 08556 7617